M-AM-SymII-3

THE STRUCTURE OF MYOSIN SUBFRAGMENT-1 AT 2.8A RESOLUTION.
((I. Rayment)) University of Wisconsin.

M-AM-SymII-4

MUTATION ANALYSIS OF THE MOLECULAR MOTOR MYOSIN.
((Kathleen M. Ruppel, Taro Q.P. Uyeda, and James A. Spudich)) Departments of Biochemistry and Developmental Biology, Stanford University, Stanford, CA 94305.

We are using site-directed mutagenesis and oligo-directed random mutagenesis to explore regions of the myosin head (Subfragment-1 or S1, the motor unit of the molecule) thought to be important for ATP and actin-binding, as well as to delineate functions of other regions of currently unknown function. Mutated myosins are expressed in *Dictyostelium* cells lacking the endogenous myosin heavy chain gene (created by gene replacement). Resultant *in vivo* phenotypes are used to identify functionally defective myosins. The altered myosins are then purified from these cells using a rapid new purification scheme, and they are characterized by a variety of methods including *in vitro* motility assays. Early mutagenesis efforts concentrated on specific amino acid changes of residues thought to be important for ATP and actin interactions. This approach yielded mutated myosins that are no longer able to bind nucleotide but which bind actin tightly (rigor-binders), myosins that have decreased affinity for nucleotide or decreased ATP turnover, and myosins with decreased stability *in vivo* and *in vitro*. More recent efforts have involved creating banks of random point mutations over short (about 20 a.a.) stretches of highly conserved myosin sequence throughout the myosin head. Initial analysis of two such banks of mutations, both centered in a block of strikingly high conservation within the 50-kDa domain, has revealed mutations that show defects in ATP hydrolysis, actin-activation of ATPase activity, or of coupling of ATPase and motility *in vitro*. Another effort has involved altering the highly variable loop structures between the 50/20-kDa junction in order to assess its importance for regulation of the rate of ATPase and speed of contraction. Sequences corresponding to smooth, cardiac and skeletal muscle myosin loops have been used to replace the *Dictyostelium* sequence, and their effects are being assayed. In collaboration with Dr. Ivan Rayment (University of Wisconsin, Madison), we are placing each of these changes on the high-resolution three dimensional structure of S1 (recently determined by Dr. Rayment and his colleagues). We are also collaborating with Dr. Ken Holmes' group (Max-Planck-Institute, Heidelberg) and Dr. Dietmar Manstein (NIMR, Mill Hill, London) to analyze the position of these mutations in relation to the docked structure of S1 bound to actin in the actin-S1 complex formed in the absence of ATP. These studies should provide a framework for understanding how myosin functions to link ATP hydrolysis to movement and force production.

POTASSIUM CHANNELS I

M-PM-A1

A G_q-LIKE G PROTEIN TRANSDUCES THE BRADYKININ ACTIVATION OF A CALCIUM-DEPENDENT POTASSIUM CURRENT IN NG108-15 CELLS.
((M.A.Wilk-Blaszczak, S.Gutowski, P.Sternweis and F.Belardetti)) Dept. Pharmacology, Univ. TX Southwestern Med. Ctr. Dallas, Dallas, TX 75235.

In differentiated NG108-15 neuroblastoma x glioma cells, bradykinin (BK) stimulates PLC, which breaks down PIP_2, generating IP_3 and DAG. By triggering Ca^{2+} release in the cytoplasm, IP_3 activates an outward $I_{K(Ca)}$. We have examined the role of a recently discovered PTX-insensitive G protein, G_q, in coupling the BK receptor to this cascade. We first studied the PTX-sensitivity of this action using the whole-cell patch-clamp technique (V_h -40 mV). After overnight incubation either with PTX (200 ng/ml, n=12) or with boiled PTX (n=7), pressure applied BK (10 nM) evoked an outward $I_{K(Ca)}$ of similar amplitude in both cases. We next perfused an antibody (AB) raised against the common C-terminal peptide of G_q and G_{11} inside the recording pipette. After 20-30 min of AB perfusion, BK evoked an outward $I_{K(Ca)}$ which was only 37% (n=7) of that evoked after perfusing preimmune IgG (n=19) or peptide-blocked AB (n=6; preimmune or peptide-blocked IgG did not affect BK responses). Finally, we examined the site of action of the AB by evoking the same $I_{K(Ca)}$ with pressure application of the calcium ionophore A23187 (20 μM). Under these conditions, intracellular AB perfusion (n=9) did not reduce the ionophore-evoked current compared to preimmune IgG perfusion (n=9). These data indicate that G_q and/or its homologs couple the BK receptor to the activation of $I_{K(Ca)}$ through activation of PLC.

M-PM-A2

NIFLUMIC ACID ACTIVATES LARGE CONDUCTANCE K_{Ca} CHANNELS.
((L. Toro, M. Ottolia, R. Olcese and E. Stefani)) Dept. Molecular Physiology & Biophysics. BCM. Houston, TX 77030

Large conductance K_{Ca} channels are important modulators of smooth muscle contractility. Their blockade produces depolarization and contraction of several smooth muscles. Conversely, their activation should lead to hyperpolarization and relaxation. Thus, the finding of drugs that selectively open this type of K channels is of significant pharmacological and therapeutical relevance. We found that niflumic acid {(trifluoro-methyl-3-phenylamino)-2-nicotinic acid}, a drug known to inhibit Ca-activated Cl channels, activates large conductance K_{Ca} channels in a dose dependent manner. Niflumic acid (20 μM) greatly increased K_{Ca} channel open probability from coronary smooth muscle incorporated into lipid bilayers. When niflumic acid was added to the external side of the channel its action was immediate; however, when the drug was added to the internal side the effect was less potent and required much more time to take place. This suggests that niflumic acid is capable to diffuse through the lipid environment and reach its site of action on the external side. The niflumic binding site is not located in the conduction pathway since high internal K could not "knock out" its action and the fast blockade induced by external TEA was not prevented by the drug. The opening of K_{Ca} channels by niflumic acid seems to be specific since activation of other K channels (DRK1 and Shaker H4) was not observed. Analogs of niflumic acid were tested; flufenamic acid {2-{{3-(trifluoromethyl)phenyl]-amino]benzoic acid} mimicked its action, while mefenamic acid {2-[(2,3-dimethylphenyl)amino]-benzoic acid} did not at equivalent concentrations. In conclusion, niflumic acid is an activator of large conductance K_{Ca} channels and an important pharmacological tool to determine the importance of these channels in cell function. Supported by grants HL47382, HL37044 and AHA-Natl. Center 900963.

M-PM-A3

NITRIC OXIDE (NO) AND cGMP-DEPENDENT PROTEIN-KINASE ACTIVATION OF LARGE CONDUCTANCE Ca^{2+}-ACTIVATED K^+ (K_{Ca}) CHANNELS IN RABBIT CEREBRAL ARTERY SMOOTH MUSCLE CELLS.
((Blair E. Robertson, Rudolf Schubert, Jürgen Hescheler and Mark T. Nelson)). Univ. of Vermont, Dept. of Pharmacology, Medical Research Facility, Colchester, VT 05446.

K_{Ca} channels help regulate arterial tone (Brayden & Nelson; Science, 256, 532-535 1992). We tested the hypothesis that arterial dilation to NO may involve activation of K_{Ca} channels. Single K_{Ca} channels in cell-attached patches from rabbit basilar artery smooth muscle cells were activated approx. 2 fold following application of 50 μM of the NO donor SIN-1 to the bathing solution. Furthermore, a membrane permeable analogue of cGMP (8PCPT-cGMP, 400 μM) also increased channel activity in cell-attached patches by approx. 3 fold. In inside-out patches, internally applied cGMP-PK (5u/μl) had no effect on its own, but in the presence of ATP and cGMP it activated the channels 9 fold (Fig. 1). ATP and cGMP also had no individual effects, suggesting cGMP activates the kinase leading to ATP hydrolysis and ultimately channel phosphorylation. These results suggest that activation of K_{Ca} channels by cGMP-PK may be involved in arterial relaxation to NO.
Fig. 1. (Conditions: Membrane Potential; + 10 mV. t = 10s. unitary current = 6.5 pA)

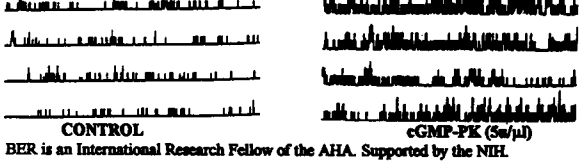

BER is an International Research Fellow of the AHA. Supported by the NIH.

M-PM-A4

IN THE ABSENCE OF EXTRACELLULAR CALCIUM, ADENOSINE (ADO) AND RELATED PURINES DECREASE THE OPEN PROBABILITY OF BK CHANNELS FROM BASILAR ARTERY SMOOTH MUSCLE.
((G. Alexander West and J. Marc Simard)) UTMB, Galveston, Texas 77550 and Univ. Washington, Seattle, WA 98104.

Purine compounds, notably ADO and ATP, have significant effects on the cerebral vasculature. We studied the effects of ADO, ATP and related compounds on large conductance Ca^{2+}-activated (BK) channels in isolated basilar artery smooth muscle cells (n=43). Whole cell, cell-attached, and inside-out patches were studied. In the absence of extracellular Ca^{2+}, ADO produced a dose-dependent decrease in macroscopic I_{BK}, with an IC_{50}=5 μM. Analysis of single BK channels in the whole cell mode showed a dramatic reduction of $N \cdot P_o$, whereas single channel conductance was minimally reduced (see Figure). In contrast, there was no significant effect on BK single channel activity in either cell-attached or inside-out patches. There was no effect of intracellular Ca^{2+} on the response. Similar results were obtained with ATP, GTP, and inosine. Pinacidil was without effect on macroscopic I_{BK}. In the presence of 1.8 mM Ca^{2+} extracellularly, the effect of ADO (5-100 μM) on I_{BK} was completely eliminated. These results suggest that there is an extracellular binding site for Ca^{2+} that is important in the regulation of BK channels and in conferring sensitivity to ADO and related purines. These results may have importance for the regulation of BK channel activity in general.

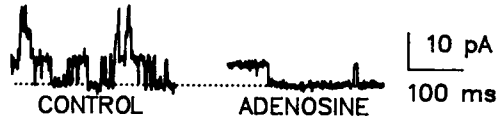

M-PM-A5

CALCIUM-ACTIVATED POTASSIUM CHANNELS IN HUMAN T LYMPHOCYTES. ((Stephan Grissmer, Angela N. Nguyen, and Michael D. Cahalan)) Department of Physiology and Biophysics, UC Irvine, CA 92717.

Using the patch-clamp technique, we have identified and characterized Ca^{2+}-activated K^+ (K(Ca)) channels in human peripheral blood (HPB) T lymphocytes. Raising $[Ca^{2+}]_i$ typically causes an average of 20 K(Ca) channels per cell to open in resting HPB T lymphocytes, and 500 K(Ca) channels per cell in activated T-cell blasts. The opening of K(Ca) channels is highly sensitive to $[Ca^{2+}]_i$ (half-activation ~400 nM, Hill coefficient of 4). At optimal $[Ca^{2+}]_i$ (1 μM) the open probability of single channels was ~0.45. The K(Ca) channels show little voltage dependence over a potential range from -100 mV to 0 mV. Compared to voltage-gated K^+ (K(V)) channels in the same cells, K(Ca) channels have nearly identical open-channel rectification, unitary conductances (12 pS in Ringer, 35 pS in K^+ Ringer), permeability ratios (K^+ (1.0) > Rb^+ (0.96) > NH_4^+ (0.17)), and voltage-dependent block by external Cs^+ or by internal Ba^{2+}. In addition, K(Ca) channels and K(V) channels are identically sensitive to block by external charybdotoxin (K_i = 3 nM). However, K(Ca) channels are less sensitive to block by either external TEA, noxiustoxin (NTX), or internal TEA, and conduct NH_4^+ current better than K^+. We conclude that while K(Ca) and K(V) channels share similarities in many open channel properties, the differences in channel gating and block by external NTX and by TEA indicate that the underlying proteins differ in several structural characteristics. Supported by NIH grants NS14609 and GM41514 and a grant from Pfizer Inc.

M-PM-A6

A COMPLETE FUNCTIONAL MAP OF THE SURFACE OF CHARYBDOTOXIN. ((Per Stampe, Ludmilla Kolmakova-Partensky, and Christopher Miller)), HHMI, Graduate Department of Biochemistry, Brandeis University, Waltham, MA 02254

The outer vestibules of many K^+ channels carry a high-affinity receptor for charybdotoxin (CTX). CTX belongs to a class of peptide toxins found in scorpion venoms. We used a genetically manipulable recombinant CTX to identify toxin residues directly involved in interaction with high-conductance Ca^{2+}-activated K^+ channels from rat skeletal muscle. The bimolecular toxin-channel interaction can be observed at the single-channel level (with channels inserted into planar bilayers) as the appearance of a toxin-induced nonconducting state longer in mean duration than the normal closed-times of 1-5 ms. The known structure of CTX (determined by 2-D NMR) guided our interpretation of results.

We mutated each of the 30 solvent-exposed residues on the CTX molecule and examined the channel-blocking kinetics of the altered toxins. (The single glycine and 6 cysteines form the interior the molecule and cannot be altered without major structural changes.) 8 residues are classified as crucial because conservative mutations lead to greater than 10-fold decrease in affinity; 13 residues are unimportant for function because radical mutations changed the affinity less than 3- fold; the remaining 9 residues fall in a group in between. 6 of the 8 crucial residues are located on a clearly defined, flat 2 x 2.5 nm surface, and the remaining 2 are close together on one side of the molecule. The unimportant sites are located on the "top" of the molecule, opposite to the crucial residues. The intermediate residues are found mostly on the three remaining sides. These results are consistent with a flat receptor site in the bottom of the channel mouth, near the end of the narrow pore and several contact points on an outer "wall" of the channel's vestibule.

M-PM-A7

POINTS OF INTERACTION OF CHARYBDOTOXIN AND A *SHAKER* K^+ CHANNEL. ((Steve A. N. Goldstein, Deborah Pheasant, Per Stampe and Chris Miller)) HHMI, Grad. Dept. of Biochem., Brandeis University, Waltham, MA.

To identify the residues of charybdotoxin (CTX) that make contact with its receptor in the outer pore of a *Shaker* K^+ channel, the binding and dissociation rates of over 70 mutant recombinant CTXs were evaluated. Channels were expressed in *Xenopus* oocytes and studied in macropatches or by whole-cell clamp in a rapid perfusion chamber. Analysis of conservative mutations showed that just 5 of the toxin's 37 amino acids profoundly influence its binding, (increasing its off-rate from 20 to 20,000-fold), while 5 positions exert a moderate influence (3 to 10-fold). The spatial geometry of these 10 toxin residues is defined by the known structure of CTX. Their arrangement offers clues, as a molecular mirror, into the nature of the channel surface coordinating a bound toxin molecule.

To identify the residues on the channel surface which make contact with CTX, the interaction of wild-type recombinant CTX with channels modified by point mutation was studied. Because the scorpion toxin receptor of *Shaker*-type K^+ channels is formed by residues in the pore-associated S5-S6 linker region, the effect of altering each of the 24 residues which surround the deep pore was evaluated.

Using these results as a guide, we have made complementary point mutations in CTX and its channel receptor site and defined both local (steric) and distant (electrostatic) points of contact. These initial results provide preliminary insights into the structural organization of the outer conduction pathway.

M-PM-A8

ENERGY BARRIER FLUCTUATIONS IN A CA-ACTIVATED K-CHANNEL REVEALED BY ANALYSIS OF SUBCONDUCTANCE STATES INDUCED BY BPTI AND DENDROTOXIN I. ((G. W. J. Moss and E. Moczydlowski)) Dept. of Pharmacology, Yale Univ. School of Medicine, New Haven, CT 06510.

Permeation through open K-channels is often assumed to involve ions hopping over stable energy barriers into fixed binding sites. Such static energy profiles represent a time-average of protein conformational states. Similarly, a "well resolved" conductance level may represent a time average of multiple short-lived conducting conformations. Thus, structural fluctuations may be crucial to the permeation process (Lauger, 1983). To address this issue we have analyzed rectifying substates induced in maxi K(Ca) channels by the homologous proteins, BPTI and DTX-I. We have previously shown that block by occlusion or changes in normal gating cannot account for this phenomenon. Planar bilayer recordings of BPTI-induced substates filtered at 500 Hz exhibit excess noise as compared to the open channel, or the subconductance events induced by DTX-I. Noise analysis indicates that BPTI-induced substates can be approximated as the filtered average of a rapid two-state process of channel flickering between high and low conductance conformations. Measurement of underlying transition rates using β-function fits of amplitude histograms predict rate constants for voltage-dependent pore fluctuations of ~4,000 to 20,000 s^{-1} at $\pm$50 mV. To verify this prediction, we patch-clamped single maxi K(Ca) channels from vascular smooth muscle cells and recorded at high resolution (8.8 kHz). We directly observed BPTI-induced channel flickering between the open state and a very low, almost zero-current level. Such recordings also reveal excess noise on DTX-induced substate events, indicating a similar switching process with much faster transition rates. We conclude that BPTI and DTX-I destabilize the normal open channel structure to cause energy barrier fluctuations at rates that are slow enough to barely resolve. Such pore fluctuations could explain noisy open states that have been observed in single-channel recordings of various cloned K-channels. Our results suggest that protein conformational dynamics play an important role in determining unitary conductance levels and rectification.

M-PM-A9

A MAXI-K CHANNEL AGONIST ISOLATED FROM A MEDICINAL HERB. ((O.B. McManus, K.L. Giangiacomo, G.H. Harris, M.E. Addy*, J.P. Reuben, G.J. Kaczorowski and M.L. Garcia)) Merck Res. Labs, P.O. Box 2000, Rahway, NJ 07065, and *Univ. of Ghana, Legon, Ghana.

Desmodium adscendens (SW) D.C. var. adscendens is a medicinal herb used in Ghana as a treatment for asthma. Crude extracts of the plant inhibited [^{125}I]-charybdotoxin (ChTX) binding to large-conductance calcium-activated potassium (maxi-K) channels from smooth muscle. A triterpenoid glycoside was isolated that inhibited [^{125}I]-ChTX binding with a K_i of 100 nM, with 80% inhibition at maximal concentrations. Kinetic analysis of [^{125}I]-ChTX binding, and of ChTX block of maxi-K channels incorporated into lipid bilayers, revealed that the triterpenoid glycoside caused a three-fold increase in the rate of toxin dissociation. These data suggest an allosteric interaction between binding sites for the triterpenoid glycoside and ChTX on maxi-K channels. In lipid bilayer and patch clamp experiments, the triterpenoid glycoside caused large reversible increases in open probability of maxi-K channels from bovine trachael and aortic smooth muscles when applied to the internal, but not the external side of the membrane. Clear increases in channel open probability were observed after exposure to concentrations as low as 10 nM. The triterpenoid glycoside shifted the voltage dependence of channel activation to more negative potentials; the maximal observed shift was 130 mV and a half-maximal shift occurred at 70 nM. Hill plots of channel open probability against drug concentration typically had slopes of about two suggesting more than one triterpenoid glycoside molecule can participate in activation of a single maxi-K channel. The triterpenoid glycoside did not activate the channel in the absence of calcium suggesting that it cannot replace calcium. We have isolated a triterpenoid glycoside from a medicinal herb that is the most potent known agonist for maxi-K channels.

M-PM-B1

μ-Aga-IV: A SPIDER TOXIN SPECIFIC FOR INSECT Na CHANNELS.
((C.J. Cohen, T. A. Bale, E.A. Ertel, V. A. Warren and M.M. Smith)) Merck Res. Labs., Rahway, NJ. 07065. (Spon. by K. Giangiacomo)

μ-Aga-IV is a peptide toxin from venom of the spider *Agelenopsis aperta* [Skinner, J Biol Chem 264:2150,(1989)]. We isolated this toxin by HPLC using insecticidal activity against blowfly larvae as the bioassay. The identification was confirmed by N-terminal sequence analysis of 30 residues and by electrospray mass spectroscopy. The mechanism of action of μ-Aga-IV was evaluated by whole cell voltage clamp studies of Na currents in locust (*Schistocerca americana*) metathoracic ganglion neurons. Freshly dispersed neuronal soma have little or no Na current, but robust Na currents are recorded from soma that are incubated overnight in saline with 20% fetal calf serum [Tribut, Pflug Arch 419:665,(1991)]. Most Na current inactivates rapidly, but a low-voltage activated component inactivates very slowly. Both components are blocked by 30 nM TTX. μ-Aga-IV enhances both components such that channel opening occurs at potentials ≈30 mV more negative than normal (see fig). This modification of Na channels can account for the spiking activity of motorneurons induced by μ-Aga-IV in house fly larvae [Adams, Neurotox '88]. μ-Aga-IV is highly selective for Na channels in insects: 0.5 μM toxin produces substantial modification in locust neurons, but 9 μM toxin has little or no effect in guinea pig atrial myocytes.

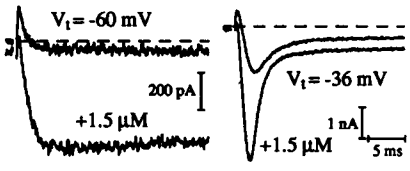

M-PM-B2

BLOCK OF CLONED HUMAN CARDIAC Na^+ CHANNELS BY LIDOCAINE: IS THE RECEPTOR GUARDED?
((Bennett PB, Chen L-Q, Kallen RG)). Dept. of Pharmacology, Vanderbilt University School of Medicine, Nashville, TN, Dept. Biochem. & Biophysics, University of Pennsylvania Philadelphia, PA.

Lidocaine induced inhibition of the cardiac sodium channel (hH1) was studied by expression of α-subunit cRNA in *Xenopus laevis* oocytes by 2-electrode voltage clamp. Twin pulse protocols were used to assess onset and recovery from block. Lidocaine (25 μM) induced 41 ± 2% block that developed with a time constant of 589 ± 42 msec (N=7) at membrane potentials between -30 and + 20 mV. In contrast over this range of membrane potentials, control channels inactivated within 20 msec and slow inactivation developed much later (τ_{SI} = 6.2 ± 0.36 sec). Recovery from block was slower than recovery from inactivation ($\tau_{RECOVERY}$ = 11 ± 0.6 msec; τ_{BLOCK} = 1.3 ± 0.2 sec) at -120 mV and block recovery was enhanced further by hyperpolarization. This apparent voltage dependence of closed channel recovery suggests a modulation of the receptor affinity depending on channel state. A receptor guarded from lidocaine occupancy by the channel "activation gates" must also be guarded from drug dissociation at negative membrane potentials (i.e. trapped). A model that traps lidocaine predicts slower recoveries at more negative membrane potentials, therefore a guarded receptor model for lidocaine block of human cardiac Na^+ channels is not consistent with experimental data and must be rejected. Realistic models of drug-channel interactions must account for the apparent state dependent change in receptor affinity. Supported by HL40608.

M-PM-B3

MECHANISM OF ZINC BLOCK IN NA-CHANNEL SUBTYPES AND MUTANTS.
((L. Schild, I. Favre and E. Moczydlowski)). Institut de Pharmacologie, UNIL., 1005 Lausanne, Switzerland, and Department of Pharmacology, Yale Univ. School of Medicine, New Haven, CT 06510.

External Zn^{2+} blocks skeletal muscle μ1 Na^+ currents expressed in Xenopus oocytes and cardiac-subtype Na^+ currents in cultured L6 cell line with K_i's of 2.9 mM and 25 μM respectively. In L6 cells Na^+-current inhibition by Zn^{2+} saturates at 85%, suggesting block to a substate level. The mutation Y401C in μ1 greatly enhances the affinity for Zn^{2+} block (K_i = 9 μM), and as for L6, Zn^{2+}-block saturates at 89%. Unitary I-V relations for BTX-modified Na^+-channels from heart were measured for symmetrical NaCl concentrations ranging from 2 to 3,0000 mM. Open channel conductance exhibits a biphasic dependence on $[Na^+]$, suggestive of double occupancy. In contrast,the Zn^{2+}-induced substate displays monophasic low affinity for Na^+. Energy barrier profiles derived by fitting I-V data to Eyring permeation models are consistent with the possibility that single Zn^{2+} ion bound in the outer vestibule at Cys 401 prevents double occupancy by Na^+ and effectively raises the barrier profile by about 6 RT units.

M-PM-B4

Temperature- and Potassium-Sensitive Skeletal Muscle Sodium Channel Mutations in Human Muscle Disease.
((L.J. Ptacek, A.L. George, R.L. Barchi, and M.F. Lepperl)) University of Utah, SLC, UT 84132, Vanderbilt University, Nashville, TN 37232; and University of Pennsylvania, Philadelphia, PA 19104.

Clinical and electrophysiological data have outlined a spectrum of similar, yet distinct, periodic paralyses including potassium-sensitive (HYPP) and temperature-sensitive (PC) forms. Recent work has revealed that these disorders result from allelic defects in the α-subunit of the adult, human skeletal-muscle sodium channel.

We have defined a potassium-sensitive mutant in the fifth putative membrane spanning segment of domain 2 (D2/S5) of the skeletal muscle sodium channel and 3 distinct mutations in D4/S3-4 in patients with the temperature sensitive phenotype. The latter 3 mutations all result in alteration of the charge in, or near the putative 'voltage sensor' of the channel.

Identification of these molecular variants and expression experiments *in vitro* will shed new light on the biophysics of this sodium channel and the manifestations of these muscle disorders in humans.

M-PM-B5

FUNCTIONAL EXPRESSION OF THE HUMAN SKELETAL MUSCLE SODIUM CHANNEL.
((M. Chahine*, P.B. Bennett, R. Horn* and A.L. George)) Department of Physiology*, Jefferson Medical College, Philadelphia, PA 19107; and Departments of Medicine and Pharmacology, Vanderbilt University, Nashville, TN 37232.

Point mutations in the adult skeletal muscle Na^+ channel (NaCh) α-subunit gene have been identified in periodic paralysis patients. Functional expression of the cloned human skeletal muscle NaCh (hSkM1) was undertaken to better understand the molecular basis of this disease. Heterologous expression of hSKM-1 was investigated in *Xenopus* oocytes and in a human embryonic kidney cells line (tsA201) using 2-electrode or whole-cell patch clamp methods, respectively. In oocytes, hSkM1 exhibited multimodal inactivation kinetics with a majority of channels inactivating slowly. Recovery from inactivation at -120 mV consisted of a fast (14 ± 4%; τ = 9 ± 2.7 msec) and a slow component (80 ± 3%; τ = 2.4 ± 0.2 sec). The $V_{1/2}$ and slope factor for inactivation were -52 ± 1.8 and 6.4 ± 0.2 mV (n=7). hSKM-1 expressed in tsA201 cells had a predominantly rapid inactivation time constant (τ=0.98 msec, 0 mV) which decreased e-fold per 31 mV. The $V_{1/2}$ and slope factor for inactivation were -77 ± 5 and 5.9 ± 0.1 mV (n=4). The results reproduce the multimodal kinetics in native muscle and indicate the importance of expression systems. Studies are in progress to further characterize the normal and disease producing mutants in this channel.

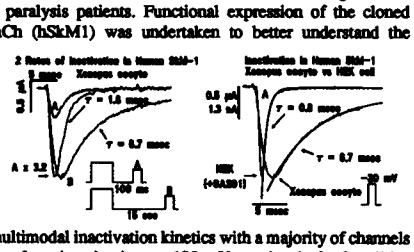

M-PM-B6

Mutants of the *seizure* locus, that affect STX binding, also alter the persistent Na current in *Drosophila* neurons.
Saito M and C.-F. Wu. Department of Biology, University of Iowa, Iowa City, IA 52242

High temperature induces seizure behavior followed by paralysis in *seizure* (*sei*) mutants of *Drosophila*. Previous studies showed altered STX binding in homogenate of *sei* flies, suggesting abnormalities in the Na channels (Jackson et al., 1984). We have shown that all-or-none action potentials in cultured *sei* neurons at 33 °C or above became plateau potentials as long as 3 sec (Saito and Wu, 1991). Previous voltage-clamp studies detected even at room temperature a reduction in the Na current density in cultured *sei* neurons (O'Dowd and Aldrich, 1988). We did not detect such a difference in our giant neuron culture system (Saito and Wu, 1991), but found a significant increase in the persistent Na current at non-permissive temperature when compared with the wild-type control (Figs.A,B, test pulse = -10mV, Hp =-70mV). Q10 for the transient (INa,t) and persistent (INa,p) Na currents were determined. The Q10 for INa,p (but not INa,t) in *sei* neurons was significantly higher (Fig.C). Deak and Hall (1989) have shown that adult flies deficient in the *sei* locus, which produce no *sei* products, also display seizure behavior at high temperature. Therefore, lack of the *sei* product could lead to hyperexcitability. This raises the possibility that the *sei* gene encodes a regulatory component such as a β-subunit of Na channels rather than the pore-forming α-subunit of a subtype of Na channels.

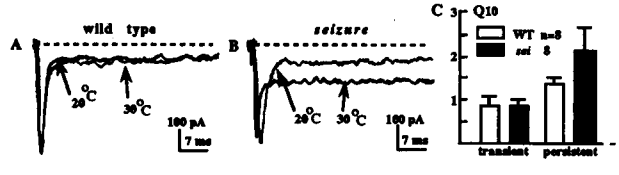

M-PM-B7

NH_2- and -COOH TAILS MEDIATE INDEPENDENTLY THE EFFECTS OF ANP ON Na^+ AND Ca^{2+} CHANNELS. ((L.A. Sorbera and M. Morad)) Department of Physiology, University of Peansylvania, Philadelphia, PA 19104-6085.

Figure 1. rat ANP1-28

Atrial natriuretic peptide (ANP) enhances the Ca^{2+} selectivity of the Na^+ channel (Sorbera & Morad, Science 247:969,1990; Sorbera & Morad, Science 252:449,1991). Here, the structure-function relation of the regulation of I_{Na} and I_{Ca} was examined in 20 ANP analogs (Genentech, Inc.). In whole cell clamped rat ventricular myocytes dialyzed with 10mM Na^+, ANP analogs were rapidly applied (>50ms) in solutions containing 10mM Na^+ to control I_{Na}. The effect of the analogs were compared to those of hANP1-28 and rANP1-28. Only those analogs with the amino terminal tail intact, hANF01 and hANF03, produced equivalent effects to the native ANP on the selectivity of the channel, i.e. enhanced the Na^+ channel current by 63.6 ± 8.3 % (n=8) and 94.0 ± 1.2 % (n=8) respectively, and shifted the reversal potential by 20-30 mV. hANF01, hANF03, rAPI, and rAPII which have deletions on the carboxylic terminal making them less effective guanylate cyclase activators, were ineffective in suppressing the Ca^{2+} channel, an effect reported to be mediated by cGMP (Gisbert & Fischmeister, Circ. Res. 62:660,1988; Sorbera & Morad, Science 247:969,1990). Urodilation of ANP (urodilatin) or oxidation of methionine on the ring of the ANP molecule also blocked the ANP effects on the Na^+ channel. hANP7-28, hANF06, h & rANP3-28, hANP4-28, hANP5-28, and rAPIII with deletions in the amino tail but with an intact carboxylic tail, suppressed only the Ca^{2+} channel by 14.1 ± 3.2 to 29.5 ± 5.8% (n=54). hANF09 with deleted carboxylic and amino tails but an intact S-S ring structure, failed to alter either the Na^+ or the Ca^{2+} channel. h & rANP8-15 which block ANP-C receptors, failed to alter the Ca^{2+} enhancing properties of ANP1-28 on the Na^+ channels. These results suggest that the SLRR amino tail (* in figure 1) is essential for enhancing the Ca^{2+} selectivity of the Na^+ channel, while the carboxylic tail is required for the I_{Ca} suppressing effect of the hormone. (Supported by NIH grant no. HL16152)

M-PM-B8

THE SODIUM CHANNEL β_1 SUBUNIT ALTERS GATING PROPERTIES OF A VARIETY OF SODIUM CHANNELS EXPRESSED IN *XENOPUS* OOCYTES. ((D.E. Patton, L.L. Isom*, W.A. Catterall* and A.L. Goldin)). Dept. of Microbiology & Molecular Genetics, U. California, Irvine, CA 92717 and *Dept. of Pharmacology, U. Washington, Seattle, WA 98195.

Rat brain sodium channels expressed in *Xenopus* oocytes by injection of α subunit RNA inactivate slowly compared to neuronal sodium channels examined *in vivo*. We have previously shown that co-expression of the rat brain β_1 subunit with the rat brain type IIA α subunit accelerates inactivation, shifts the voltage dependence of inactivation to more negative membrane potentials and increases the size of the peak sodium current (Isom et al., 1991, *Science* 256:839). These results have been extended to show that the β_1 subunit dramatically accelerates inactivation of the rat skeletal muscle sodium channel SkM1 when co-expressed in oocytes. Co-expression of β_1 also accelerates inactivation of the very slowly inactivating rat brain type III sodium channel, but to a much lesser extent. Only about a third of the current inactivates rapidly, even when the β_1 subunit is expressed at 5 times higher levels than that needed to result in fast inactivation of more than 90% of type IIA and SkM1 channels. In addition to its effects on inactivation, β_1 appears to speed up sodium channel activation. Co-expression of the β_1 subunit with a type IIA mutant sodium channel that completely lacks fast inactivation results in greatly accelerated activation kinetics, especially at more hyperpolarized potentials. The effects of the β_1 subunit on activation may be responsible for the fact that co-expression of the β_1 subunit with the rat III α subunit shifts the voltage dependence of both peak conductance and fast inactivation about 10 mV in the hyperpolarizing direction.

M-PM-B9

SODIUM CHANNEL ACTIVATION VALENCE REMAINS IDENTICAL IN BOTH PRIMARY AND SECONDARY ACTIVATION. ((M.D. Rayner, J.G. Starkus, and P.C. Ruben)) Bekesy Laboratory of Neurobiology, University of Hawaii, Honolulu, HI 96822.

In crayfish giant axons, brief (50 μs) returns to holding potential are followed by a "secondary" (2^o) activation process in which channels reactivate with kinetics faster than in the initial "primary" (1^o) activation step. After removal of fast inactivation with chloramine-T, and when both 1^o and 2^o voltage steps are to V_m >20 mV, only ~25% of total gating charge is required to first close and then reopen >90% of all sodium channels. Using a constant 1^o step and variable 2^o step, we have shown that the effective valences for both the 2^o ionic currents and 2^o charge movements are identical to those seen during 1^o activation (despite the ~75% reduction in total charge movement during 2^o activation). One interpretation of this surprising result is that, in both cases, the non-immobilizable component of gating charge alone determines the voltage dependence of channel activation. However, *full* closure of all channels during sodium tail currents requires *full* return of all gating charge (including the immobilizable component).This finding supports electrostatic coupling between the two components of gating charge, as suggested by Starkus and Rayner, *Biophys J.* 60:1101 (1992).

(Supported by PHS grants #NS-21151, #NS-29204, NIH RCMI grant #RR-03061 and American Heart Assoc. Hawaii Affiliate)

CALCIUM CHANNELS I

M-PM-C1

PERMEATION OF CALCIUM IONS THROUGH RECONSTITUTED L-TYPE CALCIUM CHANNELS INCREASES INACTIVATION RATES. ((R.L. Rosenberg and J.A. Haack)) Pharmacology, UNC-CH, Chapel Hill, NC 27599

Some L-type Ca channels reconstituted from cardiac sarcolemma into planar lipid bilayers show Ca-dependent inactivation by *global* increases in intracellular Ca^{2+} (Hirschberg et al. 1990, Soc. for Neurosci Abs 486.2). The rate of inactivation was determined from ensemble averages of single-channel recordings of (+)202-791-modified, cardiac L-type Ca channels incorporated in planar lipid bilayers. In order to determine if tightly *localized* increases in intracellular Ca^{2+} caused Ca-dependent inactivation, we studied the gating of Ca channels when the external, current-carrying, divalent cation was switched from [7.5 mM Ba^{2+}] to [7.5 mM Ba^{2+} +75 mM Ca^{2+}], and the internal solution contained 1 mM BAPTA. In 6/9 experiments, currents carried by [Ca^{2+} + Ba^{2+}] inactivated faster and more completely (bold-line ensemble average) than when the current through the same channel was carried exclusively by [Ba^{2+}] (fine-line ensemble average), even though 1 mM BAPTA was included in the intracellular chamber. These results indicate that the site of Ca-dependent inactivation is in the pore or close to the internal "mouth" of the Ca channel (cf. Imredy & Yue, 1992, Neuron 9, 197-207).

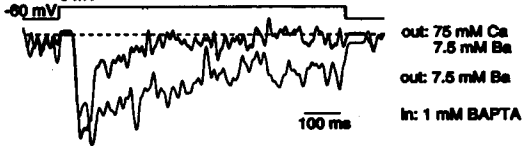

M-PM-C2

CLONING AND EXPRESSION OF A FOURTH NEURONAL CALCIUM CHANNEL BETA SUBUNIT.

Antonio Castellano, Xiangyang Wei, Lutz Birnbaumer, and Edward Perez-Reyes Department of Molecular Physiology & Biophysics, Baylor College of Medicine, Houston, Texas 77030.

Pharmacological and electrophysiological studies have demonstrated the existence of multiple types of voltage-dependent Ca^{+2} channels. Although several subunits of Ca^{+2} channels have been cloned, the subunit composition of these channels is not well known. Here we report the cloning, tissue distribution, and expression of a new brain β subunit, (β_4). Northern blot analysis indicates that β_4 is expressed almost exclusively in neuronal tissues, but also in kidney. Expression studies with β_4 indicate that it can interact with the cardiac muscle α_1, the skeletal muscle α_1, and with Ca^{+2} channels endogenous to the *Xenopus laevis* oocyte. β_4 modulation of α_1 activity is similar to the modulation induced by either β_1, β_2, or β_3. The most striking effect of β's is their ability to increase functional α_1 activity, which can be measured as either increased dihydropyridine binding to membranes from transiently transfected COS cells or increased Ca^{+2} channel activity in *Xenopus* oocytes. In addition, β_4 can modulate the following biophysical properties of the cardiac α_1 when coexpressed in *Xenopus* oocytes: it shifts the voltage dependence of activation to lower potentials, and it affects the kinetics of activation and inactivation.

M-PM-C3

ELECTROPHYSIOLOGICAL AND PHARMACOLOGICAL CHARACTERIZATION OF CLONED NEURONAL N AND L-TYPE CALCIUM CHANNELS. ((A. Stea, W.J. Tomlinson, S.J. Dubel and T.P. Snutch)) Biotechnology Laboratory, Univ. of British Columbia, Vancouver, B.C., Canada V6T 1Z3. (Spon. by M. White)

Molecular cloning studies have shown that at least five distinct classes of Ca^{2+} $\alpha 1$ subunits are expressed in the mammalian nervous system (classes A,B,C,D and E). Transient expression of the class B $\alpha 1$ subunit, rbB-I, in Xenopus oocytes resulted in whole-cell Ba^{2+} currents (up to 100 nA) recorded by 2-microelectrode voltage-clamp in a high Ba^{2+} recording solution. The rbB-I current activated slowly ($\tau \sim 65$ ms) and inactivated very little over 800 ms. From a holding potential of -100 mV the Ba^{2+} current had a threshold of activation at -30 mV and peaked at +20 mV. Half of the whole-cell Ba^{2+} current was inactivated at a holding potential of ~ -35 mV. The rbB-I current was completely blocked by 1 uM ω-conotoxin (CgTx) and was not affected by nifedipine (10 uM) or Bay K8644 (10 uM). Coexpression of rbB-I and a rat brain Ca^{2+} channel β subunit (Pragnell et al, FEBS Lett. 291:253-258) caused significant changes in the electrophysiological properties of the rbB-I induced current. The changes included: 1) an increase in the whole-cell Ba^{2+} current (up to 400 nA), 2) an increased rate of activation ($\tau \sim$ 35 ms), 3) a pronounced inactivation of the current over 800 ms, and 4) the channels were half-inactivated at a holding potential of ~ -60 mV compared with -35mV for rbB-I alone. The pharmacological properties of the current were not changed by the addition of the β subunit. Coexpression of the class C $\alpha 1$ subunit, rbC-II, with brain $\alpha 2$ and β subunits resulted in a whole-cell Ba^{2+} current characteristic of L-type Ca^{2+} channels. The current rapidly activated ($\tau \sim 4$ ms) and decayed very little over 800 ms. The rbC-II current was almost completely blocked by 10 uM nifedipine and was greatly enhanced (2-5 X) by Bay K8644. Addition of 2 uM CgTx had no discernible effect on the current.

A. Stea was the recipient of a NSERC of Canada postdoctoral fellowship.

M-PM-C4

MODULATION OF CARDIAC Ca^{2+}-CHANNEL α_1 SUBUNIT FUNCTION BY α_2 AND β SUBUNITS AS EXPRESSED IN MOUSE L CELLS. ((G. Varadi, P. Lory and A. Schwartz)) Department of Pharmacology & Cell Biophysics, University of Cincinnati, Cincinnati, OH 45267 (Sponsored by A. Matlib)

The voltage-dependent Ca^{2+} channel consists of α_1, α_2/δ, β and γ subunits. In the case of skeletal muscle, the β subunit has a profound modulatory role on α_1 function. The β subunit dramatically enhances the density of functional protein complex in the cell membrane as well as accelerates the kinetics of activation and inactivation. To study subunit modulation in the heart, the rabbit cardiac α_1 was expressed either alone or in combination with α_2 and β subunits in L cells. Functional properties of the α_1 subunit were studied using the patch-clamp technique and radioligand binding of calcium antagonists. We found that cotransfection of α_1 with α_2, β or both, elicited an increased higher current density and drug binding. The addition of β did not influence the activation kinetics; however, it caused a 3-4 fold faster inactivation of Ba^{2+} currents. Our data suggest that the primary role of the α_2 and β subunits in heart is to modulate the L-type current density. We also present several lines of evidence, using intracellular trypsin perfusion, that skeletal and cardiac α_1 subunits are differentially regulated by the β subunit.

This work was supported by NIH grants HL43231, HL22619 and by a Tanabe Seiyaku Fund.

M-PM-C5

MOLECULAR BASIS FOR DIHYDROPYRIDINE (DHP) TISSUE SPECIFICITY: SUBUNIT-DEPENDENT MODULATION OF RECOMBINANT CHANNEL ACTIVITY. ((A. Welling, Y.W. Kwan, F. Hofmann, and R.S. Kass)) Dept. Pharmakologie, Tech. Universitat Munchen, Munchen, Germany and Dept. Physiology, The University of Rochester, Rochester, NY.

We have investigated the modulation of native and recombinant calcium channel currents by the DHP nisoldipine using whole cell patch clamp procedures. Recombinant currents were expressed and measured in Chinese hamster ovary (CHO) cells stably transfected with the α_1 subunit of smooth muscle and cardiac L-type calcium channels, and native L-type currents were measured in guinea pig ventricular cells. In the absence of drug, native and recombinant α_1 channels share similar activation kinetics and voltage-dependencies. Ba^{2+} appears to be more permeant than Ca^{2+} in α_1 channels, and inactivation of recombinant channels is influenced by the permeant ion species. Inactivation, slow and voltage-dependent when Ba^{2+} is the charge carrier, is speeded when calcium carries the charge. Nisoldipine inhibits both cardiac and smooth muscle α_1 channel activity in a voltage-dependent manner: inhibition is more pronounced with depolarization. However smooth muscle α_1 channels are more sensitive to nisoldipine than native and cardiac α_1 channels: 1 nM nisoldipine causes voltage-dependent inhibition of smooth muscle α_1 channels but affects neither native nor cardiac α_1 L-channel activity. In addition, smooth muscle α_1 channels are inhibited by 10 nM nisoldipine at negative voltages (-80 mV) in contrast to native heart and cardiac $\alpha_1$channels which are unaffected at this voltage and drug concentration. Finally, at a fixed drug concentration and under identical voltage conditions, the onset of nisoldipine block of smooth muscle α_1 channels is significantly faster than either native heart or cardiac α_1 channels. We conclude that the α_1 subunit alone is sufficient to account for voltage-and Ca^{2+} dependent inactivation of L-channels as well as the voltage-dependent modulation of L-channels by DHP's. Additionally, our results show that structural differences in the cardiac and smooth muscle α_1 subunits contribute to the unique tissue specificity of DHP compounds.

M-PM-C6

MOLECULAR LOCALIZATION STUDIES OF THE DIHYDROPYRIDINE (DHP) BINDING SITE IN THE CARDIAC L-TYPE VOLTAGE DEPENDENT Ca^{2+} CHANNEL (L-VDCC) α_1 SUBUNIT REVEAL MOTIF IV S3 TO IV S6 AS ESSENTIAL ((S.Tang, A.Yatani, Y.Mori and A.Schwartz)) Department of Pharmacology and Cell Biophysics, University of Cincinnati, Cincinnati, OH 45267

DHP is an important modulator of the L-VDCCs. The DHPs bind to the α1 subunit of the L-VDCC and labeling studies have suggested several potential sites (Regulla et al,1991; Nakayama et al,1991). To molecularly identify the binding site(s) of DHPs, mutants of the cardiac L-VDCC α1 and cardiac L-type/brain P-type(DHP insensitive) chimera channels were constructed and expressed in Xenopus oocytes. The sensitivity to DHP agonist and antagonist were compared with those of the wild type cardiac α1 subunit expressed currents. Multi-point mutants in "E-F hand" and its flanking region (the region suggested by Regulla et al.) did not alter DHP sensitivity. A chimera in which the region from motif III SS2 to III S6 of the cardiac α1 (a region suggested by Nakayama et al.) was replaced with the corresponding region of the brain α1, showed no change in DHP sensitivity. On the other hand, coexpression of individual motif I and IV clones of the cardiac α1 subunit produced a DHP sensitive Ca^{2+} channel current, suggesting minimum channel structure requirement. A chimera in which the region from motif IV S3 to IV S6 of the cardiac α1 was replaced with the corresponding region of the brain α1, showed a loss of DHP sensitivity. These results suggest that the region from motif IV S3 to IV S6 is critical for DHP binding and functional effects.

M-PM-C7

EXTRACELLULAR LOCALISATION OF BENZOTHIAZEPINE/ BENZAZEPINE BINDING DOMAIN ON L-TYPE CALCIUM CHANNELS ((S.Hering,C.Strübing,M. Lakisch,J.Striessnig and H.Glossmann)) Institut für Biochemische Pharmakologie, A-6020, Innsbruck. (Spon. by J. Striessnig)

The action of the diltiazem-like Ca^{2+}-antagonists SQ32,910 and the corresponding membrane impermeable quaternary amine SQ32,428 were studied on whole cell barium currents (I_{Ba}) in A7r5 and BC3H1 cells to determine the sidedness of the benzothiazepine (BAZ) binding domain on L-type calcium channels. Both compounds competitively bind to the BAZ-binding domain of skeletal muscle Ca^{2+}-channels with K_i values of 1.3±0.2 μM and 8.9±1.1 nM, respectively. Externally applied SQ32,428 inhibited I_{Ba} dose-dependently with IC_{50}=21 μM in A7r5 cells and IC_{50}=24 μM in differentiated BC3H1 cells. Intracellular application of 100 μM SQ32,428 was without effect on I_{Ba} in both cell lines. Inhibition of I_{Ba} by SQ32,910 but not by SQ32,428 was dependent on Ca^{2+}-channel activation. Our results suggest an external localisation of the BAZ-binding domain within the α_1-subunit. The action of SQ32,910 is closely associated with the open conformational state of the L-type calcium channel.

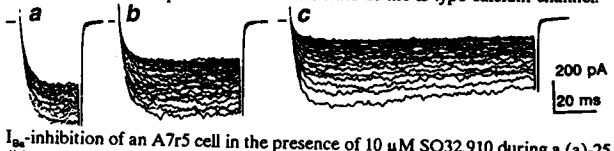

I_{Ba}-inhibition of an A7r5 cell in the presence of 10 μM SQ32,910 during a (a)-25-, (b)-50- or (c)-100-ms pulse train (1 Hz) from -60 mV to 10 mV.

M-PM-C8

SINGLE CHANNEL ANALYSIS OF NATIVE AND EXPRESSED SKELETAL MUSCLE CALCIUM CHANNELS. ((R.T. Dirksen*, T. Tanabe#, and K. Beam*)) *Department of Physiology, Colorado State University, Fort Collins, CO 80523. #HHMI, Yale University School of Medicine, New Haven, CT 06536.

Skeletal muscle dihydropyridine (DHP) receptors function both as calcium channels and as voltage sensors for excitation-contraction coupling. However, the lack of single channel data from intact skeletal muscle has limited our knowledge of the relationship between unitary channel activity and intracellular calcium release. We have measured native calcium channel activity from cultured mouse skeletal muscle in the presence of 110 mM $BaCl_2$ and Bay K8644 (5 μM). Under these conditions two distinct calcium channels, one of a lower (9.7 ± 1.3 pS, n=4) and one of a higher (14.1 ± 0.2 pS, n=9) conductance, are observed. The lower conductance channel resembles previously described T-type channels since it activates and inactivates quickly and is insensitive to DHP antagonists. The larger conductance channel (Top), which is L-type based on its sensitivity to DHP antagonists, produces an ensemble current similar to macroscopic slow L-type current previously recorded in muscle and has a maximum open probability of 0.19. This L-type current was not detected in dysgenic myotubes. However, dysgenic myotubes injected with a plasmid (pCAC6) encoding the skeletal muscle DHP receptor caused the emergence of a previously unseen high conductance (26.4 ± 0.6 pS, n=2) calcium channel (Bottom). Supported by NIH grant NS 24444.

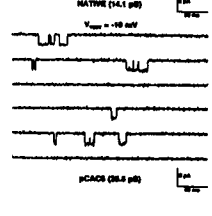

M-PM-C9

CA-PERMEABLE CHANNELS IN THE PLASMA MEMBRANE OF RAT MACROPHAGES. ((A.P. Naumov, Yu.A. Kuryshev, E.V. Kaznacheeva and G.N. Mozhayeva)) Institute of Cytology, Russian Academy of Sciences, 194064 St. Petersburg, Russia. (Spon. by B. Hille)

This study was undertaken to identify and characterize receptor-activated pathways for Ca^{2+} entry in rat macrophages. Patch clamp experiments have revealed channels permeable to di- and monovalent cations in the macrophage plasma membrane. The observed channel openings have at least three current (conductance) levels, with amplitude ratios of approximately 0.5:1.0:1.5. These three levels of openings seem to result from activity of the same channel type. The middle-level, unitary channel conductances are: 20, 19, 15, 11 and 17 pS in 105 mM $CaCl_2$, $SrCl_2$, $MnCl_2$, $BaCl_2$ and normal sodium solution, respectively. Conductances with 2 and 10 mM Ca^{2+} as the charge carrier are 10 and 14 pS, respectively. The channels are impermeable to Tris ions. In excised patches, such channel activity can be seen when nonhydrolyzable GTP analogues are added to the cytoplasmic side of the membrane. In the whole-cell configuration the same channels can be activated by addition of extracellular ATP. With 2 mM Ca^{2+} as the charge carrier, ATP evokes whole-cell currents ranging from several picoamperes to tens of picoamperes at -50 mV (mean peak value 20 pA). The data suggest that these channels constitute the main pathway for ATP-induced Ca^{2+} entry in macrophages.

MUSCLE PROTEINS

M-PM-D1

MUTANT ESSENTIAL LIGHT CHAIN EFFECTS ON CALCIUM BINDING AND REGULATION OF SCALLOP MYOSIN. ((S. Fromherz and A.G. Szent-Györgyi)) Brandeis Univ., Dept. of Biology, Waltham, MA. 02254.

The contribution of the essential light chain (ELC) to the high affinity Ca-binding site unique to molluscan myosins is being studied on reconstituted regulatory domains using mutants. Two point mutations in the EF hand-like loop of domain III, ser102met and asp94ala do not alter Ca binding. Further mutations and chimeric constructs between scallop and rat ventricular ELCs are being tested to identify sequences important for Ca binding. In order to determine the effect of these mutations on regulation simple conditions for the exchange of ELC on desensitized myosin have been developed. Two charge mutants have been constructed so that the efficiency of exchange can be monitored by urea gel electrophoresis to avoid the need of radioactive labelling (Ashiba et al. 1985 Biochem. 24:6618). One mutant has three positively charged amino acid substitutions at the N-terminus of the ELC; the other contains a short fusion of three negatively charged amino acids at the C-terminus. Both mutants exchange readily onto desensitized myosin at 40°C in the presence of 25% glycerol, 1 mM ATP and 2 mM EDTA without reducing ATPase activity. However, the extra charges on these mutants prevent rebinding of the regulatory light chain (RLC). Internal negatively charged mutants are being tested for exchange and RLC rebinding. Supported by NIH AR15963 and MDA.

M-PM-D2

SYNTHESIS OF THE MAJOR BODY WALL MUSCLE MYOSIN IN *C. ELEGANS* IS REGULATED BY THICK FILAMENT ORGANIZATION. ((G.E. White, C.M. Petry, and F.H. Schachat)) Department of Cell Biology, Duke University Medical School, Durham, North Carolina, 27710.

We are studying the relationship between thick filament protein expression and assembly of the body wall muscles of *C. elegans*. Focussing on strains which contain null mutations for either paramyosin or myosin B (the major body wall muscle myosin), we found that normal levels of myosin synthesis in *C. elegans* is dependent upon paramyosin expression. Quantitative densitometry of ^{35}S-labelled animals demonstrated that the paramyosin null synthesizes and accumulates significantly less myosin heavy chain than the wild type. In contrast, the myosin B null strain shows reduced myosin heavy chain synthesis and accumulation, but paramyosin synthesis is not affected. Missense paramyosin mutants also had reduced myosin synthesis, thereby demonstrating that the inability to form a proper thick filament core directly affects myosin synthesis. Analysis of myosin heavy chain expression in the paramyosin mutants revealed that only myosin B is affected. These results are most easily explained in terms of what is known about thick filament assembly in *C. elegans* whereby the minor myosin A and paramyosin form part of the nascent thick filament core first, with myosin B then added at the end. Thus, paramyosin mutations could affect myosin B but not myosin A while myosin B mutations would not affect paramyosin. Our observations demonstrate a strong relationship between the synthesis of myosin B and its incorporation into the thick filament and indicate that the thick filament can regulate the expression of its constituent proteins.

M-PM-D3

SKELETAL MUSCLE MYOSIN LIGHT CHAINS ARE ESSENTIAL FOR MOVEMENT. ((S. Lowey, G.S. Waller and K.M. Trybus)) Rosenstiel Research Center, Brandeis University, Waltham, MA 02254.

Myosin consists of two different light chains (LC) associated with each of two myosin heavy chains (MHC). The regulatory light chain (LC2) is wrapped around the head/rod junction, whereas the alkali light chain (ALC) is distal to LC2 in the neck region of the myosin head (S1) (Katoh & Lowey, 1989). The role of the LCs in vertebrate skeletal muscle myosin has remained obscure, since their removal from S1 does not significantly alter its actin-activated ATPase activity (Wagner & Giniger, 1981; Sivaramakrishnan & Burke, 1982). Here we have prepared MHCs which are free of both LCs in order to determine whether the LCs affect movement in an in vitro motility assay. LC-free myosin was adsorbed directly onto nitrocellulose-coated coverslips, or bound first to an anti-rod antibody, and the velocity of fluorescently labeled actin filaments was measured by video-enhanced light microscopy. We find that the loss of the LCs reduced the rate of filament movement from 8.5 μm/s to 0.8 μm/s, without significantly decreasing the ATPase activity. Reconstitution of myosin with either LC2 or ALC increased filament velocity to 1.5 μm/s and 2.5 μm/s, respectively. Readdition of both classes of LCs fully restored the myosin-directed movement to its original value. These results suggest that although the light chains may not be essential for enzymatic activity, light chain/heavy chain interactions are essential for the conversion of chemical energy into movement.

M-PM-D4

THE SEQUENCE LOCATION OF SUBSTRATE-BOUND Mg^{2+} IN MYOSIN. ((K. Ue and M.F. Morales)), U. Pacific, San Francisco.

By using a strategy similar to that which we employed in finding the tightly-held Ca^{2+} in actin [Ue, et al, 1992] we have attempted to find the location of Mg^{2+} in its complex with myosin and substrate. The tactic was to substitute for Mg^{2+} the redox metal ion Mn^{2+} (which can be shown to be effective in co-catalyzing ATPase) into the (S-1)-nucleotide complex in which the metal ion is pPDM-"trapped" [Wells & Yount (1982)] It has been shown [Berlett, et al. (1990)] that at neutral pH, in the presence of HCO_3^-, this metal ion in the presence of H_2O_2 will catalyze the oxidation of amino acid residues of proteins, thereby introducing new carbonyl groups; also [Levine, et al.(1990)] such groups can be reduced back with radioactive $NaBH_4$, at the same time labelling the affected groups. After application of this treatment to S-1 we have found that the radioactivity is confined to the 20 kDa segment of the S-1 heavy chain, more specifically to the "P-10" CNBr piece [Elzinga, M. & Collins, J.H. (1977)] of 20 kDa. We have trypsin-digested the radioactive P-10 and found that the radioactivity is mainly associated with peptide 715-721, especially Leu-716. From homology arguments Burke, et al. (1990) suggested that Asp-719, anchors the metal ion that is, in turn, chelated by the polyphosphate of the bound nucleotide. Our result experimentally confirms their expectation. Since many points in bound nucleotide are associated with either the 25 kDa or 50 kDa segments of heavy chain) bound nucleotide provides an intersegmental mechanical connection sure to be disturbed by substrate hydrolysis. Research supported by R37 HL-44200, NSF DMB-9003692, and assisted by a Fogarty Scholarship-in-Residence to M.F.M.

M-PM-D5

ANALYSIS OF THE ROLE OF MYOSIN REGULATORY LIGHT (MRLC) CHAIN PHOSPHORYLATION IN *DROSOPHILA MELANOGASTER*. **((R. Tohtong, M. Graham, R. Schaaf*, J. Hurley*, A. Simcox and D. Maughan*)) Department of Molecular Genetics, Ohio State University, Columbus, OH 43210 and *Department of Physiology and Biophysics, University of Vermont, Burlington, VT 05405.**

Drosophila muscle-specific MRLC is phosphorylated at Ser66 and Ser67. These residues align with the conserved phosphorylation sites of vertebrate MRLCs which are important for regulation of contraction. We assessed the significance of phosphorylation at these residues in the striated indirect flight muscle (IFM) by germline transformation of mutant MRLC genes in which Ser66 and Ser67 were changed to Ala. IFM ultra structure of transformants appears to be normal, indicating that phosphorylation at Ser66 and Ser67 is not required for viability and normal myofibrillogenesis. However, flies with two copies of the mutant gene (in which the only source of MRLC is the mutant form) do not fly. These flies have markedly reduced ability to beat their wings coupled with a severely attenuated stretch activation response and power output of their IFM (isolated, calcium-activated skinned fibers). These results indicate that phosphorylation of MRLC is important for normal flight muscle function in *Drosophila*, a feature more generally associated with smooth muscle than striated muscle. **Supported by NIH AR40234.**

M-PM-D6

POLARIZATION OF FLUORESCENTLY LABELED ACTIN FILAMENTS DURING MOTION IN *IN VITRO* MOTILITY ASSAY.

((S. Burlacu and J. Borejdo)) Baylor Research Institute, Baylor University Medical Center, 3812 Elm St., Dallas, TX 75226.

We have used video microscopy to measure the orientation of actin filaments during motion in in vitro motility assay. F-actin was labeled with rhodamine-phalloidin. The image of horizontally translating filaments was split into two orthogonally polarized components. The relative intensity of the two components obtained when filaments were excited with vertically polarized light was used to calculate polarization of fluorescence of the dye, i.e. the orientation of the absorption dipole of rhodamine with respect to filament axis. The orientation was different when filaments were stationary and when they were moving. The results of 54 experiments obtained when filaments were stationary are plotted in the figure (filled circles). The data is plotted in histogram form, i.e. polarization is plotted vs. the percentage of measurements which gave the particular value of polarization. The results of 25 experiments obtained when filaments were moving are plotted as open circles. There was a difference in both the shape of histograms and in the means. The 0.081 difference in means was statistically highly significant t=2.8 ($P=6x10^{-3}$). These results suggest that interactions between actin and myosin result in tranformation of polymer structure of actin. Supported by NIH.

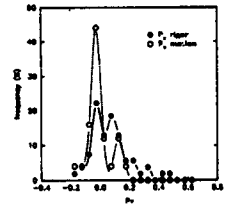

M-PM-D7

DEVELOPMENTAL STUDIES ON MOUSE CARDIAC TnI EXPRESSION.

((Ren Zhang and James D. Potter)), Department of Molecular and Cellular Pharmacology, University of Miami School of Medicine, Miami, Fl 33101

Troponin I (TnI), the inhibitory subunit of the Troponin complex, has three isoforms; fast and slow skeletal and cardiac. One of the important properties of cardiac TnI is that it contains 26-33 extra amino acids in its N-terminus, as well as two serines which can be phosphorylated by protein kinase A. When phosphorylated they may increase the rate of relaxation of the heart which results from beta-agonist stimulation. Biochemical studies have suggested that skeletal TnI may be expressed in the immature heart. We have isolated a mouse cDNA clone of cardiac TnI by screening a mouse cardiac cDNA library, and a rat cDNA clone of slow skeletal TnI using PCR, in which the primer sequences were derived from the published rat slow skeletal cDNA sequence. This rat slow skeletal muscle TnI (SMTnI) cDNA could detect mouse SMTnI RNA on Northern blots. These cDNA clones were used to study mouse cardiac development using Northern blots. Total RNA fractions were isolated from embryonic, postnatal and adult mouse heart. The Northern blot data showed that slow skeletal TnI was the major form in the early stage of cardiac development, being gradually replaced by cardiac TnI during development and disappearing in the adult mouse heart. The transition from slow skeletal TnI to cardiac TnI during development may be responsible for the observed functional differences between fetal and adult heart. (Supported by NIH HL42325).

M-PM-D8

CALCIUM PLAYS DISTINCTIVE STRUCTURAL ROLES IN THE N- AND C-TERMINAL DOMAINS OF CARDIAC TROPONIN C.

((G. A. Krudy, R. M. M. Brito, J. C. Negele, J. A. Putkey and P. R. Rosevear)) Dept. of Biochemistry, Univ. of Texas Medical School at Houston, Houston, Texas 77225.

Multi-dimensional NMR techniques and isotope labeling were used to compare the structural consequences of Ca^{2+} binding to both the low and high affinity Ca^{2+} binding sites in recombinant cardiac troponin C (cTnC3). In the absence of Ca^{2+}, the short β- sheet located between the high affinity Ca^{2+}/Mg^{2+} binding sites in the C- terminal domain was found to be absent or loosely formed as judged by the inter-residue NOEs and chemical shifts of residues in the Ca^{2+} binding loops. In contrast, the N- terminal domain β- sheet located between site II and the naturally inactive site I was present even in the absence of bound Ca^{2+}. NMR studies on apo- cTnC suggest that in the absence of bound Ca^{2+} the C-terminal domain hydrophobic cluster is mobile and loosely formed. Calcium binding mutant proteins having either an inactive Ca^{2+} binding site III (CBM-III) or an inactive Ca^{2+} binding site IV (CBM-IV) were used to further study the structural consequences of Ca^{2+} binding to each of the high affinity sites located in the C-terminal domain. Only a single active Ca^{2+} binding site was found necessary for formation of the short β- sheet between Ca^{2+} binding sites III and IV. The absence of bound Ca^{2+} at site III was found to produce greater instability in the C- terminal domain as judged from the mobility of the aromatic hydrophobic cluster within this domain. These results are consistent with a preformed hydrophobic core in the absence of Ca^{2+} in the N-terminal domain, but in the absence of Ca^{2+} a less stable or poorly formed hydrophobic core in the C-terminal domain. Thus, Ca^{2+} binding plays distinctive structural roles in the N- and C- terminal domains of cTnC.

M-PM-D9

ELECTRON PARAMAGNETIC RESONANCE SPECTROSCOPY OF TROPONIN-C AND MYOSIN LIGHT CHAIN 2.

((G.J. Wilson, W. Huang, D.R. Brown & B.D. Hambly)), Dept. of Pathology, The University of Sydney, N.S.W., 2006, Australia.

Skeletal muscle troponin-C (TnC) has 2 high specificity Ca^{2+}-binding sites in the N-terminal domain and 2 low specifity (Ca^{2+}- or Mg^{2+}-binding) sites in the C-terminal domain. Myosin light chain 2 (LC2) has only one Ca^{2+}- or Mg^{2+}-binding site in the N-terminal domain. Using electron paramagnetic resonance (EPR) spectroscopy we have studied TnC and LC2 when different ligands were bound. TnC from rabbit skeletal muscle was labelled using spin labelled maleimide (MSL) at cys-98. EPR spectra of labelled TnC showed that when Ca^{2+} or Mg^{2+} bound to TnC, the mobility of the MSL probe was reduced, with Ca^{2+} having the greater effect (see also Potter et al. (1976), J. Biol. Chem., 251:7551). The phenothiazine drug, trifluoperazine (TFP), produced a similar effect when bound to labelled TnC. Similar experiments in which expressed myosin light chain 2 (compliments of Dr F. Reinach) was specifically labelled at cys-125 using spin labelled fluorodinitroanaline (SL-FDNA) showed that ligand binding did not significantly affect SL-FDNA mobility.

The binding of divalent cations to TnC has physiological importance, being responsible both for the Ca^{2+}-activation of muscle contraction (N-terminal sites) and the stabilization of TnC in the contractile apparatus.(C-terminal sites) Thus a conformational change would be expected when these cations bind. TFP could bind to sites on the Ca^{2+}-binding proteins which are close to either the N- or the C-terminal domains (Strynadka & James (1988), Proteins 3:1). Thus changes in TnC conformation in solution could be responsible for the changes in the EPR spectra obtained upon TFP binding. The binding of TFP to myofibrillar proteins including TnC in skinned muscle fibres also affects Ca^{2+}-activation properties, indicating an effect upon Ca^{2+}-binding in physiological preparations (Kurebayashi & Ogawa (1988), J. Physiol., 403:407). Our results show that TFP can have an effect upon the structure of TnC in solution which is consistent with it affecting fibre physiological properties. The lack of an effect of ligands upon LC2 labelled with SL-FDNA is consistent with the unclear physiological role of Ca^{2+}- or Mg^{2+}-binding to the single site on LC2.

Supported by NH&MRC Australia and Faculty of Medicine, The University of Sydney.

M-PM-E1

ENRICHMENT OF INOSITOL 1,4,5-TRISPHOSPHATE BINDING IN INTERCALATED DISKS OF CARDIOMYOCYTES.

((Yoshiyuki Kijima, Akitsugu Saito, and Sidney Fleischer)) Dept. of Molecular Biology, Vanderbilt University, Nashville TN 37235

The IP_3 and ryanodine receptors have been immunolocalized in rat cardiomyocytes, at the region of intercalated disks and at the I-band of sarcomere, respectively (Kijima et al. *Circulation* 1992 abstract). In this study, binding of [^{3}H]IP_3 and [^{3}H]ryanodine was measured to cardiac subcellular fractions including longitudinal sarcoplasmic reticulum (SR), junctional SR, sarcolemma, mitochondria, and intercalated disks. The latter fraction was enriched in structures of intercalated disks as viewed by electron microscopy. The fraction displays enrichment of IP_3 binding (9.4 pmol/mg using 10 nM of ligand) v.s. < 0.2 pmol/mg in other fractions. By contrast, ryanodine binding (60 nM of ligand) was highest in junctional SR (3.3 pmol/mg). These results support our previous immuno-histochemistry, i.e. the different intracellular localization of the IP_3 and ryanodine receptors in cardiomyocytes. [New Investigatorship of AHA Florida-Affil. to Y.K; NIH-HL32711 and PO1-HL46681 to S.F.]

M-PM-E2

ISOLATION AND CHARACTERIZATION OF A CARDIAC K^+ CHANNEL MODULATED BY INOSITOL POLYPHOSPHATES (IPx).

((Yoshiyuki Kijima[#], Martin Mayrleitner[#*], Anthony P. Timerman[#], Hansgeorg Schindler[*], and Sidney Fleischer[#])) [#]Dept. of Molecular Biology, Vanderbilt University, Nashville TN 37235, and [*]Institute for Biophysics, Johannes Kepler University of Linz, Linz, Austria.

Two types of inositol 1,4,5-trisphosphate (IP_3) binding have been reported in cardiac microsomes (Kijima and Fleischer. *Biophys. J.* 61:A423, 1992). The high affinity IP_3 binding is similar to the "classical" IP_3 receptor with regard to molecular size and K_d. The low affinity IP_3 binding suggests the presence of an IP_x receptor in heart. In this study, an IP_x-modulated K^+ channel has been isolated from dog cardiac microsomes. The channel activity in planar bilayers shows permeability ratios $P_K/P_{Cl} \sim 16$ and $P_K/P_{Na} \sim 3$. It is blocked by IP_3 and inositol 1,3,4,5-tetrakisphosphate (IP_4) and by $CaCl_2$ in [mM] range. The channel shows several sub-conductance states. The channel protein is a hetero-oligomer with similar subunit composition as the cerebellar IP_x receptor (Chadwick et al. *J. Biol. Chem.* 267:3473, 1992). In summary, we find a K^+ channel in cardiac microsomes which is modulated by both IP_3 and IP_4. Therefore, its characteristics are somewhat different from those of the cerebellar IP_x receptor. [New Investigatorship of AHA Florida-Affil. to Y.K., NIH-HL32711 to S.F., and S45/07 of Austrian Res. Fonds to H.S.]

M-PM-E3

DEPOLARIZATION-INDUCED CALCIUM RELEASE FROM SR IN VITRO: ITS DEPENDENCE ON THE MAGNITUDE OF T-TUBULE DEPOLARIZATION, $[Ca^{2+}]$, AND $\Delta[Ca^{2+}]$.

((N. Ikemoto, and B. Antoniu)) Boston Biomed. Res. Inst. and Dept. Neurol. Harvard Med. Sch., Boston, MA 02114

Rapid SR Ca^{2+} release induced by double ionic replacement of triad vesicles mimicks some properties of e-c coupling in vivo. In order to let this in vitro system serve as a physiological model of e-c coupling, however, several important questions remain to be investigated; e.g. how the kinetics of the induced Ca^{2+} release change with the magnitude of T-tubule depolarization (TtDep) and with $[Ca^{2+}]$, etc. A newly devised stopped-flow technique with fluorescent Ca^{2+} probes (fluo-3 for $[Ca^{2+}] \leq 1$ μM, calcium green-5N for $[Ca^{2+}] \geq 1$ μM) permitted us to create various magnitudes of TtDep by changing the K_o/K_i ($=Cl_i/Cl_o$) ratio used for the ionic replacement from 1 up to 10 [o and i: the extra-cellular and cytoplasmic sides of T-tubules, respectively]. Increase in the magnitude of TtDep led to a sharp increase in (1) the amount of Ca^{2+} released in the fast phase, (2) the initial Ca^{2+} release rate, and (3) the rate of inactivation. TtDep-induced Ca^{2+} release was triggered at various $[Ca^{2+}]$s (0.1-5.0 μM) weakly or strongly buffered with EGTA-Ca. The fast phase of Ca^{2+} release was activated at sub-μM Ca^{2+} and leveled off at 1-2 μM, while the slow phase was activated at $[Ca^{2+}] \geq 1$ μM only when a sufficient degree of $\Delta[Ca^{2+}]$(↑) was allowed. (Supported by grants from NIH and MDA).

M-PM-E4

CYCLIC AMP PHOSPHODIESTERASES ASSOCIATED WITH MICROSOMAL SR MEMBRANES IN STRIATED MUSCLES.

((E. Rousseau, A. Eckly, C. Beaudry and C. Lugnier.)) Dept. of Physiology, Univ. of Sherbrooke, Quebec, Canada and CNRS URA 600, Université de Strasbourg, Illkirch, France.

It was proposed that a cAMP phosphodiesterase sensitive to indolidan, PDE III, was associated to SR membranes. However this PDE and other isoforms were not characterized across the spectrum of the striated muscle microsomal fractions separated on sucrose gradient. The distribution of PDE forms were analyzed by their hydrolytic activities, drug sensitivities and binding studies. Two PDE forms were identified in cardiac fractions. The major form, PDE III, was associated with junctional face membranes (FIII). Since these membranes are directly involved in controlling excitation-contraction coupling, such PDE location enhances the physiological relevance to study their implication in regulating cardiac contraction. However PDE III was absent from skeletal fractions. In both tissues PDE IV (Rolipram-sensitive) is mostly associated with the FII fraction enriched in sarcolemmal membranes. It is concluded that both forms could modulate Ca^{2+} movements in cardiac and only PDE IV in skeletal muscles. However, no PDE activity was associated with the purified ryanodine-receptor despite reports claiming the direct interaction of PDE inhibitors with the Ca^{2+} release channel. E.R. is scholar from HSFC. Supported by an MRC grant: MT 10326.

M-PM-E5

THE SARCOPLASMIC RETICULUM Ca-ATPase HAS LUMENAL Ca^{2+} SITES THAT DO NOT CHANGE THE DISSOCIATION RATES OF Ca^{2+} AND Mg^{2+} FROM CYTOPLASMIC SITES.

((J. Myung and W.P. Jencks))Graduate Department of Biochemistry, Brandeis University, Waltham, MA 02254.

The equilibrium concentration of EP formed from the SR ATPase in the presence of Pi, Mg^{2+} & EGTA with vesicles loaded with 0-60 mM $[Ca^{2+}]$ increases with increasing $[Ca]_{in}$, and then levels off at different maximal values with different $[Mg^{2+}]$. This dependence on $[Ca]_{in}$ of the concentration of EP formed from Pi & Mg^{2+} can be accounted for by the binding of lumenal Ca^{2+} to nonphosphorylated as well as to phosphorylated enzyme; it is not consistent with the binding of Ca_{in} only to EP.

The phosphorylation of $^{E}E_{Ca_2}$ by ATP with SRV loaded with 0 or 40 mM $[Ca^{2+}]$ proceeds with $k_{obsd} = 310\ s^{-1}$ in the presence of EGTA and with $k_{obsd} = 360\ s^{-1}$ in the presence of EDTA. The observed rate constants represent the sum of the rate constants for phosphorylation($k_p = 220\ s^{-1}$) and irreversible dissociation of Ca^{2+}(k_{Ca}) in the presence of EGTA, and for phosphorylation(k_p), irreversible dissociation of Ca^{2+}(k_{Ca}) and Mg^{2+}(k_{Mg}) in the presence of EDTA. The value of $k_{obsd} = 310\ s^{-1}$ gives $k_{Ca} = 310 - 220 = 90\ s^{-1}$ and the value of $k_{obsd} = 360\ s^{-1}$ gives $k_{Mg} = 360 - 220 - 90 = 50\ s^{-1}$ for both SRV loaded with 0 or 40 mM $[Ca^{2+}]$. The presence of Ca_{in} does not change the dissociation rates of Mg^{2+} and Ca^{2+}.

M-PM-E6

RATIOS OF PHOSPHOLAMBAN TO Ca^{2+}-TRANSPORTING ATPase AND PHOSPHOLAMBAN-MODULATED STIMULATION OF Ca^{2+} TRANSPORT IN STRIATED MUSCLE SARCOPLASMIC RETICULUM.

((M. A. Movsesian, G. Morris, J. Wang and J. Krall)) Veterans Affairs Medical Center & University of Utah School of Medicine, Salt Lake City, Utah and University of Calgary, Calgary, Alberta.

Levels of phospholamban (quantified immunochemically and by measurement of phosphorylation by cAMP-dependent protein kinase), Ca^{2+}-transporting ATPase (quantifiifed by measurement of Ca^{2+}-dependent, acid-stable phosphoenzyme intermediate) and phospholamban-modulated stimulation of Ca^{2+} transport (quantified by measurement of ATP-dependent, oxalate-supported Ca^{2+} accumulation in the absence and presence of cAMP-dependent protein kinase and anti-phospholamban monoclonal antibody) were compared in sarcoplasmic reticulum-enriched microsomes prepared from cardiac (rabbit and canine heart), slow twitch (rabbit soleus and canine flexor digitorum superficialis) and fast twitch (rabbit lumbodorsalis) skeletal muscle. Phospholamban was absent from fast twitch skeletal muscle and present at comparable levels in cardiac and slow twitch skeletal muscle, but ratios of phospholamban to Ca^{2+}-transporting ATPase in slow twitch skeletal muscle were less than half those in cardiac muscle, and phospholamban-modulated stimulation of Ca^{2+} transport was observed only in cardiac muscle preparations. These results indicate that phospholamban, while present in both cardiac and slow twitch skeletal muscle, may modulate sarcoplasmic reticulum Ca^{2+} transport only in the former, and that the lack of phospholamban-modulated stimulation of Ca^{2+}-transport in slow twitch skeletal muscle sarcoplasmic reticulum may reflect the lower ratios of phospholamban to Ca^{2+}-transporting ATPase in this tissue.

M-PM-E7

KINETICS OF ACTIVATION OF CALCIUM RELEASE CHANNELS BY IMPERATOXIN A, A POLYPEPTIDE TOXIN FROM THE SCORPION Pandinus imperator. ((Roque El-Hayek[1], Roberto Coronado[1] and Hector H. Valdivia[1,2])). Department of Physiology, University of Wisconsin Medical School[1] and University of Maryland Medical School[2].

Imperatoxin A ($IpTx_A$) is a polypeptide toxin of Mr 8,500 that specifically activates the ryanodine receptor/Ca release channel of sarcoplasmic reticulum (Valdivia et al PNAS, in press). $IpTx_A$ displays an exquisite selectivity for the skeletal isoform of the ryanodine receptor, enhancing the binding of [^{3}H]ryanodine to skeletal SR with an ED_{50} = 6 nM, but having no effect on cardiac SR or brain microsomes. The agonist effect of $IpTx_A$ is also seen in CHAPS-solubilized and purified ryanodine receptors, indicating a direct toxin-receptor interaction. Similar to the effect of caffeine and ATP, the Scatchard analysis shows that $IpTx_A$ increases K_D without significantly altering B_{MAX} values, suggesting a competitive interaction with the [^{3}H]ryanodine binding site. Unlike ATP, which activates binding at all [Ca^{2+}], $IpTx_A$ selectively enhances the Ca^{2+}-dependence of [^{3}H]ryanodine binding curve at low [Ca^{2+}]. This effect is synergistic with the effect of the alkaloids caffeine and doxorubicin, which also activate receptors at low [Ca^{2+}] only. This suggests a positive cooperative interaction between the toxin and the alkaloid binding sites. Ryanodine receptors reconstituted in planar lipid bilayers in the absence of ryanodine are reversibly activated by nanomolar concentrations of $IpTx_A$. The increase in [^{3}H]ryanodine binding by the toxin may therefore arise from recruitment of receptors in the open conformational state, to which [^{3}H]ryanodine binds with high affinity. The peptidic nature, selectivity, reversibility and potency make $IpTx_A$ an ideal tool to identify the structural domains of the skeletal ryanodine receptor involved in channel gating. (Supported by NIH and AHA).

M-PM-E8

CALMODULIN-DEPENDENT PHOSPHORYLATION OF THE CARDIAC SR CALCIUM CHANNEL INHIBITS CALMODULIN BINDING. ((G.M. Strasburg, M.M. Reedy, L.J. Wang, and L.R. Jones)) Michigan State University and Indiana University.

Calmodulin (CaM)-dependent kinase phosphorylation of the cardiac sarcoplasmic reticulum (SR) Ca channel protein results in increased Ca channel open state probability, and reversal of the inhibitory effect of CaM [Witcher et al., J. Biol. Chem. 266:11144 (1991)]. In these studies we have tested the hypothesis that phosphorylation of the channel protein by the CaM dependent kinase inhibits CaM binding. Wheat germ CaM was labeled with rhodamine-maleimide and binding of CaM to non-phosphorylated or phosphorylated cardiac SR vesicles was determined by fluorescence anisotropy. Binding of CaM to the channel protein in non-phosphorylated SR vesicles was consistent with two classes of sites. CaM bound to the higher affinity class of sites with a K_{d1} of 13 nM and a B_{max1} of 55 pmol/mg. Based on ryanodine-binding activity of 5 pmol/mg of the SR, these data are consistent with approximately 3 high affinity CaM binding sites per channel protein subunit. When the vesicles were phosphorylated before CaM binding experiments, the K_{d1} was 6 nM and B_{max1} was 18 pmol/mg, suggesting there was now only one high affinity CaM bound per subunit. Preliminary data indicate that phosphorylation by the cAMP-dependent protein kinase has no effect on CaM binding. These data suggest that one mechanism by which CaM-dependent phosphorylation alters channel protein function is through inhibition of CaM binding.

M-PM-E9

EFFECT OF RYANODINE ON Ca^{2+} ACCUMULATION RATE AND CAPACITY IN CANINE AND HUMAN MYOCARDIAL SARCOPLASMIC RETICULUM. ((L. R. Nimer, J. Krall and M. A. Movsesian)) Veterans Affairs Medical Center and University of Utah School of Medicine, Salt Lake City, UT 84148 (sponsored by R. Straight)

Inhibition of Ca^{2+} efflux through the junctional Ca^{2+} channel of the sarcoplasmic reticulum by ryanodine results in an apparent stimulation of Ca^{2+} accumulation in mammalian myocardial sarcoplasmic reticulum. The degree of this stimulation presumably reflects the functional ratio of ryanodine-sensitive Ca^{2+} channels to Ca^{2+}-transporting ATPase molecules. We compared the effects of ryanodine on ATP-dependent, oxalate-supported Ca^{2+} accumulation rates and capacities in sarcoplasmic reticulum-enriched microsomes prepared by homogenization and differential sedimentation of canine and human left ventricular myocardium. Incubation with 0.5 mM ryanodine increased the initial rate of Ca^{2+} accumulation (measured at 10 μM Ca^{2+}, 5 mM ATP, 5 mM oxalate, pH 7.05, 30° C) 70 $\pm$ 3 % in canine myocardial sarcoplasmic reticulum, but only 12 $\pm$ 4 % in human myocardial sarcoplasmic reticulum. In contrast, incubation with 0.5 mM ryanodine increased Ca^{2+} capacity (measured at 37° C) 121 $\pm$ 3 % in canine myocardial sarcoplasmic reticulum and 37 $\pm$ 7 % in human myocardial sarcoplasmic reticulum. These data demonstrate that Ca^{2+} capacity is more sensitive than initial rate of oxalate-supported, ATP-dependent Ca^{2+} accumulation as a measure of ryanodine-sensitive junctional Ca^{2+} channel activity, and suggest that the functional ratio of Ca^{2+} channels to Ca^{2+}-transporting ATPase molecules is significantly higher in canine than in human myocardial sarcoplasmic reticulum.

NUCLEIC ACID STRUCTURES

M-PM-F1

MANIPULATION OF SINGLE DNA MOLECULES BY LASER TRAPPING MICROSCOPY. ((S.J. Kron, J.V. Graham, S. Chu and P. Matsudaira)) Whitehead Institute, Cambridge MA 02142 and Dept. of Physics, Stanford U., Stanford CA 94305. (Spon. by C.O. Pabo)

We have installed a single beam laser optical trap (optical tweezer) on a fluorescence microscope to create a prototype laser trapping microscope. Optical tweezers use the "gradient force" due to momentum of refracted light to hold particles at the focus point of a laser beam. With latex particle handles attached to its ends, we can 1) capture one end of a single DNA molecule in solution, 2) tether this end to the glass by "welding" with the laser beam, and 3) capture the free end and move it to any position on the microscope slide, as diagrammed below. When fluorescently stained, the DNA molecule held by the optical tweezer can be imaged in real time. If the laser is blocked, the DNA relaxes to a coil, allowing measurement of dynamic properties of single DNA molecules.

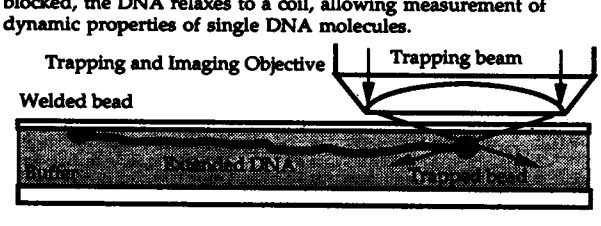

M-PM-F2

PROBE FORCE AND SPATIAL RESOLUTION IN AFM OF DNA ((Jie Yang and Zhifeng Shao)) Bio-SPM Laboratory and Department of Physiology, University of Virginia, Box 449, Charlottesville, VA 22908

Recently, several methods have been used to image DNA by AFM with reproducible results [1]. However, the condition for high resolution has not been optimized. In imaging double stranded DNA (both circular and linear), we found that the probe force is critically important for high resolution. As much as an order of magnitude improvement in resolution can be found. Using the cytochrome C spreading method developed for electron microscopy, the condition of carbon coating is crucial for reducing the interaction between the probe and the substrate, a critical factor for stable imaging. This preparation is not only suitable for AFM in air, but also stable in several organic solvents such as propanol, butanol, heptanol and octanol, where the probe force can be reduced to below 1 nN. For both in air and in solution operation, when the probe force was below 3 nN, we routinely obtained a resolution of about 3 nm with commercially available pyramid Si_3N_4 cantilevers (k = 0.06 N/m). These results seem to indicate that probe force is more critical than the tip geometry for these soft specimens, at least at the nm resolution level. Supported by the Whitaker Foundation, the US Army Research Office, NIH, and the Jeffress Trust.

[1] Yang, J., Takeyasu, K. and Shao, Z. (1992) FEBS Letters 301:173-176; Lyubchenko, Y.L. et al., (1992) Biophys. J. 61:A149; Bustamante, C. et al., (1992) Biochemistry 31:22-26; Hansma, H.G. et al. (1992) Science 256:1180-1184; Zenhausern, F. et al., (1992) J. Struct. Biol. 108:69-73.

M-PM-F3

A SOUTION STRUCTURE OF A COMPLEX OF [N-MeCys^3, N-MeCys^7] TANDEM AND [d(GATATC)]$_2$. Kenneth J. Addess, Janet S. Sinsheimer#, and Juli Feigon. Department of Chemistry and Biochemistry, the Molecular Biology Institute, and the #Department of Biomathematics, School of Medicine, University of California, Los Angeles, CA 90024.

[N-MeCys^3, N-MeCys^7] TANDEM (CysMeTANDEM), an undermethylated analogue of triostin A, is an octadepsipeptide quinoxaline antibiotic that binds specifically by bisintercalation to double-stranded DNA at NTAN sites, in contrast to triostin A, which binds specifically to double stranded DNA at NCGN sites. We have determined the three-dimensional structure of a complex of CysMeTANDEM and the DNA hexamer [d(GATATC)]$_2$ using two-dimensional ^{1}H NMR derived NOE and dihedral bond angle constraints. This is the first structure of a TpA specific quinoxaline antibiotic in complex with DNA. CysMeTANDEM binds to and affects the structure of the DNA in a manner similar to that observed in complexes of triostin A with DNA. The two quinoxaline rings bisintercalate on either side of the two central T·A base pairs and the peptide ring lies in the minor groove. The central A·T base pairs of the complex are underwound (average helical twist angle of ~-10°) and buckle inward by ~ 20°. There are intermolecular hydrogen bonds between each of the Ala NH and the AN3 protons of the TpA binding site, analogous to those observed between Ala NH and GN3 in the crystal structures of the CpG specific complexes of triostin A with DNA. However, the structure of the peptide ring of CysMeTANDEM in the complex differs from that of triostin A. This appears to be largely due to the formation of intramolecular hydrogen bonds between the two Val NH and the Ala Carbonyls, which cannot form in triostin A because the Val amide is N-methylated.

M-PM-F4

FREE ENERGY OF B–Z JUNCTION FORMATION

((D. Suh[1], R. Sheardy[2], R. Kurzinsky[2], M. Doktycz[2], A. Benight[2] & J. Chaires[1])) [1] Dept. Biochem., Univ. Mississippi Med. Center, Jackson, MS 39216; [2] Dept. Chem., Seton Hall Univ., South Orange, NJ 07079; [3] Dept. Chem., Univ. Illinois, Chicago, IL 60680

The NaCl–induced transition from the right–handed B form to a hybrid form containing both left– and right–handed DNA, joined by a B – Z junction, was investigated. Transition curves were constructed from circular dichroism spectra collected as a function of NaCl concentration for a series of 16 bp deoxyoligonucleotides. In these molecules, the dinucleotide step immediately adjacent to the B–Z junction was systematically varied. The sequence of the series (one strand of the duplex) was: 5'*CG CG CG CG CG*AMNGACTG, where *C* indicates m^{5}dC, and –**MN**– was varied to include the possible py:py stacks: –CC–, –CT–, –TC– and –TT–. Transition curves for the conversion of all deoxyoligonucleotides were found to be biphasic. Singular value decomposition was used to analyse the experimental circular dichroism spectra obtained as a function of NaCl, and showed that the transition was *not* a simple two–state process. A sequential three–state model, B ⇌ I ⇌ BZ, was derived and used to evaluate the salt dependent equilibrium constants for each step in the sequential reaction model. The results indicate that the free energy change for BZ junction formation (ΔG_j) depends on the dinucleotide sequence immediately adjacent to the junction. *Supported by:* NIH CA35636 (JC), NIH GM39471 (AB) & NSF DMB8996232 (RS).

M-PM-F5

STABILIZATION OF TRIPLEX DNA BY HYDRALAZINE AND THE PRESENCE OF ANTI-TRIPLEX DNA ANTIBODIES IN TREATED PATIENTS. ((T.J. Thomas, Y.-P. Yan, T. Thomas, J.R. Seibold, L.E. Adams and E.V. Hess)) UMDNJ-Robert Wood Johnson Medical School, New Brunswick, NJ 08903 and Univ. Cincinnati Med Center, Cincinnati, OH 45267.

Hydralazine (HYZ) is an antihypertensive drug that elicits anti-nuclear antibodies in patients as an adverse side effect. Previous studies have shown that HYZ facilitates the formation of Z-DNA. In the present study, we investigated the ability of HYZ to promote/stabilize triplex DNA form of poly(dA).2poly(dT). Under low ionic conditions (10 mM Na), the polynucleotide melted as a double helix with a Tm of 55.3°C. HYZ destabilized this duplex form by reducing its Tm to 52.5°C. Spermidine, a natural polyamine, provoked the triplex form of poly(dA).2poly(dT) with 2 melting transitions, Tm1 of 42.8°C corresponding to triplex → duplex + single stranded DNA and Tm2 of 65.4° corresponding to duplex melting. Triplex DNA formed in the presence of spermidine was stabilized by HYZ with a Tm1 of 53.6°C. These results support the hypothesis that HYZ is reactive with unusual forms of DNA and capable of converting B-DNA to a triplex form that is immunogenic. In order to test this possibility, we analyzed sera from a panel of 25 HYZ-treated patients for anti-triplex DNA antibodies using an enzyme-linked immunosorbent assay. Our results showed that 72% of HYZ-related sera had antibodies reacting toward triplex form of polynucleotides. In contrast, there was no binding of normal human sera to triplex DNA. Taken together our data indicate that HYZ and related drugs might exert their action by interacting with DNA and stabilizing higher order structures, such as the triplex DNA.

M-PM-F6

Theoretical Model Building Studies of DNA Four-Way Junctions

A. R. Srinivasan and Wilma K. Olson, *Department of Chemistry, Wright-Rieman Laboratories, Rutgers, the State University of New Jersey, New Brunswick, New Jersey 08903*

A model building scheme that combines a constrained backbone generating algorithm with simple hard-sphere packing calculations is offered to build the four-stranded structures of DNA found in Holliday junctions. Two standard B-DNA duplexes are oriented side-by-side with helix axes at different relative inclinations and then systematically rotated and translated to identify closely spaced contact-free states. Attempts are then made to introduce a sugar-phosphate chain backbone between bases on different duplexes in an energetically acceptable local conformation. The goal is to identify the multiple structural solutions associated with a particular arrangement of neighboring DNA helices in the four-way junction rather than an optimum structure. The methodology is quite general, in terms of accommodating four-way junctions with arms of variable conformations and lengths and of sizes much greater than treated heretofore. The only deformation in the structure relative to B-DNA is found at the site of backbone exchange, with base stacking completely preserved in all models. An interesting outcome of the current studies is that sterically acceptable four-arm Holliday junctions may be formed over a wide range of the angle at the cross. The dynamic mobility of the Holliday junctions may thus be inferred from the visualization of selected low-energy models. The long-range electrostatic energetics of different models corresponding to various inclinations of the contacted helices under different dielectric treatments are also assessed. (Supported by USPHS grant GM20861)

M-PM-F7

MOLECULAR STRUCTURE OF A DNA TRIPLE HELIX

G. RAGHUNATHAN [1], T. M. MILES [2] & V. SASISEKHARAN [2] [1] NCI and [2] NIDDK, NIH, Bethesda, MD 20892

A structure for the triple helix Poly dT · poly dA · poly dT is proposed. The present structure preserves the pseudo dyad between the Watson-Crick paired adenine and thymine strands, and in addition has a pseudo rotational symmetry relating the Hoogsteen paired adenine and thymine strands. The simultaneous presence of these two symmetries gives rise to a dyad between the two thymine strands. These symmetries result in identical backbone conformations for all three strands, unlike any previously proposed model for a triple helix. The proposed structure has an axial rise per residue of 3.26 A and 12 residues per turn as obtained by X-ray fiber diffraction (Arnott and Selsing, J. Mol. Biol., 88, 509, 1974). The present structure is structurally and conformationally similar to the B-form DNA and has sugar puckers in the C2'-endo region. This structure is fundamentally different from the one proposed by Arnott and coworkers, which was based on A-form DNA and C3'-endo sugar pucker. The proposed structure is stereochemically satisfactory, and it does not have the disallowed nonbonded distances present in the earlier model of Arnott and coworkers. It is energetically much more favorable than their structure.

M-PM-F8

COMBINATORICS OF THREE-DIMENSIONAL LATTICE STRUCTURES OF t-RNA. ((Brooke Lustig, David G. Covell* and Robert L. Jernigan)) Laboratory of Mathematical Biology, National Cancer Institute, National Institutes of Health, Bethesda MD, 20892. *Biomedical Supercomputing Laboratory, Program Resources Inc./Dyncorp, Frederick, MD, 21701.

The Phe t-RNA structure can be fit with lattice models, giving agreement within an RMS of 2.0 A, and specifying 76 points from a face-centered cubic lattice. Upon these points, 32 chain folds are possible. For each lattice fold, the low energy secondary structures are determined from a list of proximal bases, using a standard secondary structure algorithm. From the lists of remaining possible tertiary pairs, all possible combinations are generated, and these include 2,365,440 conformers with non-overlapping bases. The native conformation is found within the lowest 25 percent of the distribution, and the lower energy region of this distribution is found to have a large number of the 364,672 conformers that include the native secondary structure. Possible non-native conformational variations associated with the stable secondary structures include a kink in the anti-codon region and slip pairing accompanied by a bulge at the end of helical stems. Even small changes in secondary structure permit some different tertiary pairs. A full exploration of such a set of lattice points, without restrictions in volume, distances or secondary structures, involves generating an enormous number of possibilities. There are 36,484,128 possible cubic lattice configurations for the sixteen bases enclosing the internal loop of Phe t-RNA. However, substantial reductions in the numbers of lattice configurations of pairs of stems attached to the internal loop can be achieved by accounting for excluded volume.

M-PM-F9

ENERGY STORED IN THE PACKAGED DNA OF BACTERIOPHAGE T7. ((C. S. RAMAN, S. J. HAYES, B. T. NALL, and P. SERWER)) Department of Biochemistry, The University of Texas Health Science Center, San Antonio, TX 78284-7760.

To determine the non-dissipative energy invested in packaging bacteriophage T7 DNA, we have used high sensitivity titration calorimetry to measure the heat released per nucleotide pair (ΔH) when T7 DNA was expelled from its capsid at 65°C. Because expulsion of DNA leaves most of the T7 capsid intact, we have assumed that all of the energy of packaging was released as heat. The value of ΔH was -0.47±0.05 kcal mol^{-1} for wild type T7 and -0.37±0.05 kcal mol^{-1} for an 8.4% T7 DNA deletion mutant. Control titrations performed either with buffer (0.2 M NaCl, 0.01 M sodium phosphate, 0.001 M $MgCl_2$, pH 7.4) alone or with bacteriophage at a temperature (39°C) below that needed for expulsion yielded backgrounds less than 5% of the signal. The ΔH values are comparable to the energy, measured from the osmotic pressure-volume work, needed primarily to remove water from DNA during polymer induced collapse. (0.1-0.4 kcal mol^{-1} of nucleotide pair; Rau *et al* [1984] Proc. Natl. Acad. Sci. USA 81, 2621-2625). (Supported by NIH GM24365 and GM32980)

PROTEIN MOLECULAR DYNAMICS

M-PM-G1

PROTEIN DYNAMICS IN AQUEOUS AND NON-AQUEOUS ENVIRONMENTS. ((David S. Hartsough and Kenneth M. Merz Jr.)) Department of Chemistry Pennsylvania State University University Park PA 16803

We present the results of molecular dynamics simulations of a protein in an organic solvent. Our results show that while the amino acid side chains are more flexible in water, there is only a very small difference in backbone flexibility between protein in chloroform and protein in water. We propose that the major difference between the two solvent environments is the preferred orientations of the amino acid side chains. These results aid in the understanding of experimental observations and offer important insights for protein engineering in non-aqueous media.

M-PM-G2

CLASS II FORCE FIELDS FOR PEPTIDES AND PROTEINS Ming-Jing Hwang, Tom Stockfisch, Moises Hassan, Dzung Nguyen and Arnold T. Hagler. Biosym Technologies, Inc., 9685 Scranton Road, San Diego, CA 92121.

A second generation Class II molecular mechanics force field for peptides, proteins, nucleic acids and carbohydrates has been derived. This force field consists of higher order diagonal terms and includes cross terms whose force constants are well determined from fits to molecular energy surfaces calculated by *ab initio* methods. Comparisons with results from conventional Class I force fields show that the Class II interaction terms are required to give a better analytical representation for molecular properties of structures, vibrational frequencies, conformational energies and barriers, and especially for the environmental effects on these properties. For example, the Class II force field is able to account for, with a transferable set of parameters, the substantial bond length variation exhibited in nucleic acid rings and in peptide C-N bond caused by change of hybridization state at the nitrogen center from sp2 to sp3, shift in the stretching frequency of carbonyl (C=O) bond in cycloalkanones, variation in the conformational energies of molecules ranging from simple amides to nucleic acid bases, and the anomeric effect on both structural and energetic properties of carbohydrates. Finally, in addition to the properties of small molecules, results of molecular dynamics simulations with various Class I and Class II force fields on cyclic peptide crystals and proteins will be presented and the ability of these force fields to reproduce peptide and protein structures given.

M-PM-G3

COMPUTATIONAL STUDY OF CONFORMATIONAL TRANSITIONS IN THE ACTIVE SITE OF TOSYL-A-CHYMOTRYPSIN. ((Themis Lazaridis and Michael E. Paulaitis)) Department of Chemistry, Harvard University, Cambridge, MA 02138, and Center for Molecular and Engineering Thermodynamics, Department of Chemical Engineering, University of Delaware, Newark, DE 19716

The motion of the tosyl group covalently bound in the active site of α-chymotrypsin has been studied using an empirical force field. A previously developed method employing an adiabatic projection of the potential energy hypersurface onto a small number of essential degrees of freedom has been used to determine multidimensional reaction paths for the rotation of the tosyl aromatic ring within and its movement out of the specificity pocket of the enzyme. The conformation of the specificity pocket was found to change substantially under stochastic boundary, molecular dynamics simulations. The shape of the paths and the height of the calculated energy barriers were affected substantially by this conformational change. The free energy profile for tosyl ring rotation was also determined by the Free Energy Perturbation method in the presence and absence of explicit solvent water and in both cases was found to be lower than the energy barrier, indicating a positive activation entropy. Based on the calculated energy and free energy barriers the mobility of the bound inhibitor should be much lower than that observed in NMR experiments on the same system. The discrepancy is most likely due to the observed distortion of the specificity pocket during the dynamics simulation.

M-PM-G4

MOLECULAR DYNAMICS SIMULATIONS OF RUBREDOXIN AND REDOX SITE ANALOGS IN AQUEOUS SOLUTION: A COMPARISON OF THE REDOX SITE ENVIRONMENT. ((Toshiko Ichiye, Robert B. Yelle, and Brian W. Beck)) Department of Biochemistry/Biophysics, Washington State University, Pullman, WA 99164-4660.

Molecular dynamics simulations have been carried out on *Clostridium pasteurianum* rubredoxin, an iron-sulfur electron transfer protein, and on analogs of the iron-sulfur redox site in aqueous solution. The simulation of the protein in aqueous solution shows good agreement with the crystal structure. One notable feature from the analog studies is that the accessibility of the iron in the redox site to water is controlled by the C–S–Fe–S dihedral angles. The results are consistent with the experimentally observed increase in redox potential of rubredoxin over that of the Holm-Ibers analog, which has different dihedral angles than the protein. If the analog is forced to have the same dihedral angles as are found in the protein, then the relative location of the closest waters is remarkably similar to that of the two closest amide groups to the iron in rubredoxin, although in the protein there are only the two amide groups in the possible four equivalent positions for close approach. Thus, the protein environment differs from an aqueous analog both in the reduced polarity of the closest groups and in the reduced number of groups. Since these closest groups make a large contribution to the electrostatic potential at the redox site, the location and fluctuations in location of the closest groups in rubredoxin and in the analogs are described. The hydrogen bonding patterns of the closest polar groups in rubredoxin and in the analogs, which differ somewhat, are also described. In addition, the resulting electrostatic potentials and the fluctuations in them are compared.

M-PM-G5

COMPUTER SIMULATIONS OF TURN MUTATIONS IN CYTOCHROME B562

((Rajagopal Srinivasan and Shankar Subramaniam)) Beckman Institute, Center for Biophysics and Computational Biology, National Center for Supercomputing Applications, University of Illinois, Urbana, IL 61801

Cytochrome b-562 is a four helix bundle protein containing 106 residues and its three dimensional structure is characterized to 1.4 A resolution. The three residues that connect helices three and four (E81-G82-K83) have been mutagenized extensively and some of the mutant proteins fold and form stable three dimensional structures as shown by a color assay. The question posed by the computational studies was whether a priori predictions can be made as to which of the mutant sequences would fold into a wild type-like three dimensional structure. In addition the such a study would provide insight into the short-range and long range forces that stabilize the turn and yield heuristic rules to guide protein design. This study presents extensive simulations of 7 of the 30 turn sequences whose expression was attempted. Three different methodologies were used to predict the turn conformations. These include a) systematic grid search followed by Monte Carlo and simulated annealing, b) high temperature molecular dynamics and c) library search followed by simulated annealing. The results of the computer simulations on mutant structures show that a) All three methods are able to correctly predict the wild type structure. b) for the mutants that have been analyzed, all three methods predict virtually identical low energy conformations. c) mutants containing GLY or small polar amino acids at position 82 adopt the same backbone conformation as the wild type protein d) mutants with non-polar substituents at position 82 lead to turn structures that are very different from those of the wild type. The predicted order of stability is EGK = RGM > RGV > SSR > DFR > LAA > PVA.

M-PM-G6

3D STRUCTURAL PREDICTION OF THE IMMUNODOMINANT LOOP OF SEVEN ANTIGENIC VARIANTS OF FOOT-AND-MOUTH DISEASE VIRUS (FMDV), USING MOLECULAR MODELING TECHNIQUES.

((L.L. France, P. Piatty, J.F.E. Newman and F. Brown)) PIADC,USDA/ARS,Greenport, NY 11944.

The immunodominant loop of FMDV consists of residues 132-159 of VP1, one of four proteins making up the virus capsid. This loop contains both the highly conserved cell attachment site (145-147), and a hypervariable region which includes the major epitope (146-154). Although the basic structure of FMDV, serotype O, has been solved, that of the immunodominant loop could not be determined. We have used molecular modeling techniques to predict the structures of the immunodominant loops of seven antigenic variants of FMDV type A12, which differ only at positions 148 and 153 in VP1. Molecular dynamics (simulated annealing) and energy minimization were used to search conformational space for stable conformers. These results were compared with structures generated using a search of the Brookhaven Protein Data Bank for structurally conserved regions in homologous proteins. The results indicate that, for all seven antigenic variants, it is the presence or absence of proline at residue 153 and leucine at residue 148 that exerts the greatest influence on the structure of the immunodominant loop. Furthermore, the cell attachment site is predicted to be a β-turn, regardless of the substituted residue at position 148.

M-PM-G7

BROWNIAN DYNAMICS SIMULATIONS OF ANTIBODY-ANTIGEN RECOGNITION.

((Richard E. Kozack and Shankar Subramaniam)) Beckman Institute, Center for Biophysics and Computational Biology, National Center for Supercomputing Applications, University of Illinois, Urbana, IL 61801

The crystal structure for an antibody-antigen system, that of the anti-hen egg lysozyme monoclonal antibody HyHEL-5 complexed to lysozyme, is used as the starting point for computer simulations of diffusional encounters between the two proteins. The investigation consists of two parts; first, the linearized Poisson-Boltzmann equation is solved to determine the long-range electrostatic forces between antibody and antigen and then, the relative motion as influenced by these forces is modeled within Brownian motion theory. The effects of point mutations on the calculated reaction rate are considered. It is found that charged residues close to the binding site exert the greatest influence in steering the proteins into a configuration favorable for their binding, while more distant mutations are qualitatively described by the Smoluchowski model for the mutual diffusion of two uniformly charged spheres. These results can be tested by site-directed mutagenesis. (Supported in part by NIH grant RO1 GM4635.)

MEMBRANE TRANSPORT

M-PM-H1

RAPID VOLTAGE PULSES REVEAL TRANSIENT CARRIER CURRENTS IN A FACILITATED BASIC AMINO ACID TRANSPORTER

((M. Kavanaugh, E. Stefani,* and R.A. North)) Vollum Institute, Oregon Health Sciences University and *Department of Molecular Biophysics and Physiology, Baylor College of Medicine

The sodium-independent influx of basic amino acids mediated by the cloned dual function y^+ transporter/murine retrovirus receptor increases exponentially with hyperpolarization while efflux increases exponentially with depolarization. The effect of hyperpolarization on influx is not due to a voltage dependence of substrate binding because the apparent K_M approaches a minimum at hyperpolarized potentials while influx continues to increase exponentially even at saturating substrate concentrations (Kavanaugh et al. Biophys. J. 61:A425,1992). Kinetic modeling suggests that the conformational reorientation of the unliganded carrier is voltage-dependent and rate-limiting; the present studies were undertaken to record conformational transition or "gating" currents in response to rapid voltage jumps using the cut-open oocyte vaseline gap recording technique (Taglialatela et al. Biophys. J. 61:78,1992). In the absence of basic amino acids, ouabain-insensitive transient currents were observed in oocyte membranes expressing the cloned transporter. These transient currents displayed rapid kinetics and were voltage-dependent and saturable, with a midpoint of activation of -17 mV and an apparent valence of 1.2 *e*. N-Ethylmaleimide (200 μM), which blocks amino acid transport, also blocked the transient currents. The results suggest that at least one component of the voltage dependence of basic amino acid transport arises from charge movement during conformational transitions of the unliganded transporter.

M-PM-H2

Photodynamic Action of Hematoporphyrin Derivative (HpD) Activates Calcium Channel in Glioma (U-87 MG) Cells, P.G. Joshi, K. Joshi, S. Mishra and N.B. Joshi. Biophysics Department, NIMHANS, Bangalore (INDIA).

The effect of HpD mediated photosensitization on the ion transport properties of U-87 MG cells has been investigated using fluorescent indicators. HpD treatment in the dark did not produce any change in the intracellular ion concentration. However, upon irradiation with light, a large increase in intracellular calcium concentration was observed. This increase was solely due to influx of calcium as no change was observed when the cells were photosensitized in the presence of EGTA. The increase in intracellular calcium concentration varied with HpD concentration, light dose and calcium concentration. The calcium influx induced on photosensitization by HpD was repairable and was inhibited by diltiazem, a calcium channel blocker. Under similar conditions, we have not observed any leakage in potassium and sodium. Our results suggest that photodynamic action of HpD opens a voltage sensitive calcium channel and the elevated intracellular calcium level may activate a variety of cellular processes leading to cell death.

M-PM-H3

EFFECT OF *BACILLUS THURINGIENSIS* TOXIN ON THE REGULATION OF INTRACELLULAR pH IN AN INSECT CELL LINE. ((V. Vachon, M.-J. Paradis, A. Cvetkovic, J.-L. Schwartz* and R. Laprade)) GRTM, Univ. de Montréal, Montreal, Que., H3C 3J7, and *Biotechnol. Res. Inst., NRC, Montreal, Que., H4P 2R2.

In insect midgut cells, secondary active transport is energized by a vacuolar-type H^+-ATPase coupled with a K^+-H^+ antiporter (Wieczorek *et al.* J. Biol. Chem. 266, 15340 (1991)). The fluorescent pH indicator BCECF was therefore used to investigate changes in the intracellular pH of individual cells of the lepidopteran species *Spodoptera frugiperda* (Fall armyworm; SF9) in response to changes in the composition of the external medium and following the addition of CryIC, a potent biological pesticide isolated from *B. thuringiensis*, which is used extensively for the specific control of lepidopteran larvae. In the presence of K^+ and following a change in the external pH, intracellular pH approached that of the bathing medium, reaching an equilibrium within minutes. Removal of K^+ from the external medium resulted in a rapid acidification of the cells. Under these conditions, changes in the external pH had little effect on the pH of the cells. These results suggest that, in intact cells, influx of protons across the cell membrane is mediated mainly by a K^+-H^+ antiporter. In the presence of CryIC, however, the membrane became permeable to protons independently of the presence of K^+. CryIC therefore appears to interfere with the generation of the transmembrane K^+ gradient and secondary active transport by allowing protons to cross the cell membrane in a K^+-independent manner.

M-PM-H4

ANTIBODIES RAISED AGAINST THE 59 KDA Na^+/H^+ ANTIPORTER FROM BEEF HEART MITOCHONDRIA INHIBIT Na^+ FLUX IN A RECONSTITUTED SYSTEN. ((Z. Shariat-Madar and K. D. Garlid)). Department of Pharmacology, Medical College of Ohio, Toledo, Ohio 43699.

We purified and reconstituted the mitochondrial Na^+-selective Na^+/H^+ antiporter and assayed Na^+ flux using the fluorescent probe SBFI, as previously described (Garlid et al., J. B. C. 266, 6518-6523, 1991). We raised antibodies in rabbits to the 59 kDa protein that we had identified with Na^+/H^+ exchange activity. The antibodies recognized proteins of similar MW in heart, kidney and liver mitochondria from rat, dog and hamster. The anti-59 kDa antibodies inhibited Na^+ transport into proteoliposomes reconstituted with the 59 kDa Na^+/H^+ antiporter, providing support for the identification of the Na^+/H^+ antiporter protein. We are now using these polyclonal antibodies to screen a beef heart cDNA library. This research was supported in part by NIH Grants HL 36573 and HL 43814.

M-PM-H5

Ca^{2+} TRANSPORT IN THE MODEL EUCARYOTE *SACCHAROMYCES CEREVISIAE.* ((T. Dunn, Chun Zhao, T. Beeler)) USUHS, Bethesda, MD 20814

The research goal is to identify genes and proteins that regulate cytosolic $[Ca^{2+}]$ in yeast. The experimental approach is to isolate mutants with decreased tolerance to high $[Ca^{2+}]$ in the growth medium, to determine which mutants have altered Ca^{2+} metabolism, and clone by complementation genes that restore normal Ca^{2+} metabolism. A screen of 60,000 mutagenized yeast colonies yielded 19 *csg* (calcium sensitive growth) mutants that lost the ability to grow in 100 mM Ca^{2+}, but were able to grow in 100 mM Sr^{2+}. The main Ca^{2+}& Sr^{2+} sequestering organelle in yeast is the vacuole which accumulates Ca^{2+}& Sr^{2+} via a $Ca^{2+}/2H^+$-exchanger and stores Ca^{2+}& Sr^{2+} as a complex with polyphosphate. Mutants defective in non-vacuolar Ca^{2+} transport systems are likely to be Ca^{2+}-sensitive but Sr^{2+}-tolerant. Complementation analysis identifies 2 major complementation groups and 8 independent isolates. The *CSG2* gene was cloned and its DNA sequence identifies a 410 amino acid ORF containing 9 putative membrane-spanning sequences. Analysis of Ca^{2+} metabolism by the *csg2* mutant indicates that Ca^{2+} sequestration by a nonvacuolar organelle is altered. Suppressor mutants of *csg2* identify 7 complementation groups; some that require high $[Ca^{2+}]$ for growth indicating that these mutants can be used to identify other genes that regulate cellular Ca^{2+}.

M-PM-H6

SITE-DIRECTED SPIN AND FLUORESCENT LABELING OF THE LACTOSE PERMEASE OF *ESCHERICHIA coli*. H. Jung, R. Lopez, C. Altenbach*, W. L. Hubbell* & H. R. Kaback, Howard Hughes Medical Institute and *Jules Stein Eye, University of California Los Angeles, Los Angeles, CA 90024-7008.

β-Galactoside accumulation against a concentration gradient in *E. coli* is dependent upon the lactose (lac) permease, a hydrophobic, polytopic cytoplasmic membrane protein that catalyzes the coupled translocation of a single disaccharide molecule with a single proton. Based on circular dichroic measurements and hydropathy profile analysis, the protein has 12 hydrophobic domains in α-helical conformation that traverse the membrane in zig-zag fashion connected by hydrophilic loops. The 12-helix motif has been confirmed by studies on an extensive series of lac permease-alkaline phosphatase fusion proteins.

Recent studies indicate that Asp237 and Lys358, as well as Asp240 and Lys319, interact functionally, thereby suggesting that putative helix VII may lie close to helices X and XI in the tertiary structure of lac permease. In order to determine the location of these residues with respect to the membrane, the following single Cys mutants were constructed in a lac permease chimera containing the biotinylation domain from a *Klebsiella* oxalacetate decarboxylase, purified by avidin affinity chromatography, reacted with thiol-specific spin and fluorescent labels and reconstituted into proteoliposomes: D237C/K358A, D237A/K358C, D240C/K319A and D240A/K319C. The shapes of the corresponding EPR and fluorescent spectra and the results from quenching studies suggest that these residues are located in an amphiphilic environment at or close to the membrane-water interface.

M-PM-H7

CHARACTERISING SOLID SUPPORTED MEMBRANES WITH THE ATOMIC FORCE MICROSCOPE. ((H.-J. Butt, K. Seifert, K. Fendler and E. Bamberg)) Max-Planck-Institut für Biophysik, Kennedyallee 70, 6 Frankfurt/M. 70, Germany

Recently solid supported membranes have been used to study the ion transport of purple membranes (K.Seifert, K.Fendler, E.Bamberg, Biophys. J. in press.). The solid supported membrane consisted of a lipid monolayer on mercaptanised gold. The gold substrate, the mercaptane on gold, the lipid monolayer and purple membranes adsorbed onto the lipid have been studied with an atomic force microscope. Simultaneously, that is while imaging, ion transport of purple membranes and electric properties of the solid supported membrane have been measured. In this way structural information could be correlated with results of transport measurements.

M-PM-H8

TWO CONFORMATIONS OF THE UNCOUPLING PROTEIN CONTROLLED BY NUCLEOTIDE BINDING ((M. Klingenberg)) Institute for Physical Biochemistry, University of Munich, Goethestrasse 33, 8000 München 2

Purine nucleotides (ATP^{4-}, ADP^{3-}, GTP^{4-}, CDP^{3-}) inhibit H^+ translocation by the uncoupling protein (UCP). Several types of evidence show that nucleotides bind at a site different from the translocation channel. Nucleotide binding can be inhibited by mercurial and by carboxyl reagents without effecting the transport rates. Cardiolipin inhibits nucleotide binding but not transport. Nucleotide binding is strongly pH dependent in contrast to H^+ transport. Fluorescent nucleotide analogues, such as 3'dimethylaminonaphoyl (DAN)-ATP, bind at the same site as ATP but do not inhibit transport. Under competitive conditions ATP removes DAN-ATP due to tighter binding. "On"-kinetics show binding rates for DAN-ATP 20 to 100 times faster than for ATP. This was interpreted that ATP binding is limited by a conformational change of UCP from an active to an inhibited state $UCPa \rightarrow UCPa \cdot N \rightarrow UCPi \cdot N$. A two-state conformation is further supported by higher resistance to tryptic digestion of the inhibited state. DAN-ATP does not protect whereas ATP protects against proteolysis. Another fluorescent ATP derivative, DANSYL-ATP has slow "on"-kinetics and inhibits transport similar to ATP. Thus fluorescent kinetics of DAN-ATP and DANSYL-ATP permit comparing rates of formation of the primary nucleotide UCPa·N complex and of the rate limiting conformation change to UCPi·N .With ATP binding intrinsic tryptophane fluorescence of UCP is changed by 5 % . Also slight changes in the aromatic CD region of UCP reflecting primarily tyrosine can be discerned. Strong pH dependency of ATP binding to UCP reflects the unmasking of carboxyl groups in the binding centre on transition from UCPa to UCPi. Cardiolipin shifts the conformational equilibration from UCPi·N to UCPa·N.

M-PM-H9

AN HYPOTHETICAL SEQUENCE OF REACTIONS LEADING TO IRON TRANSPORT FOLLOWING DISSOCIATION FROM TRANSFERRIN IN ENDOSOMES. ((J.A. Watkins, C-Y. Li, J.D. Altazan, and J. Glass)) Hematology-Oncology Section, Center for Excellence in Cancer Research, Treatment, and Education, LSUMC-S, Shreveport, LA, 71130.

Reticulocyte iron (Fe) absorbtion via transferrin (Tf) endocytosis is a major factor in Fe metabolism. Although the exact sequence of events following Fe(III) dissociation from Tf remain uncertain, available information indicates protein-protein interactions, intramolecular and intermolecular Fe transfer, Fe(III) reduction, and translocation across the endosomal membrane are kinetically significant. Based on available data, it is reasonable to propose four models for the sequence of events following dissociation from Tf: (A) reduction before intramolecular Fe(II) transfer, (B) reduction following Fe(III) transfer, (C) reduction following Fe(III) translocation across the endosomal membrane, (D) reduction at both intra and extravesicular surfaces. Sequential additions of reductants, H^+-ATPase inhibitors, chelator effects, and second order kinetic analysis indicates multiple sites for Fe(III) reduction and pathways for intermolecular Fe transfer and suggests at least two protein mediated translocation routes. The results and considerations support Model D with the dominant pathway having the following sequence: (1) cooperative iron dissociation from Tf and redistribution among intravesicular Fe(III) acceptor sites, (2) extravesicular electron donor/acceptor reduction and transmembrane electron transfer, (3) conformational changes and configurational rearrangements, (4) Fe(III) reduction, (5) intermolecular Fe(II) transfer, (6) Fe(II) translocation, and (7) Fe(II) mobilization. These results and considerations provide a basis for further exploration of processes involved in Fe transport.

LIPID–PROTEIN INTERACTIONS

M-PM-I1

PHASE DIAGRAM AND LIPID SELECTIVITY OF LIPID–PROTEIN BILAYERS WITH HYDROPHOBIC MISMATCH

Zhengping Zhang,[1] Maria M. Sperotto,[2] Martin J. Zuckermann,[1] and Ole G. Mouritsen,[2]

[1]McGill University, Montreal, PQ, H3A 2T8, Canada; [2]The Technical University of Denmark, Building 206, DK–2800 Lyngby, Denmark

A statistical mechanical lattice model is proposed to describe the lipid–protein interactions in phospholipid bilayers with small transmembrane proteins or polypeptides which are hydrophobically mismatched to the lipid bilayer. The phase diagram has been derived by computer–simulation techniques which fully allow for thermal density fluctuations and which operate on a free–energy level and hence permit an accurate identification of the phase boundaries. The calculations predict a closed loop of gel–fluid coexistence with a lower critical mixing point. Specific heat traces across the phase diagram are presented. The theoretical results for the phase diagram and the specific–heat function are related to recent experimental measurements on phospholipid bilayers mixed with synthetic transmembrane amphiphilic peptides or with gramicidin A. The model has been extended in order to include two different lipid species characterized by different acyl–chain lengths. The lateral distribution of the two lipid species near the hydrophobic protein–lipid interface in the fluid phase of the bilayer has been derived. The results indicate that there is a very structured and heterogeneous distribution of the two lipid species near the protein and that the protein–lipid interface is enriched in one of the lipid species.

M-PM-I2

EFFECTS OF THE INITIAL BINDING OF MELITTIN ON THE FLUIDITY OF DIMYRISTOYLPHOSPHATIDYLCHOLINE SMALL UNILAMELLAR VESICLES.

((Thomas D. Bradrick, Alexander Philippetis and Solon Georghiou)) Molecular Biophysics Lab., Physics Dept., University of Tennessee, Knoxville, TN 37996. (Spon. by J. Churchich)

We have investigated the effect of the binding of bee venom melittin on the order of DMPC SUVs using stopped-flow fluorometry. Lipid vesicles, labeled with the fluorescent probe TMA-DPH, were mixed with melittin and the steady-state fluorescence anisotropy r of the probe was monitored while melittin binding took place. The millisecond time scale used for the observations was short enough that virtually no melittin-induced vesicle fusion took place; consequently, the observed effects on the lipid order and dynamics are due solely to the binding of the protein. Experiments were carried out at three different lipid-to-protein molar ratios, 180, 135 and 90, in order to examine the effects of increasing the concentration of bound melittin. For all three ratios, above the transition temperature T_m of the lipid, binding had no effect on r. The fluorescence intensity of the probe was found to increase at the same rate as protein binding, however. At T_m, melittin binding caused r as well as the fluorescence intensity of the probe to decrease at the same rate at which protein binding took place. Interestingly, varying the lipid-to-melittin molar ratio had no effect on the initial or final values of r. We also measured the transfer of energy from the tryptophan residue of melittin to TMA-DPH and found it to be negligible. This suggests that probe molecules do not preferentially associate themselves with the protein molecules. Thus, the observed effects of the protein on the bilayer appear to be long-range. In the lipid crystalline phase, the protein was found to have no effect on either r or the fluorescence intensity of the probe.

M-PM-I3

Diacylglycerol Induces Specificity and Cooperativity in the Interaction of Protein Kinase C with Phosphatidylserine

Alexandra C. Newton
Department of Chemistry, Indiana University, Bloomington, IN 47405

Protein kinase C is allosterically regulated by phosphatidylserine and diacylglycerol, two lipids that activate the enzyme by exposing its pseudo-substrate auto-inhibitory domain (*J. Biol. Chem.* (1992) 267, 15263). The interaction with phosphatidylserine displays high cooperativity in a detergent micelle system (*Biochemistry* (1992) 31, 4661). This contribution shows that the binding to phosphatidylserine in bilayers is also highly cooperative and insensitive to increasing ionic strength, but only in the presence of diacylglycerol. In the absence of this second messenger, the binding of protein kinase C to model membranes is regulated by surface charge and ionic strength, with no selectivity for headgroup other than charge. Thus, diacylglycerol is required for the specific and highly cooperative interaction of protein kinase C with phosphatidylserine.

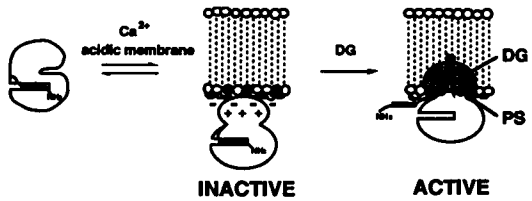

M-PM-I4

INTERACTION OF ANNEXIN VI WITH MEMBRANES: PHOSPHATIDYLETHANOLAMINE MAY RESTRICT MOBILITY IN MEMBRANES.

((Mohammad D. Bazzi and Gary L. Nelsestuen)) Department of Biochemistry, University of Minnesota St. Paul, MN 55108.

Association of annexin VI with membranes induced extensive clustering of acidic phospholipids as detected by self-quenching of fluorescent-labeled acidic phospholipids. The rates of protein-induced clustering were examined in membranes containing 10-15% fluorescent-labeled phosphatidic acid dispersed in phosphatidylcholine (PC) or phosphatidylethanolamine (PE). Both membranes supported similar levels of protein-induced fluorescence quenching. With membranes containing PC, protein-membrane association and fluorescence quenching were rapid, and were virtually complete within seconds after mixing the reagents. Membranes containing PE also exhibited rapid protein-membrane association, but showed a fluorescence quenching that was several orders of magnitude slower than membranes containing PC. Calcium chelation resulted in rapid dissociation of protein-membrane complexes and virtually complete recovery of the fluorescence signal of both membranes. The rate of fluorescence recovery was rapid in membranes containing PC, but PE-containing membranes showed slow recovery that approached the rate of phospholipid exchange between vesicles. Thus, the presence of PE appeared to severely restrict dissipation of clustered phospholipids in membranes. Membranes containing PE, N-methyl-PE, N,N dimethyl-PE, and PC showed successive increases in the rates of fluorescence quenching and recovery, suggesting that hydrogen bonding between head groups was the basis for this property. If the restricted dissipation of phosphatidic acid in PE membranes is a general property, relative mobility of membrane components and even diffusion on interior cell membranes may be influenced by this phenomenon. (Supported by NIH Grant: GM 38819.)

M-PM-I5

STRUCTURE AND ACTIVITY RELATIONSHIP OF CARDIOTOXIN - INDUCED FUSION OF SPHINGOMYELIN VESICLES (W.Wu*, K-Y Chien, and Y-C Hsu) Institute of Life Sciences, National Tsing Hua Univ. Hsin Chu Taiwan 30043 and Department of Physiology*, University of Virginia, Charlottesville, Va 22908

The activities of cardiotoxin(CTX)-induced fusion of sphingomyelin vesicles were compared for 10 HPLC-puried CTX from snake venoms of N.n.atra and N.m.mossambica. Based on both turbidity measurements and NBD-RH fluorescence energy transfer assay of the fusion process of phospholipid vesicles, CTX can be classified into two groups with distinguishly different activities. The amino acid sequences for the high-activity group, including N.m.m. CTX I, IV, V and N.n.a. CTX III, V, contain a proline residue at 31 position and hydrophobic residues near the tip of loop II. In contrast, all other five CTXs are relatively hydrophilic and lack of Pro-31 near the same region. Circular Dichroism studies on the former group of CTX further revealed that the β-sheet contents of CTXs were affected upon addition of phospholipids. It is suggested that the structure and dynamics of CTX near the tip of loop II region play important roles in CTX-induced fusion process. The present results show that the in vitro activities of CTX-induced processes could be correlated well with the ability of CTX-lipid interactions. The fact that CTX-induced depolarization of muscles cells could not be correlated with the ability of CTX-lipid interactions further indicates that lipid bilayer is not the main target for the action of CTX molecules in vivo.

M-PM-I6

ORIENTATION OF FUNCTIONAL AND NON-FUNCTIONAL PTS PERMEASE SIGNAL SEQUENCES IN LIPID BILAYERS. A POLARIZED FTIR STUDY. ((Lukas K. Tamm and Suren A. Tatulian)) Dept. of Physiology, University of Virginia, Box 449, Charlottesville, VA 22908

Synthetic peptides corresponding to the N-terminal 23 and 22 residues, respectively, of two integral plasma membrane proteins of *E. coli*, namely the mannitol- and glucitol-specific permeases of the bacterial sugar phosphotransferase system, were incorporated into single planar phospholipid bilayers supported on germanium plates. Polarized attenuated total reflection infrared spectra were recorded and order parameters were derived from the measured dichroic ratios (1). The order parameters of the two wild-type peptides which form amphiphilic α-helices in membranes (2) were -0.4 to -0.5, indicating a preferential alignment of the α-helix long axis parallel to the membrane surface. Non-functional mutant peptides of the mannitol permease sequence in which serine-3 or aspartate-4 were substituted with prolines (S3P, D4P) or lysine (D4K), but which were still largely α-helical, exhibited peptide order parameters close to zero, indicating a high degree of disorder of these peptides in the lipid bilayer. The lipids were well ordered at low concentrations of peptides in the membranes, but became disordered at high peptide concentrations. This effect of lipid disordering was more pronounced for the D4K mutant than for the wild-type mannitol peptide.

(1) Frey,S. and Tamm,L.K. (1991) Biophys. J. *60* :922-930
(2) Portlock et al., (1992) J. Biol. Chem. *267*:11017-11022

M-PM-I7

LOCATION OF SPIN-LABELED APOCYTOCHROME *c* AND CYTOCHROME *c* RELATIVE TO SPIN-LABELED LIPIDS FROM SPIN-SPIN INTERACTIONS IN ESR SATURATION STUDIES ((M.M.E.Snel, B.De Kruijff* and D.Marsh)) Max-Planck-Institut für biophysikalische Chemie, Abt. Spektroskopie, D-3400 Göttingen, Germany and *State University of Utrecht, Dept. of Biochemistry, 3508 TB Utrecht, The Netherlands.

Apocytochrome *c* spin-labeled in the N-terminal region and cytochrome *c* spin-labeled at the C-terminal were bound to fluid bilayers of negatively charged phospholipids containing phospholipid probes spin-labeled at different positions. The location of the labeled residues on the lipid-bound proteins was determined relative to the label positions in the different spin-labeled phospholipids by the influence of spin-spin interactions on the power saturation of the electron spin resonance spectra. The enhanced spin relaxation observed in the double- relative to the single-labeled systems indicates that the label on apocytochrome *c* is closest to the 14-C atom of the lipid acyl chain for the protein bound to dimyristoyl phosphatidylglycerol and to the 5-C atom for a mixture containing 85% phosphatidylcholine. For spin-labeled cytochrome *c*, the label is located close to the lipid headgroups.

M-PM-I8

MEMBRANE PROTEIN TOPOLOGY: A PRELIMINARY X-RAY STANDING WAVE STUDY OF CYTOCHROME-*c* ((J. Wang, X. Huang and M. Caffrey)) Chemistry, Ohio State University, Columbus, OH 43210; ((C. Wallace)) Biochemistry, Dalhousie University, Halifax, Nova Scotia, Canada B3H 4H7; ((M. Gelb)) Chemistry and Biochemistry, University of Washington, Seattle, WA 98195

Despite the detailed structure information available on cytochrome-*c* (cyt-*c*), the precise conformation and orientation of this peripheral protein at the membrane surface has not yet been determined. With a view to solving this topology-related problem, we have investigated cyt-*c* deposited on various membrane surfaces by means of x-ray standing waves (XSW). To this end, a selenomethionine analog of cyt-*c* ($SeMet^{80}$cyt-*c*) has been used. Negatively charged Langmuir-Blodgett (LB) monolayers of dimyristoylphosphatidylserine (DMPS) and self-assembled monolayers (SAM) of $HS-(CH_2)_n-COOH$ (n = 10 and 15) on silver mirrors served as model membranes to which cyt-*c* was attached electrostatically. X-ray fluorescence measurements performed on these model membranes produced the following results: 1) The Se-K_α fluorescence from the $SeMet^{80}$cyt-*c* films is strong and is well-resolved from background fluorescence. 2) The protein binds as a monolayer to an SAM of $HS-(CH_2)_{15}-COO^-$ with a Se monolayer-to-mirror distance of *ca.* 25 Å. 3) The protein appears to associate as multilayers or aggregates to an SAM of $HS-(CH_2)_{10}-COO^-$ and an LB film of DMPS. These results suggest that by making XSW measurements on cyt-*c* labeled with Se-Met at different positions in the protein it should be possible to establish unambiguously the orientation of the protein at the membrane surface. Supported by NIH DK 36849 and DK 45295.

OTHER CHANNELS

M-PM-J1

USE OF CHIMERAS TO LOCALIZE REGIONS DETERMINING ION SELECTIVITY IN POTASSIUM CHANNELS ((Lise Heginbotham and Roderick MacKinnon)), Harvard Medical School, Boston, MA 02115.

Potassium channels and non-selective cyclic nucleotide-gated cation channels (CNG channels) display considerable sequence similarity, especially in the regions thought to form the channel pores (P-region). This homology is particularly striking in light of the fact that the channels differ in their ion selectivity. To ascertain which parts of this region are important in determining the ionic selectivity, we have inserted portions of the CNG channel P-region into the corresponding portion of the Shaker K+ channel. The amino terminal half of the pore, which is quite conserved between these two channels, does not appear to determine potassium selectivity. In contrast, transfer of the non-conserved carboxyl terminal portion of the CNG channel P-region into the Shaker channel results in a voltage-activated channel which is non-selective. This chimeric channel displays another characteristic of CNG channel pores: it is blocked by low concentrations of divalent cations. Reversion chimeras, in which portions of the Shaker P-region are introduced into the CNG channel, are currently being tested for their properties of ion selectivity.

M-PM-J2

DIVALENT CATION BLOCK IS AFFECTED BY MUTATIONS OF AN ACIDIC RESIDUE IN THE PORE REGION OF cGMP-GATED CHANNELS. ((Michael Root and Roderick MacKinnon)) Program in Biophysics and Dept. of Neurobiology, Harvard Medical School, Boston, MA, 02115.

Divalent cation blockade plays an important physiological role in the function of the cGMP-activated cation channel from retina. Recent work on Shaker K^+ channels has demonstrated that a deletion mutation in the pore, suggested by the cGMP-gated channel sequence, not only renders the Shaker K^+ channel nonselective for monovalent cations, but also confers an external divalent blockade. This divalent sensitivity has been shown to depend upon the acidic residue adjacent to the deletion. Our studies here involve the corresponding residue in the cGMP-gated channel. When this residue is Glu or Asp, the channel is highly sensitive to external divalent cations in the form of permeant block. However, if an uncharged residue (Asn, Gln, Gly) is substituted, then the affinity for external divalent ions decreases by two orders of magnitude. These results strongly suggest that this residue forms part of a divalent cation binding site in the pore of cGMP-activated channels.

M-PM-J3

THE BLOCKING EFFECT OF Ca AND Mg ON THE cGMP ACTIVATED CURRENT IN RETINAL RODS.

((F. Sesti and V. Torre)) Dipartimento di Fisica, Via Dodecaneso 33, Genova 16146, Italy.

Properties of cGMP activated channels were studied in inside-out patches excised from retinal rods of the tiger salamander Ambystoma tigrinum. The addition of 0.5 and 1 mM Ca or Mg to the medium bathing the cytoplasmic side of the patch, blocked in a voltage dependent way the macroscopic current activated by 100 μM cGMP. At membrane voltages between -100 and 100 mV, in patches excised from the outer segment the single channel activity induced by 2 μM cGMP was reduced by adding Ca, but single channel events of a smaller size, could be clearly detected by simply increasing the cGMP concentration. In patches excised from the inner segment, containing only one cGMP activated channel, the blocking effect of 0.5 or 1 mM Mg in the presence of 100 μM cGMP was antagonized by increasing the cGMP concentration to 500 μM. The blocking effect of Ca in the presence of 100 μM cGMP was not relieved by increasing the cGMP concentration to 500 μM. These results show that millimolar amount of cytosolic Ca reduces both the open probability and the single channel conductance while cytosolic Mg has a major effect on the open probability and not on the single channel conductance.

M-PM-J4

CYTOSOLIC ACIDIFICATION ENHANCES THE ACTIVATION BY cAMP OF THE CHANNEL IN RETINAL ROD OUTER SEGMENTS.

((C. Sanfilippo and A. Menini)) Istituto di Cibernetica e Biofisica, C.N.R., Genova, Italy.

Cation channels directly activated by cGMP control the flow of ions across the surface membrane of vertebrate rods. These channels can also be activated by cAMP but, at neutral pH, the maximal current is lower than the one activated by cGMP and the concentration ($K_{1/2}$) necessary to activate half of the maximal current is higher for cAMP than for cGMP. We measured macroscopic currents in excised inside-out patches from retinal rod outer segments of the tiger salamander as a function of cGMP or cAMP concentrations as the cytosolic pH was lowered. The maximal current activated by cGMP was reduced, but the $K_{1/2}$ for channel activation was not affected. On the contrary, cytosolic acidification enhanced the activation of the channel by cAMP, both increasing the maximal current and reducing the $K_{1/2}$. These results suggest that titratable groups at the cytosolic side of the channel are important in the activation of the channel by cyclic nucleotides.

M-PM-J5

PERMEATION IN THE CYSTIC FIBROSIS TRANSMEMBRANE CONDUCTANCE REGULATOR (CFTR) CHLORIDE CHANNEL.

((J.A. Tabcharani and J.W. Hanrahan)) Department of Physiology and Respiratory Health NCE, McGill University, 3655 Drummond St., Montréal, Québec, Canada H3G 1Y6

CFTR is a non-rectifying, low-conductance Cl channel which mediates cAMP-stimulated chloride transport in epithelial cells and is defective in cystic fibrosis. Although regulation of CFTR has been studied in some detail, less is known regarding its permeation. CFTR channels display Goldman-type rectification in cell-attached patches; conductance is 8.7 pS (37°C) or 6.0 pS (22°C) near the membrane potential when the pipette solution contains 154 mM Cl and 10 mM TES. The I/V relationship becomes linear after excision into symmetrical solutions and conductance increases to 10.9 pS (37°) or 7.0 pS (22°C). The relationship between conductance and Cl activity is hyperbolic and can be fitted with a Michaelis-Menten-type function with K_M = 38 mM and maximum conductance of ~10 pS (22°C). A substate with conductance approximately half that of the fully open state is also observed. Biionic reversal potentials measured immediately after exposing the cytoplasmic side to test anions indicate $P_I(2.1) > P_{Br}(1.3) > P_{Cl}(1.0) > P_F(0.1)$, consistent with a "weak field strength" site. However, iodide currents become blocked within 1-2 min. and once this occurs, the extrapolated reversal potential shifts strongly in the negative direction indicating that $P_{Cl} > P_I$. This block and hysteresis in the I/V relationship occurs with 20 mM thiosulfate present, therefore it is probably not caused by trace I_3^- or other polyiodides. The relative conductances for cytoplasmic anions under initial biionic conditions are $G_{Cl}(1.0) > G_I(0.6) > G_{Br}(0.5) > G_F(0.3)$. The initial sequence for extracellular anions is $G_I(1.7) > G_{Cl}(1.0) > G_{Br}(0.6) > G_F$(n.a.). Among other anions examined, $P_{NO3}(1.7) > P_{Cl}(1.0) > P_{formate}(0.3) > P_{acetate}(0.2) > P_{ethanesulfonate}$, $P_{propionate}$, P_{HCO3}, $P_{pyruvate}$, $P_{gluconate}$. Unhydrated radii of permeant and impermeant anions suggest the pore diameter of CFTR is ~0.55 nm.

Supported by the NIH(NIDDK) and Canadian CF Foundation.

M-PM-J6

THE CARDIAC cAMP-DEPENDENT Cl⁻ CONDUCTANCE IS ENCODED BY AN ALTERNATIVELY SPLICED ISOFORM OF CFTR.

((B. Horowitz, S.S. Tsung, P.C. Levesque, P. Hart, and J.R. Hume.)) University of Nevada, School of Medicine, Reno NV 89557.

Activation of cAMP-dependent Cl⁻ channels in heart modulates resting membrane potential and action potential duration in response to autonomic stimulation. Recent data has demonstrated that the CFTR (cystic fibrosis transmembrane regulator) gene product is expressed in heart and is responsible for the observed cAMP-dependent Cl⁻ conductance. At this time it is not clear to what extent the CFTR gene product expressed in heart is identical to the known structure of CFTR expressed in epithelial cells. In this study, we employed the polymerase chain reaction (PCR) to amplify cDNA from rabbit ventricle and cloned fragments corresponding to the 12 transmembrane spanning domains (TSI-TSXII) of the epithelial CFTR transcript. Comparison of the amino acid sequence of human epithelial CFTR with the deduced sequence from rabbit heart indicated deletion of a 30 amino acid segment in the first cytoplasmic loop of CFTR which corresponds to known locations of intron-exon junctions in human CFTR, indicating that CFTR is an alternatively spliced isoform in heart. Outside of the alternatively spliced region, the heart CFTR isoform from rabbit displays greater than 95% identity to human epithelial CFTR. Southern analysis of heart reverse transcription PCR products only showed hybridization to cardiac tissues which electrophysiologically exhibit the cAMP-dependent Cl⁻ conductance in native cells. The functional and clinical significance of expression of a specific isoform of the CFTR Cl⁻ channel in mammalian heart remains to be determined. [Supported by NIH grant HL-30143 (J.R.H.). P.C.L. was supported by an NIH postdoctoral fellowship and S.S.T. was supported by a Medical Student Research Fellowship (NIDDK grant DK-07478-11)].

M-PM-J7

PARA-SULFANATO-CALIXARENES ARE POTENT BLOCKERS OF COLONIC CHLORIDE CHANNELS.

((A. K. Singh[1], R. K. Juneja[2], R. Wang[1], J. L. Atwood[2] and R. J. Bridges[1])) [1]Dept. of Physiology & Biophysics, Univ. of Alabama, AL 35294, [2]Dept. of Chemistry, Univ. of Alabama, Tuscaloosa, AL 35486

Calixarenes were tested on the outwardly rectifying Cl channel incorporated into planar lipid bilayers (PE:PS: 7:3). Plasma membrane vesicles derived from rat colonic enterocytes were used as a source of Cl channels. Calixarene effects were evaluated on the outer membrane side of the channel after first recording control channel activity.

p-Sulfonato-calixarenes caused long-lived zero conductance closures (block) of the colonic Cl Channel. Blockade was completely reversed upon exchange with calixarene-free buffer. The duration of the block periods increased with the size of the p-sulfonato-calix[n]arene: n=4, 3-4 s; n=6, 30-40 s; n=8, >>100 s. Kinetic analysis revealed the calixarenes act as open channel blockers at a single binding site with K_D's of n=4, 700 nM; n=6, 400 nM; n=8, 50 nM. Methylation of p-tetra-sulfonato-calix[4]arene (TS-calix[4]arene to yield 5,11,17,23-tetrasufonato-25,26,27,28-tetramethoxy calix[4]arene (TS-TM-calix[4]arene) led to a dramatic improvement in potency. TS-TM-calix[4]arene caused long-lived block periods lasting 100-300 s and a half maximal decrease in percent open time at less than 3 nM. Crystallographic studies demonstrate methylation results in a switch from a cone conformation to a 1,3-alternate conformation and this accounts for the higher potency of TS-TM-calix[4]arene over TS-calix[4]arene.

M-PM-K1

REMOVAL OF STABLE TYROSINE RADICAL, D^+, AFFECTS THE STRUCTURE OR REDOX PROPERTIES OF TYROSINE Z IN MANGANESE DEPLETED *SYNECHOCYSTIS* 6803 PHOTOSYSTEM II PARTICLES.

((R.J. Boerner, K.A. Bixby, A.P. Nguyen*, G.H. Noren, R.J. Debus*, & B.A. Barry)) Univ. of MN, St. Paul, MN 55108, *Univ. of CA, Riverside, CA 92521.

Photosystem II contains two redox active tyrosines, D^+ and Z^+, which have identical EPR lineshapes. Tyrosine Z conducts electrons between the primary donor and the manganese catalytic site. The physiological role of the dark stable tyrosine radical, D^+, is not known. To understand the function of D^+, we have characterized two site-directed mutations at tyrosine D in the transformable cyanobacterium, *Synechocystis* sp. PCC 6803, through the use of purified photosystem II particles (Noren, G.H., Boerner, R.J., & Barry, B.A. (1991) *Biochemistry, 30*, 3943-3950). In these mutants, tyrosine D has been changed to either a tryptophan (YW160D2) or a phenylalanine (YF160D2). In manganese depleted mutant particles, a light induced EPR signal is observed. This signal is made up of a stable component, due to a chlorophyll radical, and an unstable component. The lineshape of the unstable, oxidized component, referred to as M^+, is obtained by subtraction. M^+ has a different lineshape from tyrosine Z^+/D^+, but a similar *g*-value of 2.004. Up to one M^+ spin per reaction center can be photooxidized. The characteristic light induced Z^+ EPR signal that is detected in wild type is not detected in the mutants. The lineshape of M^+ is similar to the lineshape of the light induced photosystem II radical observed in a site-directed mutant in the D1 polypeptide (YF161D1) (Noren, G.H., & Barry, B.A. (1992) *Biochemistry 31*, 3335 - 3342). Optical measurements in wild type and mutant (YF160D2, YW160D2) manganese depleted PSII particles show that charge recombination kinetics between Q_A^- and an oxidized redox active component are similar, within a factor of two. We conclude that lack of the stable tyrosine D^+ alters the structure or redox properties of tyrosine Z in manganese depleted preparations.

M-PM-K2

THE EFFECT OF SITE-DIRECTED MUTAGENESIS AT POSITION M210 ON THE ENERGIES OF THE CHARGE SEPARATED STATES P^+B^- AND P^+H^- IN REACTION CENTERS OF *Rb. sphaeroides*,

M. Volk, W. Neumann, A. Ogrodnik, K.A. Gray, D. Oesterhelt and M.E. Michel-Beyerle, Inst. für Physikalische u. Theoret. Chemie, Technische Univ. München, 8046 Garching (Germany)

The exchange of tyrosine M210 (Y) to phenylalanine (F) in reaction centers (RCs) of *Rb. sphaeroides* slows primary charge separation from 3.5ps to 16ps [1]. This could be due to effects of YM210→F on the energies of the states involved and/or to structural changes. The magnetic field dependent recombination dynamics of P^+H^- (P: primary donor, H: bacterioheophytin) in quinone depleted RCs allows conclusions on the energies of P^+H^- and P^+B^- (B: accessory bacteriochlorophyll). P^+H^- recombines on the ns timescale either to the groundstate P with the rate k_S or, after hyperfine induced singlet-triplet-mixing (STM), to the triplet state ^3P with k_T. An external magnetic field hinders STM, thus reducing the yield Φ_T of $^3P^*$ and slowing the recombination of P^+H^-. The values of k_S of $0.011ns^{-1}$ (90K) and $0.03ns^{-1}$ (290K), as determined from the magnetic field dependence of the radical pair lifetime τ_{RP} and Φ_T, are 30% smaller than in wild-type RCs (WT) [2]. This effect is explained by a decrease of the superexchange matrixelement between P^+H^- and PH due to an increase of the energy of P^+B^- by $1000cm^{-1}$ as predicted for the replacement of the polar Y by the unpolar F [3]. From the width of the magnetic field dependence of Φ_T the rate k_T in the mutant is estimated to be smaller than in WT by 10% at 290K, but larger by 10% at 90K. This temperature dependence is shown to arise from the energy of P^+H^- being larger ($\simeq 400cm^{-1}$) in the mutant than in WT. Thus, the effects of YM210→F on the recombination dynamics of P^+H^- can be explained by energetic effects only.

[1] Finkele et al. (1990) Biochem. 29, 8517, [2] Ogrodnik et al. (1988) Biochim. Biophys. Acta 936, 361, [3] Parson et al. (1990) Biochim. Biophys. Acta 1017, 251.

M-PM-K3

POLARIZED LIGHT AND KINETIC OPTICAL STUDIES ON THE BETA MUTANT AND ASSOCIATED DOUBLE MUTANTS OF REACTION CENTERS*.

((C. Schenck, S. Corey, C. Kirmaier and D. Holten)), Dept. Biochem., Colorado S. U. and Dept. Chem., Wash. U.

In the bacterial reaction center (RC) a bacteriopheophytin electron acceptor (H_L) is reduced in 3 ps by the excited special pair, P*. In previous work[1], we have shown that a single point mutation ((M)L214H) results in incorporation of a functional bacteriochlorophyll (β_L) at the H_L binding site. As a consequence, there is a decrease in the free energy change (ΔG) of the initial reaction, and there are corresponding changes in the kinetics of the initial charge separation. We have introduced several additional mutations into the RC, in an effort to further decrease ΔG for the forward reaction.

Mutations at Glu L104, believed to form a stabilizing hydrogen bond with the C-9 keto group of the electron acceptor, have only small effects on the kinetics of electron transfer and presumably on the energetics[2,3]. ΔG for the initial reaction in one double mutant ((M)L214H/(L)E104V) could be as small as 45 meV, yet the forward reaction rate decreases by only 20% relative to the beta mutant. This provides further evidence for an unusually weak ΔG dependence of the initial rate.

Transient flash photolysis measurements support the notion that β_L is reduced after a flash (i.e., we do not observe the transient reduction of B_L, the monomer bacteriochlorophyll). Transient photoselection measurements reveal that the β_L anion transition moment is rotated by 10-15 degrees (relative to WT) toward the transition moment of P, and that the rotation is insensitive to mutagenic replacement at L104. Room temperature and low temperature linear dichroism studies also exhibit evidence that the Qy transition moment of β_L is rotated with respect to the C_2 symmetry axis of the protein. One interpretation of these results is that the molecular framework of β_L is rotated in its binding site when compared to H_L. *Support by NIH and NSF. [1]C. Kirmaier et al.(1991) *Science* 251, 922; [2]L. Hanson et al.(1987) *Prog. Photosyn. Res.* 3, 311; [3]M.E. Michel-Beyerle et al.(1988) *Biochim. Biophys. Acta* 932, 52.

M-PM-K4

EPR AND ENDOR STUDIES OF Q_A^- IN REACTION CENTER SINGLE CRYSTALS FROM *RB. SPHAEROIDES* R-26 IN WHICH IRON WAS REPLACED BY Zn.*

((W. Lubitz)) Max-Volmer-Institut, Tech. Univ., Berlin, D-1000 Berlin 12, Germany; ((R.A. Isaacson, E.C. Abresch and G. Feher)) Physics Dept., Univ. of Calif., San Diego, La Jolla, CA.

Single crystals of reaction centers (RCs) from *Rb. sphaeroides* R-26 biosynthetically enriched in zinc (25% Zn, 75% Fe) were grown as described (1). Reduction of the crystals with sodium dithionite yielded the anion radical of the primary quinone acceptor, Q_A^- (2). The angular dependences of the EPR and ENDOR spectra were measured at 17 °C with H_o in the ab plane. The following preliminary results were obtained: $g_{min} = 2.0028$ (1), ΔH (ptp der.) = 4.3 G, $g_{max} = 2.0058$ (1), $\Delta H = 5.1$ G. The ^{1}H-ENDOR spectra with H_o along the g_{min} and g_{max} axes are shown in the figure. Experiments are in progress to determine the angular dependence in the other 2 crystallographic planes. An analysis of these data will yield the values and axes of the electronic g- and hyperfine tensors. From these and the known 3-dimensional structure (1) the direction of the hydrogen bonds and distances of the ^{1}H nuclei to the quinone oxygens will be deduced. (1) J.P. Allen, G. Feher, T.O. Yeates, H. Komiya and D.C. Rees (1987) *PNAS USA* 84, 5730. (2) G. Feher, R.A. Isaacson, M.Y. Okamura and W. Lubitz (1985) in *Antennas and Reaction Centers of Photosynthetic Bacteria*, M. Beyerle, Ed., Springer-Verlag, Berlin, pp. 174. *Supported by DFG (Sfb 312), NSF (DMB 89-15631) and NATO (CRC 910468).

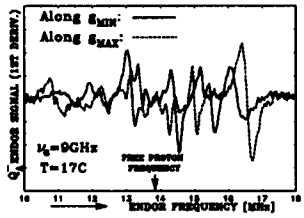

M-PM-K5

UV DIFFERENCE SPECTRUM ASSOCIATED WITH SLOW PROTON UPTAKE IN GLU-L212→GLN MUTANT RCs FROM *Rb. sphaeroides*.*

((P.H. McPherson, M.L. Paddock, M.Y. Okamura and G. Feher)) Physics Dept. 0319, Univ. of Calif., La Jolla, Ca 92093-0319.

In EQ(L212) RCs (Glu-L212→Gln) the uptake of one proton by doubly reduced Q_B is slowed dramatically to ~1 s^{-1} (pH 6.5), but the uptake of the other proton and the electron transfers to Q_B remain fast (> 1000 s^{-1}) (1,2). To determine which species protonates slowly, i.e., either $(Q_BH)^-$ or a residue that rapidly transfers a proton to $(Q_BH)^-$, we measured the UV absorbance changes that occur concomitant with the slow proton uptake. The resulting difference spectrum at pH 6.5 (Fig.) resembles that obtained from the protonation of $(QH)^-$ in 80% ETOH (3). This suggests that the slow protonation in the EQ(L212) RCs is associated with the reaction $(Q_BH)^- + H^+ \rightarrow Q_BH_2$. The discrepancy at $295 < \lambda < 325$ nm between the EQ(L212) mutant and model compound could be due to: i) overlap of RC absorbance changes (which presumably also cause the minima at 360 and 400 nm) with the $(Q_BH)^-$ absorbance; ii) differences in the absorbance of $(Q_BH)^-$ in the RC and $(QH)^-$ in solution. *(1) Paddock et al., (1989) PNAS 86 6602. (2) McPherson et al. (1990) Biophys. J. 57 404a. (3) Morrison et al. (1982) in "Function of Quinones in Energy-Conserving Systems" pp. 35 (Academic Press).* *Work supported by NSF and NIH.

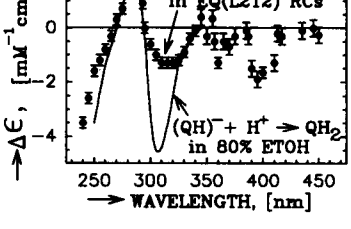

M-PM-K6

THE ROLE OF ASP-L213 IN PROTON TRANSFER IN BACTERIAL RCS FROM *RB. SPHAEROIDES*.*

((M.L. Paddock, S.H. Rongey, P.H. McPherson, A. Juth, G. Feher & M.Y. Okamura)) Physics Department, University of California, San Diego, La Jolla, CA.

Reaction centers (RCs) convert light into electrochemical energy through the double reduction and protonation of a bound quinone molecule Q_B. Several amino acid residues have been implicated in proton transfer to reduced Q_B, including Asp-L213 (1,2). Replacement of Asp-L213 with Asn [DN(L213)] resulted in a dramatically reduced proton/electron transfer $k_{AB}^{(2)}$ (Table) consistent with slowed proton transfer. The charge recombination k_{BD} was also reduced (Table) indicating a stabilized Q_B^-. Replacement with Glu [DE(L213)], a similar residue to the native Asp, only partially restored $k_{AB}^{(2)}$, but not k_{BD}. A spontaneous revertant, containing the replacements Asp-L213→Asn and Arg-L217→Cys [DN(L213)/RC(M233)], results in the removal of a positive charged residue; it displayed partially restored $k_{AB}^{(2)}$ and restored k_{BD}. These results suggest that two different effects are important for proton transfer: i) a contiguous proton transfer chain is important, as shown by the faster $k_{AB}^{(2)}$ observed in the DE(L213) compared to the DN(L213) RCs and ii) proper electrostatics near Q_B are important, as shown by the faster $k_{AB}^{(2)}$ observed in the revertant. **Thus, Asp-L213 is important for its role as a component of a proton transfer chain as well as for its role in establishing proper electrostatics for fast proton transfer.** (1) Rongey *et al.* (1991) Biophys. J. 59, 142a. (2) Takahashi & Wraight (1990) BBA 1020, 107-111. *Supported by NSF and NIH.

Rate constant (measured in s^{-1})	Native	DN(L213)	DE(L213)	DN(L213)/ RC(M233)
$k_{AB}^{(2)}$ ($DQ_AQ_B^- + 2\,H^+ \rightarrow DQ_AQ_BH_2$)	1500	0.25	16	80
k_{BD} ($D^+Q_AQ_B^- \rightarrow DQ_AQ_B$)	0.7	0.04	0.02	1.8

M-PM-K7

THE PROTON-COUPLED ELECTRON TRANSFER REACTION $Q_A^-Q_B + 2H^+ \rightarrow Q_AQ_BH_2$ ($k_{AB}^{(2)}$) IS ACCELERATED BY ASP RESIDUES AT L213 OR M44 IN REACTION CENTERS FROM *RB. SPHAEROIDES*.*

((S. H. Rongey, M. L. Paddock, G. Feher and M. Y. Okamura)) Physics Dept., Univ. of Calif., San Diego, La Jolla, CA. 92093

Replacement of Asp-L213 with Asn in the reaction center (RC) from *Rb. sphaeroides* drastically slowed $k_{AB}^{(2)}$, resulting in a photosynthetically deficient mutant (1,2). This effect on $k_{AB}^{(2)}$ is reversed by the additional mutation Asn-M44 → Asp, restoring photosynthetic viability to the mutant bacteria consistent with recent results from a mutant of *Rb. capsulatus* (3). This double mutant is analogous to *Rps. viridis* which has Asn at L213 and Asp at the position homologous to M44. Another mutant that had Asp residues, at both the L213 and M44 sites, exhibited nearly a 10 fold increase in $k_{AB}^{(2)}$ over the native rate. These results show that an Asp at either L213 or M44 provides near native $k_{AB}^{(2)}$ rates and that Asp residues at both sites results in an even faster rate. Measurements of the stability of Q_B^- (as in 2) indicate the Asp residues at L213 and M44 are negatively charged. **Thus, the proton-coupled electron transfer reaction $k_{AB}^{(2)}$ is accelerated by the presence of negatively charged Asp residues near Q_B.** *Supported by NSF and NIH. (1) S.H. Rongey, *et al.* (1990) *Biophys. J.* 59, 142. (2) E. Takahashi and C.A. Wraight (1990) *B.B.A.* 1020, 107. (3) D.K. Hanson, *et al.* (1992) *Photosyn. Res.* 32, 147.

Strain	Residue (Charge) L213	Residue (Charge) M44	$k_{AB}^{(2)}$ (s^{-1})
DN(L213)	Asn	Asn	0.25
Native	Asp (-)	Asn	1,500
DN(L213)/ND(M44)	Asn	Asp (-)	1,300
ND(M44)	Asp (-)	Asp (-)	13,000

M-PM-K8

CHIMERIC MUTAGENESIS OF *RB. CAPSULATUS* REACTION CENTERS INCORPORATING CHLOROFLEXUS AURANTIACUS SEQUENCE.

((D.M. Gallo, A.K.W. Taguchi, N.W. Woodbury)) Department of Chemistry and Biochemistry and the Center for the Study of Early Events in Photosynthesis, Arizona State University, Tempe, AZ 85287-1604

In the reaction center (RC) of photosynthetic bacteria, replacement of the axial His ligands of the special pair with nonpolar alkyl residues leads to the incorporation of bacteriopheophytin (Bpheo) in place of bacteriochlorophyll (Bchl). Replacement of the His ligands of the monomer Bchls (B_A and B_B) in *Rhodobacter capsulatus* with Leu has been performed, but RCs from these mutants were not stable to conventional isolation procedures (Bylina et al. (1990) *Biochem.* 29, 6203). *Chloroflexus aurantiacus* contains a Leu at the position of the B_B His ligand found in purple nonsulfur bacteria and a Bpheo is in the B-branch monomer binding pocket. Based upon sequence homology and structural information, the B-branch monomer binding pocket of *Rb. capsulatus* was replaced with the homologous region from *C. aurantiacus*. The replacement contained the following changes: Val M171→ Glu, Pro M174→ Ala, Tyr M175→ His, Phe M176→ Lys, Ser M179→ Ala, His M180→ Leu. This mutant, CAR 1.0, was not able to grow photosynthetically, and RCs were unstable to isolation. Photosynthetic revertant analysis yielded nineteen isolates, all of which appear to be second-site revertants, not involving the α, β, L and M genes of the *puf* operon. RCs were isolated from several of the revertants and they all exhibited similar characteristics. Most notable, is an apparent splitting of the Q_Y monomer Bchl peak. The two resulting transitions are at approximately 785 nm and 800 nm. Also, the oscillator strength of the Bpheo Q_Y transition is increased relative to that of P. Light-dark difference spectra of RCs and chromatophores indicate that the RCs can undergo primary electron transfer. Further purification and cofactor analysis are currently underway.

VISUAL RECEPTORS I

M-PM-L1

VISUAL TRANSDUCTION IN TRANSGENIC MOUSE RODS EXPRESSING DIFFERENT FORMS OF TRANSDUCIN.

((C. Makino[1], D. Baylor[1], J. Lem[2], M. Simon[2], C. Raport[3], J. Hurley[3])) [1]Dept. Neurobiology, Stanford Univ., [2]Div. Biology, California Inst. Technology, [3]Dept. Biochemistry, Univ. Washington.

In visual transduction the G-protein transducin couples photoexcitation of rhodopsin to phosphodiesterase (PDE) activation. Active PDE hydrolyzes cGMP which causes cationic channels to close and the photoreceptor to hyperpolarize. How do the number of copies of transducin and the speed of transducin shutoff affect the kinetics and sensitivity of transduction? Mouse rods were induced to express a transgene encoding for rod transducin, cone transducin or mutant transducins with greatly reduced GTPase activities. Light responses of individual rods were then observed with suction electrode recording. At low levels of expression, transduction was little affected. Moderate expression of mutant cone transducin lowered the flash sensitivity without changing the response kinetics. The failure to change the light response was surprising. Possibly, mutant transducin was not activated as efficiently as wild type or mutant transducin's slow shutoff was compensated by feedback mechanisms. At higher expression the flash response was prolonged, the dark current was reduced and the flash sensitivity lowered further. (Supported by NIH grant EY05750).

M-PM-L2

THE EFFECT OF RECOVERIN-LIKE CALCIUM-BINDING PROTEINS ON THE PHOTORESPONSE OF RETINAL RODS.

((M. Gray-Keller[1], A. Polans[2], K. Palczewski[3] & P. Detwiler[1])) University of Washington, Dept. of Physiology & Biophysics[1] and Ophthalmology[3], Seattle, WA and R.S. Dow N.S.I. of Good Samaritan Hospital[2], Portland, OR.

In a rod photoreceptor the light-induced hydrolysis of cGMP leads to a decrease in internal [Ca^{++}] which promotes recovery of the photoresponse by stimulating the activity of guanylate cyclase (GC). *In vitro* biochemical studies suggests that recoverin, a 26 kDa Ca-binding protein in bovine ROS, mediates the low-Ca activation of GC and may facilitate recovery of the light response. To physiologically evaluate this proposal we dialyzed recoverin and two of its homologues into functionally intact ROS of Gecko lizard while simultaneously monitoring the light response using whole-cell recording. Recoverin, visinin and a 26 kDa Ca-binding protein (Gecko p26) were purified from bovine, chicken and Gecko retina respectively. Homology of Gecko p26 to recoverin and visinin is indicated by its reactivity with anti-visinin and anti-N-terminal recoverin antibodies. Gecko p26 was immunocytochemically localized solely to photoreceptor cells. ROS detached from their inner segments were dialyzed with standard internal medium containing ATP and GTP in the absence and presence of either recoverin, visinin or Gecko p26. All three Ca-binding proteins delayed rather than accelerated the onset of recovery, giving rise to a photoresponse larger in amplitude and slower in kinetics than cells dialyzed with control solution. The proteins had no affect on the resting dark current level which is a measure of basal GC activity. The addition of either calmodulin, calcium or BAPTA to standard internal medium did not mimic the suppression of response recovery observed with the 26 kDa proteins. Our observations do not support the proposal that recoverin mediates the low-Ca activation of GC. However, a delay in the onset of recovery is consistent with the proteins affecting turnoff of the transduction cascade, for example, by inhibition of rhodopsin kinase activity.

M-PM-L3

STRUCTURE AND LIGHT-INDUCED CONFORMATIONAL CHANGES IN SPIN LABELED CYSTEINE MUTANTS OF RHODOPSIN

(J.Resek, Z.T.Farahbakhsh, W.L. Hubbell and H.G.Khorana) Depts of Biology & Chemistry, MIT, Cambridge, MA 02139 and Jules Stein Eye Institute & Dept of Chemistry & Biochemistry, UCLA, Los Angeles, CA 90024-7008

Cysteine mutants of rhodopsin modified with a nitroxide spin label were used to examine protein structure and conformational changes upon bleaching. A rhodopsin "base" mutant was constructed in which the native cytoplasmic cysteines C140, C316, C322 and C323 were changed to serine. With this as a basis, 5 additional mutants were generated by placing single cysteines in rhodopsin cytoplasmic loops at positions 62, 65, 140, 240 or 316. The mutants were expressed in COS cells, regenerated with 11-*cis* retinal and purified to give a 280/500 nm ratio of 1.6-1.9. Each of the mutants was modified with a sulfhydryl-specific spin label and EPR spectra were recorded in lauryl maltoside (LM) and digitonin (Dig). In the base mutant, 0.25 moles of label were incorporated per mole of chromophore, whereas in the mutants with single cysteine residues, 1.3-1.6 moles of label were incorporated per mole of chromophore. Both the molecular mobility and the collision rates of the nitroxides with chromium oxalate indicated that residues 65, 140, 240 and 316 were exposed to the aqueous environment while the mobility of the nitroxide at position 62 indicated that this site lies in the protein interior. Changes in rhodopsin conformation upon bleaching were examined in Dig and LM. In Dig, bleaching arrests the protein at MI, and produces little change in the mobility of the attached nitroxides. In LM, MII is the dominant species and significant changes were detected at C140 and C316. These data indicate that the light-induced conformational changes in the cytoplasmic loops do not take place before MII formation.

(Supported by grants NIH GM28289 and AI 11479 (H.G.K.), NIH EY06189 (J.R.), and NIH EY05216 (W.L.H.)).

M-PM-L4

ACTIVATION AND REGENERATION OF BOVINE RHODOPSIN IN DETERGENT MICELLES.

((S.Subramaniam, R.R.Franke†, A.V.Kiselev)) Johns Hopkins University School of Medicine, Baltimore, MD 21205 and †Rockefeller University, New York 10023.

Using a pH electrode, we have measured protonation changes that accompany light activation of purified bovine rhodopsin solubilized in 0.1% dodecyl maltoside. At pH 7.1, light absorption triggers a net proton release from rhodopsin into the aqueous medium (τ~ 20 sec), whereas at pH 5, a rapid (τ ~1sec) protonation of rhodopsin is observed. Illumination at intermediate pH values results in a superposition of the release and uptake signals, indicating that different side chains are involved in the two events. Upon illumination of rhodopsin at pH 7.1 in the presence of GTP and purified transducin, GTP is hydrolyzed as detected by a net proton release. Addition of phosphodiesterase and cGMP to this mixture results in cGMP hydrolysis. These observations show that it is possible to functionally reconstitute rhodopsin/transducin/phosphodiesterase interactions in dodecyl maltoside micelles. To study rhodopsin regeneration, we have measured chromophore formation upon addition of 11-cis retinal to bleached purified opsin in egg PC, DMPC or DPPC bilayers. At 18°C, where egg PC is above, and DMPC, DPPC are below their respective chain melting temperatures, >80% regeneration is observed in egg PC, and <30% in DMPC and DPPC vesicles. However, in the presence of 0.6% CHAPS, ~60% regeneration is found with all three lipids, demonstrating that rhodopsin formation in bilayers requires a fluid membrane.

M-PM-L5

RHODOPSIN FUNCTION IS MODULATED BY PROPERTIES OF THE MEMBRANE LIPID BILAYER. ((Nicholas J. Gibson and Michael F. Brown)) Department of Chemistry, University of Arizona, Tucson, Arizona 85721.

We have tested the hypothesis that the characteristic lipid composition of biomembranes is associated with influences on the conformational state of intrinsic membrane proteins which govern essential biological functions. The key event in visual **signal transduction** involves the MI-MII conformational change of rhodopsin.[1,2] Lipid acyl chain length and degree of polyunsaturation, as well as lipid headgroup size and charge, have all been shown to affect the MI-MII transition. The nature of the forces exerted on rhodopsin by the membrane, however, has yet to be established. We have studied this question by incorporating rhodopsin into recombinant membrane vesicles of varying lipid composition. The extent of the MI-MII transition, for both recombinants and native rod outer segment membranes, has been measured using **flash photolysis** techniques. We have found that the pK for the MI-MII acid-base equilibrium depends on the lipid composition.[3] Lipid substitution experiments suggest that non-specific lipid-mediated **material properties** of the bilayer, particularly curvature and lateral stresses, are important determinants of rhodopsin function. [1]J.M. Beach *et al.* (1984) *Biophys. J.* 45:292a. [2]T.S. Wiedmann *et al.* (1988) *Biochemistry* 27: 6469. [3]N.J. Gibson and M.F. Brown (1991) *Photochem. Photobiol.* 54: 985.

Supported by NIH Grant EY03754.

HETEROLOGOUS EXPRESSION OF EXCITABILITY PROTEINS

M-PM-WS1-1

Workshop: Heterologous Expression of Excitability Proteins, S. Cheng, Genzyme Corp., Framingham, MA; R. Farley, USC, LA, CA; E. Huang, Caltech, Pasadena, CA; A. Karlin, Columbia U. Col. of Phys. & Surg., NY, NY; C. Miller, Brandeis U., Waltham, MA; H. A. Lester, (Organizer), Caltech, Pasadena, CA

The proteins of membrane excitability (voltage-gated ion channels, ligand-gated ion channels, 7-helix receptors, ion-coupled transporters, and ATPase pumps) have been appreciated functionally for many decades, for they endow cells with the ability to respond to external stimuli and to generate their own stimuli. Recently, structure-function studies on these proteins have been dominated by the heterologous expression cycle, which allows researchers to begin with cDNA clones for these proteins, express them functionally in foreign cells, make cleverly chosen mutations at suspected important amino acids, and measure function of the altered protein. The next stages of knowledge will require new concepts and techniques. S. Cheng describes biochemical and functional characterization of CFTR expressed in the milk of transgenic mice. He hopes to express enough CFTR for high-resolution functional studies and for use as a therapeutic agent. R. Farley discusses the expression of Na, K-ATPase in yeast cells, with emphasis on the identification of a functional role for the β subunit. The data indicate that the structure of the β subunit influences the interaction of the pump with potassium ions. E. Huang describes attempts to construct synthetic neurons by expressing voltage-gated channels in previously unexcitable mammalian cells. New insights have derived from the attempt to describe voltage trajectories in these cells as the sum of known parts. A. Karlin describes a new tactic in oocyte expression: site-directed mutagenesis combined with clever group-specific reagent chemistry. His results suggest that β-strands, not α-helices, may line the ion channel at the nicotinic receptor. C. Miller discusses present systems for heterologous expression of potassium channels for protein-level biochemistry.

EXTRUDED LIPOSOMES. A RE-EVALUATION

M-PM-WS2-1

OSMOTIC CHARACTERISTICS OF EXTRUDED LUVs

Tom Madden, University British Columbia

M-PM-WS2-2

SHAPE CHARACTERIZATION OF EXTRUDED PHOSPHOLIPID VESICLES. ((Stéphane G. Clerc and T.E. Thompson)) Department of Biochemistry, University of Virginia, Charlottesville, VA 22908

Single lamellar phospholipid vesicles formed by extrusion (Hope et al., Biochim. Biophys. Acta 812:55-65, 1985) have been used in many types of experiments. It is generally supposed that these vesicles, usually in the size range of 100-200 nm diameter are spherical in shape. The shape, however, may with some components and system compositions be non-spherical. Knowledge of the actual shape is necessary in order to calculate the volume of the internal compartment and bilayer area per vesicle. Actual vesicle shapes for individual systems can and should always be determined by negative stain and freeze fracture electron microscopy. Changes in shape after preparation can be generated osmotically and followed by monitoring changes in fluorescence intensity of self-quenched fluorophores trapped in the internal aqueous compartment of the vesicles. Supported by NIH grant GM-14628.

M-PM-WS2-3

THE INFLUENCE OF MEDIUM COMPOSITION AND PREPARATIVE PROCEDURE ON SOLUTE ENTRAPMENT IN EXTRUDED VESICLES

Doug Pfeiffer, Ohio State University

M-PM-WS2-4

LIPOSOMES PREPARED BY FREEZE-THAW EXTRUSION VARY WITH LIPID AND AQUEOUS PHASE COMPOSITION--ONE LAB'S EXPERIENCE. ((A. Walter)) Dept. Physiol. & Biophys., Wright State University, Dayton, OH

In our quest for the perfect--i.e., easy to prepare in any quantity with no solvent or detergent--liposome, we utilized The Extruder™. The Extruder™ is a high pressure filter device used with polycarbonate filters with pores of well-defined diameter (Nuclepore). Lipid dispersed in aqueous solution as MLVs was first frozen and thawed repeatedly (10 x) to decrease the number of lamellae and average diameter of the MLVs and then the suspension was extruded 10x through 0.1 μm pore diameter filters. The resulting preparations were highly reproducible for a given set of conditions. PS formed spherical liposomes that were smaller than the filter diameter (70 nm vs. 100 nm). For many encapsulated solutions the apparent encapsulated volume was as expected for the diameter. However, dipicholinic acid (DPA) was excluded. When p-xylene-bis-pyridinium bromide (DPX, 90 mM) was in the aqueous phase the average diameter increased at least 10 nm. Extruded egg PC liposomes were larger than PS liposomes. Egg PC/cholesterol liposomes had both larger encapsulated volumes (mannitol) and diameters (gel filtration) than liposomes without cholesterol. Cryo-TEM revealed that the shape of PC liposomes was not necessarily spherical. These products of extrusion must indicate features of the physical chemical characteristics of each system and how these interact with the extrusion process.

M-PM-WS2-5

EXPERIENCES WITH A HAND-HELD, SYRINGE-DRIVEN EXTRUSION DEVICE. R. C. MacDonald Department of Biochemistry, Molecular Biology and Cell Biology, Northwestern University, Evanston, IL 60208.

Many research applications require milligram quantities of extruded liposomes in aqueous phase volumes of a few ml. For such purposes, a syringe-driven extrusion device provides a very convenient vesicle preparation procedure. Gas-tight syringes of up to 1 ml volume provide sufficient pressure to force liposome suspensions through polycarbonate filters having 100 nm diameter pores. To provide complete emulsification and to save time, a push-pull design is appropriate. For such operation, it is essential to support the filter on both sides. Furthermore, it is desirable to have a small hold-up volume. These requirements are easily met in an inexpensive device with which vesicles can be prepared in a minute or two. Lipid concentrations of at least 100 mg/ml can be extruded. Judging from the turbidity in the syringe in which the sample is originally loaded, there are some large particles that are never extruded to the far side, however, these comprise a very small portion of the total lipid, for recoveries from the other syringe are of the order of 95%. There seem to be no significant differences between vesicles extruded through a single filter and those extruded through two filters in tandem, although the approach to miminum turbidity as a function of number of passes is slightly different in the two cases. Freezing and thawing does not seem to be necessary. The vesicles produced by extrusion through 100 nm diameter pores are 80-100 nm, as measured by negative stain electron microscopy or quasi-elastic light scattering.

M-PM-WS2-6

Using Low-pressure Extruded Liposomes in the Laboratory. P. L. Yeagle, Department of Biochemistry, University at Buffalo School of Medicine, Buffalo, NY 14214

Low-pressure extruded liposomes, or large unilamellar vesicles (LUV), have been used in this laboratory for fusion experiments and for studies on the interaction of anti-viral peptide fusion inhibitors with bilayer surfaces[1]. They have advantages over LUV previously used in that no detergent or solvent is left to contaminate the preparation. Low pressure extrusion is a slow, inefficient process, but does not lead to unusual vesicle morphologies. Perturbations to observed ^{2}H quadrupole splittings and to ^{31}P CSA are observed because the size of the LUV leads to some motional averaging of these powder patterns. Formation of LUV apparently does not lead to significant changes in lamellar-hexagonal II phase transitions, however.
This work was supported by grants from NIH (AI26800; DE05608).
[1] Virology, 182, 690-702 (1991); Biochemistry, 31, 3177-3183 (1992)

DNA ELECTROPHORESIS

M-PM-WS3-1

EFFECT OF POLYACRYLAMIDE GEL PORE RADIUS ON DNA MOBILITY ANOMALIES. ((Nancy C. Stellwagen)) Department of Biochemistry, University of Iowa, Iowa City, IA 52242.

The dependence of the anomalous mobilities of certain DNA restriction fragments on polyacrylamide gel pore radius has been studied, using molecular weight ladders prepared from normal and anomalously migrating 147 bp fragments from the plasmid pBR322. If the gel pore radius is increased by decreasing the acrylamide concentration at constant crosslinker ratio (the usual method of increasing gel pore size), the mobility anomalies decrease with increasing gel pore radius. However, if the gel pore radius is increased by decreasing the crosslinker ratio at constant acrylamide concentration, the mobility anomalies decrease with increasing gel concentration until the DNA radius of gyration and the gel pore radius are approximately equal, after which the mobility anomalies become independent of gel pore radius. Therefore, mobility anomalies are directly related to gel pore radius only when the polyacrylamide concentration is held constant. Supported by GM 29690.

M-PM-WS3-2

QUANTITATIVE IMAGING OF ELECTROPHORETIC GELS*. ((John C. Sutherland)) Biology Department, Brookhaven National Laboratory, Upton, NY 11973.

Gel electrophoresis is widely used to separate and characterize proteins, nucleic acids, and other biopolymers. However, most applications use only qualitative information due, in part to difficulties of quantitating data obtained from photographic and radiographic film. During the past decade, systems that record directly quantitative images of electrophoretic gels and blots have been developed and are coming into widespread use. I shall review: the labeling of biomolecules, the quantitative recording (without film) of their distribution in gels and blots following electrophoretic separations, and systems for the storage and analysis of such images. Examples of the use of charge-coupled devices for the quantitative imaging of fluorophore labeled DNA and photostimulable phosphor imaging of radiolabeled DNA in studies of DNA damage and repair, and genomic mapping will be presented.

*Supported by the Office of Health and Environmental Research, USDOE, and by grant HG00371 from the National Center for Genome Research, NIH.

M-PM-WS3-3
DNA ELECTROPHORESIS

Organizer: Mark M. Garner, National Institutes of Health

Speakers:
Y. L. Lyubchenko, University of Nevada, Reno
P. Serwer, University of Texas Health Sciences Center
J. Noolandi, Xerox Research Center of Canada

FROM STRUCTURE TO PERMEATION IN OPEN IONIC CHANNELS

M-PM-WS4-1

WORKSHOP 5

FROM STRUCTURE TO PERMEATION IN OPEN IONIC CHANNELS

Organizer: ((Robert S. Eisenberg))

The anatomy of channel proteins is becoming better known as the techniques of molecular biology yield structural results. The functions of channels are quite well known from measurements in the Hodgkin-Huxley and Neher-Sakmann traditions. A hierarchy of theories should be needed to link atomic structure of channels to their macroscopic function, starting with simulations of molecular dynamics of channel proteins and their contents, proceeding through stochastic analysis of ions in the channel's pore, ending with a macroscopic description of single channel currents as actually measured. Bob Eisenberg will present a *Poisson-Nernst-Planck* theory in which the electric field within the pore is calculated from channel structure, instead of being assumed *a priori*. This *PNP* theory predicts many characteristics of biological channels, although it describes a channel of just one conformation in which ionic points flow through each other. Duanpin Chen will show that the electric field--the barriers and wells of potential--in such a theory varies substantially with experimental conditions, producing many coupling phenomena and some gating phenomena observed in real channels and transporters. Olaf Andersen will describe the currents and fluxes in a gramicidin channel that a useful theory must predict.

M-PM-WS4-2

POISSON-NERNST-PLANCK *(PNP)* THEORY OF AN OPEN IONIC CHANNEL. ((Robert Eisenberg and Duanpin Chen)) Dept. of Physiology, Rush Medical College, 1750 W. Harrison, Chicago IL

The structure of an ionic channel is the location of its atoms and their permanent electric charge. The electric field within a channel's pore is determined by all types of charge, namely the permanent charge of the channel protein, the mobile charge of ions within the pore, and the induced charge in pore and protein. Permanent charge is significantly shielded by permeating ions whose concentration and flux in turn depend on the electric field. A channel and its contents form a thoroughly coupled system, requiring simultaneous analysis of electric field and electro-diffusion, as do semiconductors like transistors. Asymptotic analysis of a *PNP* theory gives surprising results. Even though its pore is always open, in just one conformation, and its ions are points, able to flow through each other, its net and unidirectional fluxes are ***not*** independent if the pore contains an access resistance or selectivity filter. Rather, the fluxes vary together, as bath concentrations are varied. The electric field changes shape because the shielding of the permanent charge varies: potential barriers can change into potential wells (i.e., binding sites) as concentrations change. In this way, fluxes are coupled to concentrations in the bath, and to one another, as they are in traditional single file channels or mediated transport systems.

M-PM-WS4-3

POISSON-NERNST-PLANCK *(PNP)* THEORY OF IONIC CHANNELS. ((Duanpin Chen and Robert Eisenberg)) Dept. of Physiology, Rush Medical College, 1750 W. Harrison, Chicago IL

PNP theory predicts many characteristics of biological channels, although it describes a channel of just one conformation in which ionic points can flow through each other. Rectification, saturation of conductance with concentration, and flux interactions arise naturally in the theory, if the pore contains an access resistance or selectivity filter, because the shape of the electric field changes with experimental conditions. The spatial variation (1) of ionic charge (2) of potential (3) and of the energy of the charge at that potential reveals how each characteristic of real channels can arise even in such an oversimplified model. When the permanent charge distribution has four maxima, as in thyristors or "Numa rings", three *IV* relations satisfy the steady-state equations. Two are stable. One contains few ions to shield the permanent charge or carry current, perhaps corresponding to a closed channel. The other contains enough ions to shield the permanent charge and carry a large current, perhaps corresponding to an open channel. The unstable state may describe a transient or inactivating channel. We have constructed and are integrating a time dependent version of the *PNP* theory to see if the evolution or switching of these states can account for the time dependent properties of channels.

M-PM-WS4-4

ION MOVEMENT THROUGH A SINGLE-FILING CHANNEL
((O. S. Andersen, M. D. Becker, R. E. Koeppe II, and J. Procopio))
Cornell Univ. Med. Coll., New York, NY 10021, Univ. Arkansas, Fayetteville, AR 72701, Univ. Sao Paulo, 05508 Sao Paulo, SP, Brazil.

We have examined the kinetics of alkali metal cation ion movement through gramicidin channels using either a combination of tracer flux and small-signal conductance measurements or single-channel current-(voltage,concentration) measurements. Based on X-ray scattering results of Olah et al. (*J. Mol. Biol.* 218:847, 1991) the results were analyzed in terms of 3-barrier-2-site models with either single or double ion occupancy (3B2S1I or 3B2S2I); these discrete state models were further enhanced by incorporating interfacial polarization (IP) and aqueous diffusion limitation (DL). Neither the 3B2S1I nor the 3B2S2I model was able to account satisfactorily for the current-(voltage,concentration) results in [Val^1]gramicidin A channels (0.01 to 5.0 M salt; 25 to 500 mV). Based on statistical model selection the most satisfactory discrete state model was 3B2S2I with the inclusion of both IP and DL. Using this 3B2S2I-(DL,IP) model one can account for the results. The model was tested using Monte Carlo methods, which demonstrated that the fit is robust. At low potentials the 3B2S2I-(DL,IP) model reduces to a simple 3B2S2I model, but with "lumped" rate constants that include the effects of DL. The tracer flux and small-signal conductance measurements could be fit to this model using rate constant that are comparable to the lumped rate constants. We have used the 3B2S2I-(DL,IP) model to understand how Trp→Phe substitutions alter channel function. The results show that a Trp→Phe substitution at the channel entrance alters all rate constants for ion movement through the channel - and the height of the energy barrier at the channel center.

M-PM-WS5-1
STRUCTURE AND FUNCTION OF CYTOCHROME bc_1 AND bf COMPLEXES
Organizer: Peter Rich, Glynn Research Institute, U.K.

OVERVIEW OF CURRENT BIOPHYSICAL AND GENETIC DATA RELATING TO STRUCTURE OF bc COMPLEXES
Dan Robertson, University of Pennsylvania, Philadelphia

Open Discussion of Structure including: STRUCTURE PREDICTION AND MUTANT STUDIES; X-RAY AND ELECTRON DIFFRACTION; SPECTROSCOPY INCLUDING EPR, ENDOR, CD, MCD; MODEL HAEM SYSTEMS

OVERVIEW OF CURRENT CONTROVERSIES ON THE MECHANISM OF THE bc COMPLEXES
Peter Rich, Glynn Research Institute, U.K.

Open discussion of Mechanism including: CHEMISTRY OF THE Q-REACTIVE SITES; ELECTROGENIC REACTIONS; MONOMER/DIMER QUESTIONS; DCCD AND PUMPING MECHANISM; SHORT AND LONG RANGE CONFORMATIONAL EFFECTS

THE ROLE OF ACCESSORY PROTEINS IN PROTEIN REFOLDING

M-PM-WS6-1
THE ROLE OF ACCESSORY PROTEINS IN PROTEIN FOLDING
Organizer: George Lorimer, E. I. du Pont de Nemours Co.

Speakers: G. Lorimer
J. Buchner, University of Regensburg, Germany
T. Kiefhaber, Stanford University Medical Center

MUSCLE MECHANICS AND ULTRASTRUCTURE

M-Pos1
N-TERMINAL ACTIN PEPTIDES INHIBIT FORCE AND VELOCITY IN SKELETAL AND CARDIAC MUSCLE.
((Joseph M. Metzger)) Dept. of Physiology, Univ. of Michigan, School of Medicine, Ann Arbor, MI 48109.

The functional binding domains of actin and myosin during muscle contraction are not well understood. Previous solution biochemical studies have provided evidence that the acidic amino acid rich N-terminal region of actin may be an important myosin binding site during contraction. The aim of the present study was to determine the functional domain(s) of the myosin binding site on actin by activating permeabilized cardiac myocytes and skeletal fibers in the presence of peptide sequences that correspond to the N-terminal region of actin. Initial studies centered on the highly conserved 18-28 amino acid sequence of actin. Maximum Ca^{2+} activated isometric force was depressed in a concentration dependent manner in the presence of this peptide with the effect being greater in cardiac than in either slow or fast skeletal fibers. Results also indicated that maximum shortening velocity was inhibited in the presence of the peptide. Upon removal of the peptide, force and velocity were restored to control values indicating the effects on contraction were fully reversible. Effects on contraction due to other N-terminal peptide fragments were also examined. Of these, peptide 1-9 was most effective in inhibiting force (K_{in} = 2.1 mM) and peptide 10-17 was the least effective (K_{in} = 9.1 mM). The effect of these peptides to inhibit contraction appears unrelated to the net charge since the inhibition of contraction due to peptide 18-28 (zero net charge; K_{in} = 5.4 mM) was intermediate to peptides 1-9 (-4 net charge) and 10-17 (-1 net charge). These results suggest that the N-terminal region of actin may represent a functional binding domain for myosin during contraction in both cardiac and skeletal muscle fibers.

M-Pos2
TROPONIN C AND ALTERED CA^{2+} SENSITIVITY OF CONTRACTION IN CARDIAC MYOCYTES FROM TRANSGENIC MICE.
((Joseph M. Metzger*, Michael S. Parmacek+, Eliav Barr+, Karen L. Cochrane#, Loren J. Field#, and Jeffrey M. Leiden+)) Dept. of Physiology*, Univ. Michigan, School of Medicine, Ann Arbor, MI 48109, Dept. of Medicine+, Univ. of Chicago, Chicago, IL 60637, and Krannert Institute of Cardiology#, Indiana School of Medicine, Indianapolis, In 46202

Force production falls precipitously during ischemia in the heart. The mechanism of this effect is unknown but appears to be due in part to ischemia-induced intracellular acidification. We tested here whether troponin C, the Ca^{2+} binding protein subunit of the thin filament regulatory system, may mediate the effect of low pH to depress contraction in heart. We studied individual cardiac myocytes obtained from transgenic mice in which the native cardiac isoform of troponin C was replaced by the skeletal isoform of troponin C to determine if the isoform of troponin C present in heart would alter low pH-induced contractile dysfunction. Our findings indicate that the Ca^{2+} sensitivity of contraction of cardiac myocytes that expressed skeletal troponin C was markedly less affected by reduced pH than that in native cardiac myocytes. Upon lowering pH from 7.00 to 6.20 the shift in the mid-point of the tension-$[Ca^{2+}]$ relationship (i.e. pCa_{50}, where pCa is $-\log[Ca^{2+}]$) was 1.27 ± 0.03 (n=7) pCa units in control cardiac myocytes and 0.96 ± 0.04 (n=11) pCa units in transgenic cardiac myocytes, a value significantly less than that in controls ($P < 0.001$). These findings demonstrate that TnC plays an important role in determining the profound sensitivity of cardiac muscle to acidosis.

M-Pos3

PHALLOIDIN-INDUCED TENSION AND ATPase CHANGES IN SKINNED STRIATED MUSCLE FIBERS AND MYOFIBRILS.

((Anna Bukatina*, Franklin Fuchs, and Yi-Peng Wang)) Department of Physiology, University of Pittsburgh School of Medicine, Pittsburgh, PA 15261 and *Inst. Theor. Exp. Biophysics, Russian Acad. Sci., Pushchino, Russia 142292.

We studied the effect of phalloidin (PH), an actin-stabilizing peptide, on the functional properties of skinned fibers and myofibrils from rabbit psoas (fast, FM), rabbit soleus (slow, SM), and bovine ventricle (cardiac, CM) muscle. Within 5-10 min. following the addition of PH to activated skinned fibers the FM exhibited a transient increase in tension (phase 1) followed by a relaxation (phase 2), and then an increase in tension (phase 3) (see also Bukatina and Morozov, 1979). With SM phase 3 was very small or absent. With CM phase 1 and 2 were very weak and phase 3 was dominant. The PH effect was generally reduced at low pCa. It is possible that time-dependent changes in force are related to the known (Cano, et al, 1992; Szczesna and Lehrer, 1992) time-dependent spread of PH binding from the ends of the thin filaments to the Z line. Myofibrillar ATPase activity was stimulated by PH, with maximal stimulation occurring at high pCa. The magnitude of the ATPase increase was correlated with the magnitude of phase 3 tension, this being greatest in CM. With the latter there was also an increase in Ca^{2+} sensitivity (~ 0.1 pCa unit). The fact that both PH and Ca^{2+} promote crossbridge cycling (see also Son'kin et al, 1983) suggests a crucial role for actin in contractile regulation. Supported by NIH grant AR 10551.

M-Pos4

PEPTIDERGIC ENHANCEMENT OF TENSION GENERATION IN CRUSTACEAN SKELETAL MUSCLE FIBERS.

((A. Romero, J. Monterrubio, L. Lizardi and C. Zuazaga)) Institute of Neurobiology, Univ. of Puerto Rico Med. Sci. Campus, San Juan, PR 00901

Mechanical activation of tonic flexor muscle fibers of the crustacean *Atya lanipes* is strictly dependent on extracellular Ca^{2+}, even though the fibers do not generate Ca^{2+} action potentials (Bonilla *et al.* Tissue & Cell 24: 525, 1992). Sulfhydryl alkylating agents induce Ca^{2+} action potentials and enhance mechanical responses (Lizardi *et al.* J. Membr. Biol. 129: 167, 1992). We have been investigating whether putative crustacean peptide cotransmitters have effects similar to those of the sulfhydryl specific reagents on *Atya* muscle. Using immunohistochemistry we found that proctolin-like peptides are contained within neurons which innervate the muscle. Bath-applied proctolin (10^{-6} M) increased 30 to 175% the isometric tension generated by a fiber in response to directly injected depolarizing current pulses (80-200 nA; 400 ms). The peptide's effect on depolarization-induced tension was found to be dose-dependent and to depend on extracellular Ca^{2+}. Proctolin had no effect on resting tension, did not change the resting membrane potential, and did not induce Ca^{2+} action potentials. These results suggest that proctolin enhances Ca^{2+} channel activity and, thus, tension. Proctolin's enhancement of Ca^{2+} channel activity is less than that produced by the sulfhydryl alkylating agents because it does not induce Ca^{2+} action potentials. Our results are compatible with the possibility that, in *Atya* muscle fibers, an intracellular source contributes significantly towards the elevation of the intracellular Ca^{2+} required for contraction. Supported by NIH (NS-07464, RR03051).

M-Pos5

2,3-BUTANEDIONE-MONOXIME (BDM) HAS SIMILAR EFFECTS ON NUCLEOTIDE TRIPHOSPHATE HYDROLYSIS IN SOLUTION AND ON THE MECHANICAL PROPERTIES OF MUSCLE FIBERS.

((Betty Belknap, Howard D. White, Ed Pate, and Roger Cooke)) Dept. of Biochem., Eastern Virginia Medical School, Dept. of Biochem. and CVRI, UCSF, and Dept. Math., WSU.

BDM has been shown by several laboratories to inhibit the contraction of muscle fibers. In order to more fully understand the molecular mechanism of this inhibition, we have made parallel studies of the affect of BDM upon the steady state kinetics of hydrolysis of a series of nucleoside triphosphate substrates by actomyosin-S1 in solution and on the mechanical properties of glycerinated muscle fibers. The primary effect of BDM on steady state hydrolysis of CTP and ATP in solution is a four-fold increase in both Kapp of actin activation of hydrolysis and S1 binding to actin measured by active enzyme centrifugation. BDM inhibits the maximum rates of hydrolysis of ATP and CTP by less than 30 percent. However, the maximum rates of hydrolysis of GTP and aza-ATP, substrates that are hydrolyzed more slowly than ATP by actomyosin-S1, are doubled by 30 mM BDM. Actin binding in the presence of GTP or aza-ATP is essentially unchanged. Similar effects are observed in skinned muscle fibers. BDM decreases both active tension and unloaded shortening velocity while utilizing ATP as substrate but increases both the active tension and the unloaded shortening velocities produced by GTP. The inhibition of effective substrates and enhancement of poor substrates are both consistent with BDM stabilizing an A.M.NDP.Pi state. Supported by NIH grants HL41776, AR36943, HL32145 and by AHA.

M-Pos6

EFFECT OF C-TERMINAL CALDESMON FRAGMENTS ON TENSION AND STIFFNESS OF RELAXED AND ACTIVATED ASYNCHRONOUS FLIGHT MUSCLE.

((GRANZIER, H.L.M+, LIN, J.J.*, WANG, C.-L. A.**, WANG, K+.)) +Clayton Found. Biochem. Inst., Dept. of Chem. & Biochem., Univ. of Texas, Austin TX 78712. *Depar.t of Biology, University of Iowa, Iowa City, Ia.52242 **Dept. of Muscle Research, Boston Biomedical Research Institute, Boston, Ma 02114. (Spon. by A. Brady).

Weakly-binding cross bridges have been proposed by several groups to represent an essential intermediate state for active force generation in vertebrate skeletal muscles. Our recent studies of insect (Lethocerus) flight muscle fibers that had been treated with gelsolin to remove thin filaments revealed the presence of weak bridges in relaxed insect flight muscle under physiological conditions (21-23°C and 195 mM ionic strength) (See our accompanying abstract). As a complementary approach, we have applied the technique introduced by Brenner et al. (1991) that uses caldesmon to inhibit cross-bridge interaction in vertebrate muscle. This technique is here refined by using cloned C-terminal fragments of both human fibroblast caldesmon (CAD39, Novy et al. 1991) and smooth muscle caldesmon (a 27 kd fragment beginning at Lys 579, Wang et al., 1991), that bind to actin and inhibit actomyosin interaction in solution.

We found that neither fragment affects passive tension of insect fibers while they both significantly depressed high frequency stiffness of passive fibers in a dose-dependent and reversible manner. The depression was largest at low ionic strength (40 mM) and a smaller but significant depression existed even at 195 mM. Active tension was depressed to a similar extent as passive stiffness. Both passive stiffness and active tension recovered after removal of caldesmon fragments by washing. Interestingly, the degree of stiffness depression at the various ionic strengths by the caldesmon fragments is similar to that measured after thin filament removal with gelsolin. Our results suggest that weak-binding bridges exist in relaxed insect flight muscle under physiological conditions. Insect flight muscle appears to be an attractive system to study the characteristics of the weak-binding cross-bridge.

M-Pos7

EFFECT OF ANTIBODIES AGAINST THE N-TERMINAL SEGMENT OF ACTIN ON STIFFNESS AND ACTIVE FORCE OF SKINNED RABBIT PSOAS FIBERS.

((B. Brenner*, G. DasGupta#, E. Reisler#)) *Univ. of Ulm, FRG; #UCLA, USA.

F_{ab}(1-7), antibody fragments against the first seven N-terminal residues on actin, were previously shown to inhibit binding of myosin subfragment-1 (S-1) to actin both in the absence and presence of nucleotides including MgATP (G. Gupta & E. Reisler, Biochem. 1991, 1992). In addition, in the presence of ATP acto-S-1 ATPase was inhibited but to a larger extent than expected from inhibition of S-1 binding to actin. It was concluded that F_{ab}(1-7) can act to inhibit both the binding of S-1 to actin in the presence of ATP and a catalytic step in the ATP hydrolysis cycle.

We diffused the F_{ab}(1-7) into skinned rabbit psoas fibers to examine whether these antibody fragments can also interfere with cross-bridge binding to actin and force generation. Measurement of rapid stiffness under relaxing conditions was used to examine the extent of cross-bridge attachment in preforce-generation states. We found that inhibition of active force is much more sensitive to F_{ab} than inhibition of relaxed stiffness. In the presence of 0.05-0.1mg/ml of the F_{ab}(1-7), force could be fully abolished both at high (170mM) and low (50mM) ionic strength, while relaxed stiffness was reduced by only 20-30%. At 2-4 times higher [F_{ab}(1-7)] relaxed stiffness was inhibited by some 70%. When active force was fully inhibited at the low ionic strength (<2% of original active force), fiber stiffness in the activating solution was still comparable to that in the relaxing solution at the same ionic strength. This suggests that the more effective inhibition of active force compared to relaxed stiffness does not result from a better inhibition of weak cross-bridge binding to actin at high Ca^{++}. Instead, at least part of the observed inhibition of active force by F_{ab}(1-7) apparently occurs without inhibition of weak cross-bridge attachment to actin and may result from interference at a point subsequent to weak attachment of cross-bridges to actin.

M-Pos8

CALMIDAZOLIUM BINDING TO TROPONIN (TN) DECREASES RELAXATION RATES IN SKINNED FROG MUSCLE FIBERS.

((Philip A. Wahr, J. David Johnson, and Jack A. Rall)) Dept. of Physiology and Dept. of Medical Biochemistry, Ohio State University, Columbus, OH 43210.

Mechanically skinned fibers from the tibialis anterior muscle of *R. temporaria* activated at 10° C with pCa 5.5 were made to relax by photolysis of 2 mM diazo-2, a caged Ca2+ chelator. The time to 20% relaxation, t_{20}, was 26 ± 2 ms (mean ± S.D.) with a rate constant in the exponential phase, r_c, of 31 ± 9 s^{-1}, N = 5. At 10° C, calmidazolium (2 μM) lowered the off rate of Ca2+ from the Ca2+ specific sites on purified TN C from 247 to 87 s^{-1} and on whole TN from 10.5 to 4.2 s^{-1}. Calmidazolium (5 μM) also slowed diazo-2 relaxation of skinned fibers to t_{20} = 38 ± 11 ms and r_c = 21 ± 3 s^{-1}, N = 5. In intact fibers, stimulated electrically to produce a brief tetanus, relaxation is much slower, with t_{20} = 155 ± 18 ms, and r_c = 17 ± 3 s^{-1}, N = 7. Thus: A) in skinned fibers the rate of Ca2+ dissociation from TN significantly affects the relaxation rate, and B) in intact fibers Ca2+ sequestration may be the rate-limiting step in relaxation.

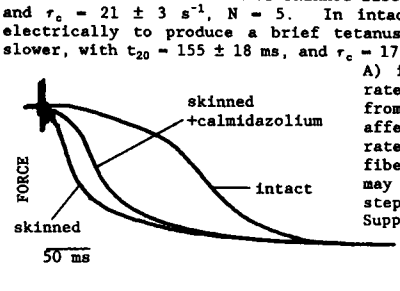

Supported by: AHA, Ohio Affiliate.

M-Pos9

MODEL OF THE RELEASE OF MYOSIN HEADS FROM ACTIN IN RAPIDLY CONTRACTING MUSCLE FIBERS. ((R. Cooke and E. Pate)) Dept. Biochem. and CVRI, UCSF, and Dept. Math., WSU.

In actively shortening muscle, a detached myosin cross-bridge is thought to attach to an actin binding site and exert a positive force through some powerstroke distance, h. The cross-bridge is then carried by movement of the filaments into a region where it exerts a negative, resistive force until it detaches from actin. At V_{max}, the sum of the positive forces produced by attached cross-bridges must balance the negative forces. We have previously shown that this balance allows one to relate h, V_{max}, and the rate of cross-bridge release at low substrate concentration, where the rate of cross-bridge release is limited by the rate of substrate binding. Data suggest that h is approximately 10 nm. At higher substrate concentration, the step limiting cross-bridge release in the negative force region is less certain, and models suggest that some negatively-strained cross-bridges are carried into regions where their free energy exceeds that of the detached state. We modify the previous model to include rapid detachment of cross-bridges whose free energy exceeds that of the detached state. This model explains two aspects of muscle contraction: (1) the rate limiting step in the negative force region is slow, and is of the order of magnitude of an isomerization which has been observed in studies of the kinetics of acto-S1 in solution. (2) at high shortening velocities, the observed rate of ATP hydrolysis decreases since a cross-bridge can interact with multiple actins before releasing products and binding another ATP. The model again suggests h is approximately 10 nm. Supported by NIH grants HL32145, AR36943 and by AHA.

M-Pos10

A COMPREHENSIVE MATHEMATICAL DESCRIPTION OF THE EFFECTS OF CHEMICAL INTERVENTIONS ON THE CROSSBRIDGE CYCLE OF MUSCLE ((M.P. Slawnych, C.Y. Seow, A.F. Huxley, and L.E. Ford)) University of British Columbia, Vancouver; University of Chicago, Chicago, IL 60637; Trinity Colllege Cambridge, UK (Spon. B.H. Bressler)

To better interpret our experiments on muscle, we developed a convenient computer program to write and solve a system of linear differential equations describing the rates of change of any arbitrary number of states in a crossbridge cycle. In the solutions to be presented, the rate "constants" for physical transitions (crossbridge attachment, power stroke, detachment) vary with the axial position of the myosin head relative to the actin attachment sites, whereas the rate constants of chemical transitions (substrate binding, hydrolysis, product release) are independent of this position. The scheme in Fig. 1 produces qualitative agreement with the effects of chemical interventions in skinned fibers. Both raising ADP and lowering ATP concentration increase isometric force to a greater extent than stiffness, suggesting a detention of bridges in a high force state (Biophys. J. **61**:A294). Raising phosphate depresses isometric force to a greater extent than stiffness and slows the rapid, partial (Phase 2) force recovery following a sudden shortening step, suggesting that phosphate detains bridges in a low force state (Seow & Ford, these abstracts). Additional transitions are needed to explain the velocity increase and more extensive and more rapid late force recovery seen in high phosphate at high pH. The program is used to predict experimental results obtained with different schemes.

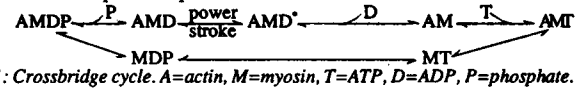

Fig. 1: Crossbridge cycle. A=actin, M=myosin, T=ATP, D=ADP, P=phosphate.

M-Pos11

THE SEGMENT-LENGTH-CLAMP TECHNIQUE INDUCES ERRONEOUS LENGTH-TENSION RELATIONS: A MATHEMATICAL MODEL STUDY. ((M.A.T.A. Sontrop, P.M.L. Janssen, B.G.V. van Heijst, E.L. DeBeer, P. Schiereck.)) Dept. Med. Physiol. & Sports Medicine, Utrecht University, NL - 3521GG Utrecht.

The segment-length-clamp technique maintains a constant muscle-segment length for isometric tension measurements. The feedback system used for length control is hampered by both electronic noise and limited resolution of the optical length-measuring system. This feedback noise can be considered as white noise added to the reference signal used in the control loop. As a result of this white noise the segment length varies continuously. The response of the crossbridge to these length changes is asymmetric: a small stretch induces a long-living force-generating state, while a small release is soon followed by detachment. The question arises whether this asymmetric behaviour significantly alters the true isometric force.

To quantify the effect of the noise on force, we simulated the effect of addition of white noise on two crossbridge models, the Huxley-Simmons model and the Julian-Sollins-Sollins model. The first model describes two crossbridge states, both able to generate force. In the second, the crossbridges are either in a strong-binding, weak-binding or detached state. Addition of a noise of 0.4% / half sarcomere to the crossbridge models has a significant impact: in the Huxley-Simmons model a redistribution of crossbridge states in favour of strong-binding takes place. Consequently, the measured force is predicted to increase by 35% over true isometric force. In the Julian-Sollins-Sollins model the pertubations induce a higher fraction of detached bridges, thereby decreasing force by 32% relative to isometric. In conclusion, the white noise present in the feedback system of segment-length-clamps alters crossbridge distribution, thereby generating erroneous length-tension relations.

M-Pos12

ON THE REGENERATION OF THE ACTIN-MYOSIN POWER STROKE IN CONTRACTING MUSCLE. Yi-der Chen and Bernhard Brenner. Laboratory of Chemical Physics, NIDDK, NIH, Bethesda, MD 20892, USA and Department of General Physiology, University of Ulm, Ulm, FRG.

The transient behavior of muscle in double- or multiple-step length perturbations as carried out experimentally by Lombardi et al (Nature 355, 638-641 (1992)) is simulated with a conventional crossbridge model, which has been shown previously (Eisenberg et al. Biophys. J. 29, 195-227 (1980)) to be able to account for many mechanical as well as biochemical data of muscle. The rate of regeneration of the quick tension recovery of the model is found to be fast and comparable to that measured by Lombardi et al. For multiple-step "stair-case" type length releases, the tension response reaches a steady state shape after 3 or 4 steps and the average ATP turnover is much slower than the regeneration of the quick tension recovery, as observed experimentally. Our simulation demonstrates that the experimental findings of Lombardi et al can easily be reproduced by this simple conventional crossbridge model, in which the completion of one work-producing power stroke is coupled to the hydrolysis of one ATP molecule. Thus, to account for the data of Lombardi et al, there is no need to assume that crossbridge can execute multiple power strokes per ATPase cycle, although crossbridges may well be able to do so. The mechanism that underlies the fast regeneration of the quick tension recovery in this conventional model is discussed.

M-Pos13

LOCATION AND CROSSREACTIVITY OF SCALLOP MINI-TITIN. ((P. Vibert, S. Edelstein, L. Castellani and B. Elliott)) Rosenstiel Center, Brandeis University, Waltham, MA 02254.

We have isolated mini-titins from both the striated and the smooth muscles of molluscs (Vibert et al., Biophys. J. 61, A286 (1992)) and have made antibodies to mini-titin from scallop striated muscle. Immuno-EM localizes mini-titin in scallop striated muscle to the distal region of the A-band, extending about one molecular length (~0.2 μm) in from the tips of the thick filaments. This antibody crossreacts with mini-titins in scallop smooth and Mytilus catch muscles, as well as with proteins in striated muscles from Limulus, Lethocerus (flight), and crayfish. It labels the A/I junction (I-region in Lethocerus) in these striated muscles as well as in chicken skeletal muscle. Antibodies to the repetitive region and also to the kinase domain of nematode twitchin crossreact with scallop mini-titin in Western blots and label the A/I junction of scallop myofibrils by immunofluorescence. EM of single molecules shows that antibodies to twitchin kinase bind to scallop mini-titin near the break in the rod where the "tailpiece" begins. The titin family thus includes mini-titins from molluscan striated and smooth muscles, various arthropod proteins (Limulus mini-titin; insect and crayfish projectins), as well as nematode twitchin. Moreover, a motif related to the twitchin kinase domain appears to be present in a number of invertebrate mini-titins, as well as in vertebrate titin.

M-Pos14

CAN CHEMICAL FIXATION BE AVOIDED WHEN CRYOSECTIONING STRIATED MUSCLE? ((J.F. Ménétret and R. Craig)) U. Mass. Med. Center, Worcester, MA 01655

We have cryosectioned skinned, cryoprotected scallop striated adductor muscle and lobster dorsal tail muscle using the Tokuyasu method. After thawing on a grid and removing the cryoprotectant, the sections have been observed by negative staining. Sections of lobster muscle fixed in the rigor state show the characteristic "chevron" structure and a first and sometimes second order of the 38nm layer line (ll); if chemical fixation is omitted prior to sectioning, the 5.9nm ll is also seen. Sections of unfixed rigor muscle, relaxed on the grid, show unlabelled actin filaments; accordingly the 38nm ll disappears while the 5.9nm ll remains. Sections of scallop muscle fixed in the relaxed state show a clear 14.5nm periodicity; if chemical fixation is avoided reflections on the 48nm layer line are also seen, indicating preservation of helical symmetry of the myosin heads around the thick filaments. Sections of unfixed muscle enabled us to avoid possible artefacts related to chemical fixation and may in the future give us the opportunity to study dynamic aspects of muscle structure. Sections obtained by these techniques may also be studied by cryo-electron microscopy. (Supported by a postdoctoral fellowship from MDA (JFM) and NIH grant AR34711 (RC).)

M-Pos15

ELECTRON MICROSCOPIC STUDIES OF ISOLATED CHICKEN SKELETAL MUSCLE THICK FILAMENTS. ((R. W. Kensler and J. Woodhead)). Division of Cell Biology and Biophysics, School of Biological Sciences, University of Missouri-Kansas City, Kansas City, MO 64110; and Department of Anatomy and Neurobiology, Medical College of Pennsylvania, Philadelphia, PA 19149.

Procedures for the isolation of relaxed skeletal muscle thick filaments with near-helically ordered arrays of myosin crossbridges have previously been reported for frog (Kensler and Stewart. 1983. J. Cell Biol. 96:1797), fish (Kensler and Stewart. 1989. J. Cell Sci. 94:391), and rabbit (Kensler and Stewart. 1992. Biophys. J. 61:A301). We report here that thick filaments from chicken pectoralis muscle can similarly be isolated with a well ordered near-helical arrangement of crossbridges as seen in negatively stained and platinum shadowed preparations. This periodicity is confirmed by optical diffraction and computed transforms of images of the filaments. These show a strong series of layer lines near the expected orders of a 43 nm near-helical periodicity as expected from X-ray diffraction (Huxley and Brown. 1967. J. Mol. Biol. 30:383). We further demonstrate that the periodicity, like that of rabbit thick filaments, is temperature sensitive. Our goal is to further analyze the structure and arrangement of myosin in these native filaments for comparison with the results of the electron microscope and X-ray diffraction studies of chicken S1-subunit crystals (Winkelmann, Baker, and Rayment. 1991. J. Cell Biol. 114:701).

M-Pos16

DIFFUSION OF FLUORESCENTLY LABELED PROTEINS INTO SKINNED SKELETAL MUSCLE FIBERS OBSERVED BY CONFOCAL MICROSCOPY. ((T. Kraft*, M. Messerli+, B. Rutishauser+, J.-C. Perriard+, T. Wallimann+, B. Brenner*)) *Univ. of Ulm, D-7900 Ulm, FRG; +ETH-Hönggerberg, CH-8093 Zürich, Switzerland.

To probe elementary mechanisms of muscular contraction, frequently it is necessary to diffuse proteins or protein-fragments into demembranated muscle fibers. Diffusion of proteins into skinned muscle fibers cannot easily be predicted since it depends on factors such as the size and shape of the proteins, the space available between the lattice of fiber proteins, and interactions of the proteins during diffusion with fiber proteins. The architecture of the sarcomeres is not homogeneous and thus may affect diffusion in different regions of each sarcomere differently, possibly resulting in defined routes of diffusion for some proteins.

Using the BioRad MRC-600 confocal microscope allowed optical sectioning of muscle fibers with 0.3-0.4 μm thickness such that background fluorescence coming from fiber parts out of the focal plane was minimized. Furthermore we could follow the time course of diffusion of fluorescently labeled proteins into the fibers in 3 dimensions with sufficient spatial resolution to detect specific diffusion routes for some proteins, reflecting (1) the size of the available space and (2) possible interactions with fiber proteins.

We used this method to follow diffusion of e.g. caldesmon, antibodies, creatine-phosphokinase, pyruvate-kinase and N-ethylmaleimide-modified myosin S-1 (NEM-S1) into rabbit psoas fibers. We found that equilibration for some proteins is surprisingly slow (Caldesmon-fragments several hours, NEM-S1 several days), suggesting that it is not simply limited by the size and shape of the protein but also by its interaction with fiber proteins (e.g. NEM-S1 binding to actin).

Furthermore, the use of confocal microscopy allows to follow the binding of proteins to distinct sites within each sarcomere with resolution that is sufficient to directly characterize specific binding patterns even along the myofilaments.

M-Pos17

ELECTRON MICROSCOPE STUDY OF CONTRACTING MUSCLE FIBERS DURING FAST MECHANICAL TRANSIENTS. ((Hernando Sosa, Greta Ouyang, and Hugh Huxley)) Rosenstiel Center, Brandeis University, Waltham, MA 02254.

In order to investigate possible structural changes in the cross-bridges associated with muscle force production, we have set up a system to rapidly freeze muscle fibers during contraction. Our system allows us to apply a length transient to the fibers at a predetermined time before freezing. This time interval can be set with a sub-millisecond precision. The aim of this project is to arrest the muscle ultrastructure immediately after the rapid tension recovery period that follows a sudden length change of about 1% applied to a contracting muscle (Huxley & Simmons 1971). Bundles of glycerinated rabbit psoas fibers were used for these experiments. One end of the fibers were attached to a fast moving lever in order to apply the length transients. Length changes up to 2% of the fiber length were complete in about 200 usec (Cambridge Technology Inc. Model 6350). The ability of the muscle fibers to recover tension after the length transient was checked in parallel experiments using a tension transducer with a frequency response of about 4.5 Khz attached to the other end of the fiber bundle. The bundles were frozen by plunging into liquid ethane (-177 to -180°C). The frozen bundles were freeze substituted in acetone containing 4% tannic acid, post fixed with osmium and uranyl acetate, plastic embedded and sectioned for EM observation. The electron micrographs obtained reveal excellent ultrastructural preservation and optical diffraction patterns showed layer lines up to 5.9 nm (actin). Preservation appeared to be particularly good when 15% glucose was used as a cryoprotectant. Many areas in isometric contraction showed regular series of approximately perpendicular lines extending from the thick to the thin filaments in the 11 planes, presumably representing the tail-end portion of myosin heads attached to actin with only weak labeling of the actin helical repeat, but conforming more closely to the axial repeat of the myosin backbone (14.3nm). Preliminary analysis of the optical diffraction patterns has not shown a large decrease in the 14.3 nm reflection intensity in released muscles as in X-ray diffraction studies of frog muscle, but a number of such specimens showed relatively stronger labeling of the actin 36 nm repeat. We are continuing the analysis of these patterns. Supported by NIH ARE38899 and by a grant from the Lucille P. Markey Charitable Trust (H.E.H.).

M-Pos18

TWO DIMENSIONAL X-RAY DIFFRACTION FROM SKINNED RABBIT MUSCLE FIBERS. **((L.C. Yu*, D.X. Gilroy*, S. Malinchik*, S. Xu*, B. Brenner*)) *National Institutes of Health. *University of Ulm, FRG.**

Earlier two dimensional X-ray diffraction studies (Matsuda & Podolsky, PNAS, 1984) showed that both myosin layer lines and rigor features were present while an estimated 80% of the cross-bridges were weakly attached to actin in skinned rabbit fibers under relaxing conditions at low ionic strength (μ) and low tem-perature. We reexamined with special emphasis on avoiding possible ATP depletion in the fibers as the cause for rigor-like features. Diffraction patterns were recorded by an imaging plate detector system. The bundles produced similar equatorial intensities, throughout the exposure (≈ 2 hr), as previously seen in our single fiber results. Under low μ, 5°C, relaxing conditions, myosin layer lines up to 6 orders, some with distinct maxima, were recorded but prominent actin reflections associated with rigor were absent. In lowering μ from 100mM to 30mM under relaxing conditions, the myosin layer lines become stronger and sharper. However, most prominently, the intensity of meridional reflections at 215Å increased by ≈ 5 fold, while meridional 143Å reflection appeared to decrease slightly. The results suggest that weak attachment of cross-bridges and/or lowering of μ appear to affect projected mass and distribution of cross-bridges at the surface of the thick filament and also affect the ordering of the filament lattice.

M-Pos19

THE ORGANIZATION OF MYOSIN/PARAMYOSIN FILAMENT FROM CRAYFISH ABDOMINAL FLEXOR MUSCLE. ((M.Chen,H.B.Li*,A.Y.Li, N.H.Zhou,F.R. Yang*)) Shanghai Institute of Physiology, Chinese Academy of Sciences,Shanghai 200031,China. *Computer Center,Shanghai Medical University, Shanghai 200032, China.

Electron microscopic observations on the crayfish (Procambarus clarkii) abdominal flexor muscle revealed the significant differences in the sarcomere characteristics and myofilament arrangement between superficial and deep flexor (Y.M.Zhong, S.K.Huang & M.Chen, A.Biol.Exp.Sinica, 24:329, 1991). Further electrophoretic analysis of isolated thick filaments and protein purification and immunochemical localization of myofibrils indicate that the thick filament from crayfish contains myosin and paramyosin.

Electron micrographs of transverse section of thick filaments from crayfish deep abdominal flexor muscle have been analysed with computer image processing techniques. The rotational power spectra of the filaments show peaks for six-fold rotational frequences. The rotational averaging image of transverse section of thick filament exhibits that the mantle of thick filament is made of 12 subfilaments which arrange in six groups. Similar studies are underway using crayfish superficial abdominal flexor muscle.

The Project is Supported by National Natural Science Foundation of China.

M-Pos20

STRUCTURAL CHANGES IN CROSS-BRIDGES OF SKINNED MUSCLE FIBERS ACTIVATED BY PHOTOLYSIS OF CAGED Ca^{2+} AND RAPIDLY FROZEN FOR ELECTRON MICROSCOPY ((J.M. Murray, T.D. Lenart, C. Franzini-Armstrong & Y.E. Goldman)), Univ. of Pennsylvania, Phila., Pa. 19104.

To investigate the structural changes underlying the cross-bridge power stroke we applied time-resolved electron microscopy and computerized image processing to chemically skinned fibers from frog sartorius muscle during rapid activation. Single fibers were activated from the relaxed state by photolysis of DM-Nitrophen (Kaplan & Ellis-Davies, *PNAS* 85:6575, 1988), and ultra-rapidly frozen at various times after activation (Lenart et al. *Biophys. J.* 61:A286, 1992). Samples were freeze substituted in 0.1% tannic acid and 4% OsO_4 in acetone, and embedded in araldite. Electron micrographs from overlap zones were digitized, orthogonalized to remove shear, and scaled to equalize the spacing of the 14.3 nm meridional spot of the Fourier transform. Active cross-bridges showed many shapes and angles; many were perpendicular to the fiber axis. Average power spectra (analogous to diffraction patterns) were obtained by summing the magnitudes of 17-96 Fourier transforms of overlap regions for samples frozen in the relaxed and rigor conditions and at 12 ms, 33 ms, and 220 ms after photorelease of Ca^{2+}. In the average power spectra 12 ms after Ca^{2+} release, the 14.3 nm meridional reflection was weaker than in relaxed fibers, but then strengthened again during tension development. The 22 and 43 nm meridional intensities were weak after activation. A 36 nm actin layer line appeared at 12 ms and became more intense as tension developed, but remained weaker than in rigor. At 33 and 220 ms, the 43 nm and 36 nm layer lines were separated by a clear gap. After normalization, difference power spectra were obtained by subtraction. Power spectral differences between relaxation and the three time points after Ca^{2+} release showed gradual intensification of the 36 nm layer line as force developed. The results show that despite the highly variable shape of active cross-bridges, they adopt a degree of actin helical periodicity. This order increases during active force development and is maximal in rigor. Supported by HL15835 to the PMI and by the MDA.

M-Pos21

DISTRIBUTION OF MASS IN ACTIVATED, FREEZE-SUBSTITUTED MUSCLE STUDIED IN CROSS SECTIONS. ((K. Hirose, J. M. Murray, C. Franzini-Armstrong & Y. E. Goldman)) University of Pennsylvania, Philadelphia, PA 19104.

X-ray diffraction studies show movement of mass from thick to thin filaments when a muscle fiber goes from the relaxed to active or rigor states. However, possible mirror-asymmetry in azimuthal position of cross-bridge mass around the thin filaments would not be seen in X-ray data. EM images of thin cross sections should retain this asymmetry. Glycerinated rabbit fibers were slam-frozen at various times after photolysis of caged ATP in the presence of calcium (Hirose et al., Bioph.J., 59, 577a, 1991). Control fibers were frozen in the relaxed or rigor states. Frozen samples were freeze-substituted and embedded in araldite. Cross-sectional micrographs of overlap regions were digitized and interpolated onto a regular hexagonal lattice. The computed diffraction pattern averaged from several regions of rigor fibers showed significant peaks up to ~6 nm. The unit cells of the interpolated images were six-fold-rotationally averaged. Density maps from several areas were averaged to form the final image. Mirror asymmetry was strongly present in rigor, but not apparent in active fibers at 50 ms. The difference maps of (rigor-relax) and (active-relax) showed density loss after release of ATP at the thin filament sites and gain near the thick filament surface. The map of (50ms-rigor) showed asymmetric density distribution with respect to the line connecting thick and thin filaments, with some density gain between neighboring thin filaments and loss near the thick filament surface. These results suggest that the average position of the cross-bridges in active fibers differs from rigor both laterally and azimuthally. Rigor, but not active (50ms) cross-bridges slew around the thin filament preferentially in one direction. Supported by NIH HL 15835 to PMI and NSF MCB-9113313 to JMM.

M-Pos22

X-RAY DIFFRACTION PATTERNS FROM INSECT FLIGHT MUSCLE IN THE ISOMETRICALLY CONTRACTING STATE. ((M.K. Reedy * & T.C. Irving#)) *Dept. Cell Biology, Duke University, Durham NC, 27710; #MacCHESS, Dept. of Biochemistry, Cornell University, Ithaca NY, 14853.

Our goal is to resolve to 5 nm and eventually to 5 ms, the structural changes accompanying force production in asynchronous fibrillar insect flight muscle (IFM) by combining quick-freeze electron-microscopy with time-resolved synchrotron X-ray diffraction (TR-SXRD) on the high flux wiggler beam lines at CHESS. Previous TR-SXRD of contracting IFM has been restricted to a few strong reflections, as "seen" by 1-D detectors during transient stretch-activated contractions. We seek full 2-D patterns from sustained steady-state contractions. By using high [Ca^{2+}] (1mM) and low ionic strength (~40-100 mM) we have obtained strong steady isometric contractions from IFM with lifetimes of many 10's of seconds. Complete 2-dimensional axial patterns could be obtained on a 50 cm camera (CHESS A-1 station) in 30 s on Fuji image plates. Similar patterns could be obtained on the new 2m small-angle camera (CHESS F-1 station) in 50-200 ms. Contracting muscle patterns show qualitative differences from relaxed patterns including intensification of (1) reflections on the 19.3 nm layer line and (2) those on the 11th actin layer line at 7.03 nm. We are now poised to look at this state in more detail. 5 ms time resolution by TR-SXRD seems achievable by summing, and may be used to explore transients associated with steady-state contraction, including those imposed by sudden length steps.
Supported by MDA &NIH AR14317 (MKR) and by NIH RR01646-09 (MacCHESS)

M-Pos23

TWO DIMENSIONAL X-RAY DIFFRACTION DIAGRAMS FROM CONTRACTING MUSCLE RECORDED ON IMAGING PLATES WITH MILLISECOND TIME RESOLUTION USING SYNCHROTRON RADIATION. ((Hugh Huxley, Alex Stewart & Hernando Sosa)) Rosenstiel Center, Brandeis University, Waltham, MA 02254, ((Tom Irving)), MacCHESS, Dept. of Biology, Cornell University, Ithaca, New York 14853.

We have assembled a small angle X-ray scattering system for muscle research on the 25 pole wiggler beam line F1 at the Cornell Synchrotron Radiation Facility (CHESS). This double-focused mirror monochromator beam line provides an exceptionally high total flux, approximately 10^{13} photons per second at 0.9Å wavelength. The beam is collimated by a remotely-controlled three slit system, and with a two meter flight tube between specimen and detector very clear patterns extending from the first myosin layer line at 429Å to beyond the actin 27.3Å meridional reflection can be recorded in a single exposure of 200 milliseconds or less. The specimen is scanned rapidly over the X-ray beam to spread out radiation damage, and no deterioration of the patterns is apparent during several such exposures. In order to achieve high time resolution, the X-ray beam is interrupted by a rotating metal disc with a slot in it of appropriate width. The rotation is accurately synchronized to a chosen time point during contraction which can be changed between successive contractions usually spaced about two or four minutes apart. A metal screen blanks off alternate halves of the imaging plate (centered on the X-ray beam) during successive contractions, so that images from the control and experimental conditions are collected on the two halves of the same image plate. The required total exposure can readily be built up from one or two millisecond time-slots during one or two such series. Ancillary beam shutters with higher X-ray absorption but correspondingly slower opening speeds were found to provide adequate protection against hard radiation which otherwise reaches the detector continuously. This system is being used to study the behavior of the entire 2D X-ray diagram during rapid structural transients in muscle, especially ones associated with Huxley-Simmons type quick releases, which may represent a partially synchronized population of crossbridges carrying out their working strokes. Supported by NIH ARE38899, by a grant from the Lucille P. Markey Charitable Trust (H.E.H.), and by NIH RR01646-09 (MacCHESS).

M-Pos24

ANALYSIS OF FACTORS THAT AFFECT EQUATORIAL X-RAY DIFFRACTION INTENSITIES FROM MUSCLE FIBERS. ((S.Malinchik and L.Yu)) NIAMS/LPB, NIH, Bethesda, MD 20892

Increases in the equatorial intensity ratio I_{11}/I_{10} has been widely used as an indication of crossbridge attachement. However, such interpretation is an oversimplification, as demonstrated previously (Lymn, Biohys. J., 1978; Yu, Biophys. J. 1989). In this study, three dimensional models are constructed which include both the thick and the thin filaments with various distributions of cross-bridges in the lattice. Parameters are chosen which may simulate various physiological conditions. The results further emphasize that attachment of cross-bridges is not the only factor that affects I_{11}/I_{10} ratio. For example, (i) radial movement of center of crossbridge shell surrounding thick filament could cause substantial decrease in I_{10} (≈50%) while I_{11} changes little (< 10 %); (ii) as the population of ordered cross-bridges surrounding thick filament decreases but that of disordered cross-bridges increases in the lattice: I_{10} decreases little (< 20%) while I_{11} could increase by 150%; (iii) if azimuthal distribution of crossbridges surrounding thick filament becomes anisotropic and predominantly along myosin-actin lines: I_{10} ≈ constant while I_{11} could rise by 130%. Furthermore, decrease in lattice spacing without changing cross-bridge configurations results in increases in both I_{10} and I_{11} leading to an increase in I_{11}/I_{10}. Disorder of thick filaments results in decrease in both I_{10} and I_{11} but similar disorder of thin filaments results in increase in I_{10} and decrease in I_{11}. To distinguish causes of change, one could follow changes in individual intensities, and further, study intensities of higher equatorial orders, reflection widths and background levels.

M-Pos25

CHANGES IN MASS DISTRIBUTION IN THE LATTICE OF FROG SKELETAL MUSCLE DURING THE SHIFT FROM RELAXATION TO CONTRACTION OR RIGOR. ((Q. Li, T. C. Irving and B. M. Millman)) Biophysics Group, Dept. of Physics University of Guelph, Ontario, Canada N1G 2W1 and MacCHESS, Dept. of Biochemisty, Cornell University, Ithaca NY 14853.

We have studied the contracting and rigor states of skeletal muscle by X-ray diffraction using both a laboratory source and 0.155 nm radiation from the CHESS synchrotron at Cornell University. Both muscle states involve an interaction between myosin heads and actin filaments. Equatorial patterns showing the first eight orders of the hexagonal A-band lattice (1,0 to 4,0) were obtained from frog sartorius muscles at rest and in contracting and rigor states. Difference Patterson diagrams were constructed which demonstrated a shift of the mass centres of myosin heads towards actin filaments during the change from relaxation to either contraction or rigor. The largest mass loss is from a region 13 nm from the centres of the myosin filaments. In the rigor case, the mass is lost from regions lying on the 1,0 planes, whereas this localization is less striking in the contracting case. These results support earlier results obtained from electron density reconstructions (Li et al., 1992, Biophys. J., 61:A302). When the lattice spacing is changed by either adding sucrose to the Ringer's solution or diluting the Ringer's solution, the intensity ratio of the 1,0 and 1,1 reflections is unchanged, but the absolute intensities of both reflections decrease linearly with the decrease in lattice spacing.

M-Pos26

THE MERIDIONAL X-RAY DIFFRACTION PATTERN FROM VERTEBRATE SKELETAL MUSCLE IN RIGOR. ((J-C. Chen, T. C. Irving, B. G. Nickel and B. M. Millman)) Dept. of Physics, University of Guelph, Ontario, Canada N1G 2W1 and MacCHESS, Dept. of Biochemisty, Cornell University, Ithaca NY 14853. (Spon. by G. Renninger)

Detailed X-ray diffraction patterns were obtained from glycerol-extracted rabbit psoas muscles in salt solution over a range of pH (5.5 - 8.4) using the high-energy synchrotron source at Cornell University (CHESS). Analysis of reflections along the meridian showed a series of reflections which could be indexed as either orders of the thick or thin filaments (periodicities: 43.2 and 5.50 nm respectively) or interference orders between the thick and thin filament periodicities. In particular, a reflection at 9.95 nm could only be ascribed to crosslinking between the thick and thin filaments. These observations and interpretation are similar to those made in the case of insect flight muscle (Holmes, et al., 1980, Proc. Roy. Soc. B 207:13-33). Clear sampling along the first meridional layer line (at 36.5 nm) could be observed in some patterns. Although not exactly matching the lattice spacing, this sampling appeared to be correlated with the equatorial lattice spacing, indicating three-dimensional order in the filament lattice of these muscles during rigor.

M-Pos27

BIREFRINGENCE OF MUSCLE.

((P.S. Blank, X. Wu and F.D. Carlson)) Johns Hopkins University, Baltimore, MD 21218.

Total birefringence, B, was measured during the relaxed and rigor states of single, skinned, rabbit psoas muscle fibers as a function of sarcomere length and temperature. Intrinsic birefringence, B_I, was measured using refractive index matching metrizamide solutions. Form birefringence, B_F, was calculated as $B_F = B - B_I$. At full overlap (15 C), B, B_I, and B_F, were significantly lower in the rigor state. This difference was consistent with an ~ 25 degree shift, away from the fiber axis, in the average cross-bridge orientation ($\Theta_{Rigor} = \Theta_{Relax} + 25$). At no overlap (15 C), B, B_I, and B_F were similar in the relaxed and rigor states; the average cross-bridge orientation was the same. The lower value of B at 2 C was consistent with an increase in the average cross-bridge orientation. In the relaxed state, B_I (15 and 2 C) decreased with increasing sarcomere length. In the rigor state, B_I (15 C) remained constant. Muscle birefringence is sensitive to cross-bridge orientation. These results, when combined with birefringence measurements on the active state, will be useful in distinguishing between models of crossbridge dynamics. Supported by USPHS 12803 to F.D.C.

M-Pos28

CONTRACTION-INDUCED MOVEMENTS OF WATER IN SINGLE FIBERS OF FROG SKELETAL MUSCLE.

((K. Trombitás†, P. Baatsen‡, J. Schreuder†, and G. H. Pollack.†)) †Center for Bioengineering, WD-12 University of Washington, Seattle, WA 98195, and ‡Department of Physiology, Catholic University of Louvain, Brussels, Belgium.

Although X-ray diffraction measurements imply almost constant filament separation during isometric contraction, such constancy does not hold at the cell level. Cell cross-section increases substantially during isometric contraction (Neering *et al., Biophys. J.* 59:926-932, 1991). This expansion could arise from accumulation of water drawn from other fiber regions, or from water entry into the cell from outside. To distinguish between these hypotheses, we froze single fibers of frog skeletal muscle that were jacketed by a thin layer of water. Frozen fibers were freeze-substituted, sectioned transversely, and examined in the electron microscope. In fibers frozen during contraction, we found large accumulations of water just beneath the sarcolemma, less in deeper regions, and almost none in the fiber core. Such gradients were absent or diminished in fibers frozen in the relaxed state. The water was not confined to the myofibril space alone; we found large water spaces between myofibrils, particularly near mitochondria. The pattern of accumulation, between myofibrils and around mitochondria, implies that the driving force for water movement lies outside the filament lattice, and may therefore be osmotic. The fact that the distribution was nonuniform—highest near the sarcolemma and lowest in the core—implies that the water was drawn from the jacket surrounding the cell. Thus, the contractile cycle may be associated with water entry into, and exit from, the cell.

M-Pos29

MYOSIN HEAD ORIENTATION IN SKINNED MUSCLE FIBERS MEASURED WITH A NOVEL BIREFRINGENCE-INTERFERENCE MICROSCOPE

((Neil Millar, Alf Månsson & Malcolm Irving)) Dept. of Biophysics, Kings College London, London WC2B 5RL UK.

Muscle fibres are birefringent: they have a higher refractive index for light polarised parallel to the fibre axis ($n_{||}$) than for light polarised perpendicular to the fibre axis ($n_{\perp}$). The birefringence of striated muscle is associated with the thick filaments, and changes in myosin head orientation cause changes in birefringence. Birefringence measurements can therefore be used to monitor changes in myosin head orientation in unmodified muscle fibers. Here we measure both **birefringence retardation** ϕ (the phase lag between the parallel and perpendicular components of light passing through the fiber), and **interference retardation** θ (the phase lag between light passing through the fiber and through the solution (refractive index n_{sln})). Dividing ϕ by θ, we obtain the **normalised birefringence** $(n_{||} - n_{\perp}) / (n_{||} - n_{sln})$. This quantity is more useful than conventional birefringence since it depends only on protein orientation, not on changes in fiber shape or volume. Measurements are made using a HeNe laser focused to a 6μm spot at the fiber, and retardations are measured electronically using de Sénarmont phase analysers (J.Microscopy, **108**,251,1976) allowing real time measurement of normalised birefringence. Normalised birefringence was constant (±5%) in different parts of a single glycerinated rabbit psoas muscle fiber even when the light path length through the fiber changed by a factor of 2. Normalised birefringence decreased by 11.2 ± 1.2% (mean ± sem, n=5, 15-20°C, μ=0.1M) in rigor compared to relaxing conditions. This corresponds to a change in the mean orientation of myosin heads of about 20°, consistent with previous conclusions (J.Mol.Biol. **210**,113,1989). Supported by Wellcome trust (UK).

M-Pos30

MAPPING ANGULAR TRANSITIONS OF CROSS-BRIDGES IN MUSCLE FIBERS USING MULTIPLE EXTRINSIC PROBES.

((Thomas P. Burghardt, Daniel J. Toft and Katalin Ajtai)) Department of Biochemistry & Molecular Biology, Mayo Foundation, Rochester, MN 55905.

Fluorescence polarization (FP) and electron paramagnetic resonance (EPR) spectroscopy are highly sensitive techniques for investigating the orientation of extrinsically labeled myosin cross-bridges in muscle fibers. In practice, their sensitivity to protein rotation depends critically on to orientation of the probe in the myosin-fixed reference frame. A cross-bridge rotation that rotates the bound probe about its symmetry axis will go undetected by FP and EPR. We combine data from different probes (both FP and EPR probes) that are variously oriented within the cross-bridge to remove this degeneracy. Combining data from multiple probes also permits us to extend to angular resolution of the individual probe angular distributions. With enhancements involving the use of luminescent/paramagnetic probes we extend the angular resolution to the theoretical limit. TPB is an Established Investigator of AHA. This work is supported by NIH (R01 AR 39288), NSF (DMB 88-19755), AHA (900644), and Mayo Foundation.

M-Pos31

MYOSIN HEAD ROTATION IN MUSCLE FIBERS MEASURED USING POLARIZED FLUORESCENCE PHOTOBLEACHING RECOVERY.

((Edward H. Hellen, Katalin Ajtai and Thomas P. Burghardt)) Department of Biochemistry & Mol. Biology, Mayo Foundation, Rochester, MN 55905.

The interaction of myosin with actin is of great importance in the mechanism of muscle contraction. In the rotating cross bridge model of muscle contraction a rotation of the myosin head while bound to actin generates the force causing contraction. Steady state fluorescence polarization results are consistent with this model, showing large differences in the orientation of myosin heads labeled with rhodamine for muscle fibers in the states of rigor, relax, active, and ADP. We are using polarized fluorescence photobleaching recovery (PFPR) to investigate the rate and range of rotation of the myosin head group in rabbit skinned psoas muscle fibers. Measurements have been made with muscle fibers specifically labeled at SH-1 with 5'-iodoacetamido tetramethylrhodamine in the static states of rigor, relax, and ADP, with the goal of making the measurement on active fibers. Results show that in the rigor and ADP states the myosin head is tightly associated with actin, and in the relax state the myosin head rapidly (faster than 200 microsec.) accesses a large but restricted range of orientation. TPB is an Established Investigator of AHA. This work is supported by NIH (R01 AR 39288), NSF (DMB 88-19755), AHA (900644), and Mayo Foundation.

M-Pos32

KINASE RELATED PROTEIN, A PROTEIN WHICH PROMOTES THE ASSEMBLY OF SMOOTH MUSCLE MYOSIN MINIFILAMENTS IN THE PRESENCE OF ATP. ((V.P.Shirinsky, A.V. Vorotnikov, K.G. Birukov, A.K. Nanaev, J.R. Sellers, M. Collinge, T.J. Lukas and D.M. Watterson)) Cardiol. Res. Cntr., Moscow, Russia.; NHLBI, NIH, Bethesda, MD. and Dept. of Pharmacol. Vanderbilt Univ. Nashville, TN.

The smooth muscle kinase related protein (KRP) is a low molecular weight acidic protein with amino acid sequence identity to the carboxyl terminal part of myosin light chain kinase (MLCK) from smooth muscle and nonmuscle tissues. This unusual relationship is the result of the KRP gene being located within the MLCK gene (Collinge et al. Mol.Cell.Biol. 12, 2359, 1992). We have found that chicken gizzard KRP forms complexes with unphosphorylated smooth muscle and nonmuscle myosin in vitro, but weakly binds to the phosphorylated myosins. KRP reverses the depolymerizing effect of ATP on unphosphorylated myosin and promotes the assembly of minifilaments of side-polar morphology as revealed by electron microscopy. KRP binds to HMM as well as myosin, but not to myosin rod or V8 protease generated S1 fragment, suggesting that KRP binds to the hinge region of myosin. Quantitation of Northern blots of KRP and MLCK mRNA's, and Western blots of KRP and MLCK protein indicate that the KRP:MLCK ratio is greater than 10:1 in gizzard tissue, indicating that KRP is as abundant as myosin in smooth muscle. Altogether the results are consistent with a model in which KRP is one of the "missing links" in smooth muscle biochemistry and plays the a structural role in stabilizing myosin filaments.

M-Pos33

MOLECULAR PROPERTIES OF MYOSIN LIGHT CHAIN KINASES REVISITED: ON ISOFORMS AND MODELS OF CALCIUM SIGNAL TRANSDUCTION ((T.J. Lukas, M. Collinge and D.M. Watterson)) Dept of Pharmacology, Vanderbilt University. Nashville, TN 37232-6600

We have used a multidisciplinary approach to elucidate the primary structure and functional domains of the calmodulin (CaM) regulated myosin light chain kinase (MLCK) from chicken smooth muscle and nonmuscle tissues. The CaM Regulatory Unit was shown (1-3) to be composed of overlapping, functionally coupled sequences referred to as the CaM binding or recognition segment and the autoinhibitory segment: AKKLSKDRMKKYMARRKWQKTGHAVRAIGRLSS. It was also shown (3) that the CaM Regulatory Unit is preceded by a linker sequence (NCTQCLQHPWLQKDTKNME) that couples the CaM Regulatory Unit to the catalytic domain. Substitution and deletion mutagenesis in this region produced a set of constitutively active enzymes with retention of substrate specificity. Recent replacement molecular models (4) are consistent with these prior reports (1-3). Most recently, we have used selective probes based on the MLCK gene (5) and site-directed antibodies to peptides in the nonmuscle MLCK sequence to selectively monitor the more abundant forms of MLCK in smooth muscle tissue extracts.

1. Lukas et al., 1986, Biochem. 25:1458-1464.
2. Lukas et al., 1988, CSHSQB 53:185-193.
3. Shoemaker etal., 1990, J. Cell Biol. 111:1107-1125.
4. Knighton et al., 1992, Science 258:130-135.
5. Collinge et al., 1992, Mol. Cell. Biol. 12:2359-2371.

M-Pos34

PHOSPHORYLATION OF A 25 kDa PROTEIN ASSOCIATED WITH SMOOTH MUSCLE ACTIN, TROPOMYOSIN AND CALPONIN. ((W.T. Gerthoffer, J. Pohl, M. Montella and J. McHugh)) Dept. of Pharmacology, Univ. Nevada School of Medicine, Reno, NV 89557-0046.

Contraction of mammalian smooth muscles is associated with phosphorylation of several contractile proteins and despite considerable information on phosphorylation of the 20 kDa myosin light chains, the control of muscle contraction in smooth muscles in not completely understood. To further investigate the phosphoproteins important in smooth muscle contraction we labeled canine tracheal and colonic smooth muscles overnight (22° C) with ^{32}P. Tissues were stimulated with carbachol, histamine or K^+, then frozen in acetone/5% trichloroacetic acid. A crude thin filament extract was made containing (moles protein/mole actin): actin (1); tropomyosin (0.99); calponin (0.11); and an unidentified 25 kDa protein (0.39). Caldesmon and calponin were phosphorylated as was the prominent 25 kDa protein. In additional studies, we found that heat treatment for 4 hours at 42° increased the amount of the 25 kDa protein relative to actin in both tracheal and colonic smooth muscle. The results suggest that the 25 kDa is heat inducible in the time span in which heat shock proteins are expressed. It may be that small proteins homologous to the heat shock (hsp) family are constituitively expressed in mammalian smooth muscle and are associated with actin filaments. Supported by NIH grants DK41315 and HL48183.

M-Pos35

EVIDENCE FOR INTERACTION BETWEEN 11kDa SMOOTH MUSCLE CALCIUM BINDING PROTEIN AND CALDESMON. ((R. S. Mani, W.D. McCubbin and C.M. Kay)) Medical Research Council Group in Protein Structure and Function, Department of Biochemistry, University of Alberta, Edmonton, Canada T6G 2H7.

A low molecular weight calcium-binding protein, designated as SMCaBP-11, has been isolated in a homogeneous form from chicken gizzard. The protein exists as a dimer of molecular weight 21000 in benign medium. Upon binding calcium, the protein undergoes a conformational change. When the protein was excited at 280 nm, the tyrosine fluorescence emission maximum was centered at 306 nm. Ca^{2+} addition resulted in a nearly 15 percent decrease in intrinsic fluorescence intensity. Fluorescence titration with Ca^{2+} exhibited two classes of calcium-binding sites with Kd values of 0.2 and 80 μM.

Caldesmon is a smooth muscle regulatory protein that interacts with actin, myosin, tropomyosin and calmodulin. It inhibits actin activated ATPase activity of myosin and myosin subfragments and this inhibition can be reversed by calmodulin in the presence of Ca^{2+}. Caldesmon was examined for its ability to interact with 11kDa SMCaBP using affinity chromatography and the fluorescent probe acrylodan. Effect of 11 kDa SMCaBP on the inhibitory effect of caldesmon on the Acto-S_1 ATPase was also studied. Like calmodulin, 11kDa protein could release the inhibitory effect of caldesmon in the presence of Ca^{2+}. For complete reversal one needs 0.5 mole of 11 kDa protein based on the molecular weight of the dimer i.e. one subunit per mole of caldesmon was required. When caldesmon was applied to 11kDa protein-sepharose in the presence of Ca^{2+}, most of the caldesmon was bound to the column and could be eluted with EGTA indicating that there is a direct interaction between caldesmon and 11kDa, SMCaBP.

Acrylodan labelled caldesmon when excited at 375 nm had an emission maximum at 505 nm. Addition of 11kDa SMCaBP resulted in a two fold increase in fluorescence intensity and this was accompanied by a blue shift in the emission maximum (i.e. max = 492 nm) suggesting that the probe now occupies a more non polar environment. Titration of labelled caldesmon with 11kDa protein indicated a strong affinity for this protein. When 11kDa protein was added to labelled caldesmon in the presence of EGTA, there was no indication of any interaction. 11kDa protein was at least as potent as calmodulin in reversing the inhibitory effect of caldesmon, making it a potential Ca^{2+} factor in regulating caldesmon in smooth muscle.

M-Pos36

CALDESMON BINDS PREFERENTIALLY TO A CONFORMATION OF MYOSIN RESEMBLING THE 10S FORM ((Frank W.M. Lu & Joseph M. Chalovich)) East Carolina School of Medicine, Greenville, NC 27858-4354 USA

We have shown earlier that caldesmon binds to myosin and this binding is dependent on ATP. Thus, in the presence of ATP, the binding is strengthened by 20-fold and the stoichiometry changes from 2 caldesmon's per myosin molecule to 1:1 (Hemric & Chalovich, JBC 19672, 1990). The binding increases with ATP concentration and reaches its maximum at 1 mM ATP. Attempts to bind caldesmon to ATP affinity columns have been unsuccessful and we assumed that the nucleotide induced changes reside in myosin. Specifically, we wished to determine if caldesmon bound more tightly to the inactive 10S form of myosin. To test this hypothesis, myosin was modified with N-ethylmaleimide to stabilize the 6S state (Chandra et al. JBC 202, 1985). This modification had no effect on the binding of caldesmon to myosin in the absence of ATP. However, ATP did not enhance the binding of NEM-myosin to caldesmon. This suggests that the strong binding of caldesmon to myosin is dependent on a conformational change in myosin similar to the 6S-10S conformational change. This observation presents the interesting possibility that intact caldesmon, containing the myosin binding site, not only inhibits the binding of myosin to actin but may further inhibit contraction by stabilizing the inactive 10S form of smooth muscle myosin.

M-Pos37

CROSS-LINKING OF THE NH_2-TERMINAL DOMAIN OF CALDESMON TO ACTIN. Philip Graceffa; Boston Biomed. Res. Inst., Boston, MA 02114.

Caldesmon (CaD) cys-580, in the C-terminal actin-binding domain, can be rapidly and effeciently disulfide cross-linked to cys-374 of actin by incubating caldesmon with actin modified at cys-374 with 5,5'-dithiobis(2-nitrobenzoic acid) [Graceffa & Jancso (1991) JBC 266,20305]. Further incubation (±tropomyosin) slowly leads to a second disulfide cross-link between the other cysteine in CaD, at position 153 in the N-terminal domain, and cys-374 of another actin monomer. The yield of the second cross-link was insensitive to ionic strength from 40 to 500 mM NaCl, whereas the CaD-actin binding strength decreased enormously over this range. These results suggest that the N-terminal domain of CaD is largely dissociated from and projects out from the actin filament at all salt concentrations studied and becomes slowly cross-linked to modified-actin during collisions with the actin filament. Support for these conclusions came from photocross-linking actin to CaD, specifically labeled at either of its cys with benzophenone-iodoacetamide. Cross-linking yields were high with CaD labeled at cys-580 but close to zero for CaD labeled at cys-153. These findings are consistent with previous knowledge that C-terminal fragments of CaD bind to actin whereas N-terminal fragments do not. Since the N-terminal domain of CaD binds to myosin, such projections, if they exist in vivo, could link myosin filaments to actin filaments and possibly form the molecular basis of the economic maintenance of tone in smooth muscle.

M-Pos38

ELECTRON MICROSCOPIC STUDIES OF CALDESMON BINDING TO ACTIN-TROPOMYOSIN FILAMENTS. ((K. Mabuchi, J. J.-C. Lin[1] and C.-L. A. Wang)) [1]Dept. of Biology, University of Iowa, Iowa City, IA 52242, and Dept. of Muscle Research, Boston Biomedical Research Institute, Boston, MA 02114

We have shown on the basis of electron microscopic observations that the way chicken gizzard caldesmon (CaD) binds to synthetic rabbit skeletal actin filaments differs from that it does in native thin filaments (J. Muscle Res. Cell Motility, in press); the majority of CaD bind to F-actin with only one end of the molecule, leaving the other end projecting away from the filament. With the aid of a monoclonal antibody specific against the N-terminal region of CaD we also noticed that either end of CaD was capable of interacting with actin, although the C-terminal end appeared to be the preferred site. In contrast to the reconstituted system, labeling of gizzard native thin filaments (prepared according to Marston & Lehman, Biochem. J., 231, 517, 1985) with the same antibody indicated that CaD was in its entire length associated with the filament. In this work we examined the possibility that tropomyosin bound to F-actin might enhance the interaction between CaD and actin. The number of antibody molecules complexed with CaD *on* F-actin was compared to the number of antibody molecules "tethered" to F-actin via CaD in the presence and absence of tropomyosin. We found that in both cases at least 60% of the antibody molecules were associated with the filament in a tethered structure. Our observations suggest that tropomyosin does not affect the mode of binding of CaD to F-actin in the reconstituted system, and therefore, other factor(s) must be sought to explain the difference seen in the native system. (Supported by grants from NIH and AHA)

M-Pos39

INTERACTIONS OF CALDESMON WITH N-TERMINAL ACTIN MUTANTS

Rachelle Crosbie[1], Carl Miller[1], Joseph M. Chalovich[2], Peter A. Rubenstein[3], and Emil Reisler[1]
[1]Dept. of Chemistry and Biochemistry, UCLA, Los Angeles, CA. 90024 [2]Dept. of Biochemistry, East Carolina University School of Medicine, Greenville, NC. 27858 [3]Dept. of Biochemisty, University of Iowa, Iowa City, IA. 52242

N-terminal yeast actin mutants were used to assess the role of N-terminal acidic residues in the interactions of caldesmon with actin. The yeast actins differed only in their N-terminal charge, as indicated: 1) 4Ac Actin: Ac-Met-Asp-Glu-Asp-Glu-Val (4 acidic charges); 2) Wildtype actin: Ac-Met-Asp-Ser-Glu-Val (2 acidic charges); 3) DNEQ: Ac-Met-Asn-Ser-Gln-Val (neutral charge); 4) ΔDSE: $^{+}H_3N$-Val (1 basic charge). Cosedimentation experiments revealed similar binding of caldesmon to α-actin and each yeast actin ($K_a \approx 1.1 \times 10^6$ M^{-1}). However, caldesmon inhibition of acto-S1 ATPase was affected by alterations in the N-terminus. This inhibition was similar for wildtype, 4Ac, and α-actin (80%). The neutral and deletion mutants showed little inhibition (15%) of acto-S1 ATPase activity. We also examined the polymerization of G-actin by caldesmon by both pyrene fluorescence and light scattering. The skeletal, wildtype, and 4Ac actins had similar rates and extents of polymerization while the neutral and deletion mutants showed very slow rates of polymerization. These results are discussed in terms of multiple contact sites between actin and S-1 and caldesmon.

M-Pos40

CALDESMON MAY INFLUENCE TROPOMYOSIN'S POSITION ON ACTIN.

((W. Lehman[1], R. Craig[2] and P. Vibert[3])) [1]Department of Physiology, Boston University School of Medicine, Boston, MA 02118; [2]Department of Cell Biology, University of Massachusetts Medical School, Worcester, MA 01655; and [3]Rosenstiel Center, Brandeis University, Waltham, MA 02254.

Three-dimensional helical reconstructions of negatively stained thin filaments isolated from chicken gizzard smooth muscle in EGTA show actin monomers whose bi-lobed shape and connectivity are very similar to those seen in reconstructions of frozen-hydrated skeletal muscle thin filaments. Some of these reconstructions, especially those from filaments in which a strand of protein is visible by eye in the electron micrographs, reveal in addition a continuous thin strand of density that follows the long-pitch actin helices, in contact with the inner domain of each actin monomer. Gizzard thin filaments treated with Ca^{++} calmodulin, which dissociated caldesmon but not tropomyosin, have also been reconstructed. Under these conditions, but using a smaller sample of filaments than examined in EGTA, reconstructions have also revealed a bi-lobed actin monomer, as well as a continuous surface strand that now appears to be closer to the outer domain of actin. The strands seen in both states thus presumably represent tropomyosin. It appears that caldesmon may fix tropomyosin in a particular position on actin in the absence of calcium. This position might not allow tropomyosin to potentiate acto-myosin ATPase, making caldesmon an inhibitor of contraction in vivo.

M-Pos41

CALDESMON CONTENT IN VERTEBRATE SMOOTH MUSCLES.

((W. Lehman*, D. Denault* and S.B. Marston+)) *Boston Univ. Sch. Med., Boston, MA 02118, +Nat'l Heart & Lung Inst., London, U.K.

Caldesmon (CD) and tropomyosin (TM) can be selectively and quantitatively extracted from vascular and visceral smooth muscle following heat-treatment; all other smooth muscle proteins are precipitated by this procedure. Estimates of CD:TM molar ratio in heat-extracts by SDS-PAGE densitometry are 1 CD:5.1-5.3 TM for rabbit and sheep aorta and 1 CD:5.9 TM for rabbit stomach and chicken gizzard. Taking TM as a reference of thin-filament content in intact muscle, it follows that the relative CD contents in the above tissues are similar. CD in heat-extracts was identified by western-blotting and by its anomalous migration on 4 different SDS-PAGE systems, in which CD runs as a single band but with different Mr in each. Assuming that the CD band in gels of total (unfractionated) smooth muscle tissue consists of CD alone, SDS-PAGE densitometry yields a molar ratio of 1 CD:4.4 TM:30 Actin for the unfractionated arterial tissue and 1 CD:6 TM:37 Actin for gizzard, values consistent with those above. Smooth muscles appear to contain different thin-filament classes, and CD-rich filaments can be isolated from vascular and visceral tissues in approx. equal yield, suggesting pools of CD-filaments in each that are similar in magnitude; if, as we proposed, CD is restricted to specific filaments in all smooth muscles in a molar ratio of 1 CD:2 TM:14 Actin, then the CD-filaments would account for approx. 35-45% of the total thin-filament pool in arterial smooth muscle and slightly less in visceral muscles.

M-Pos42

FUNCTIONAL DOMAINS OF CHICKEN GIZZARD AND HUMAN AORTA CALDESMON DETERMINED WITH EXPRESSED FRAGMENTS GENERATED BY SITE-DIRECTED MUTAGENESIS ((C.S. Redwood, P.A.J. Huber and S.B. Marston))
Dept Cardiac Medicine, NHLI, Dovehouse st., LONDON, SW3 6LY, UK

From the sequence and from studies of proteolytic fragments an extended 4 domain model of caldesmon structure was proposed as shown.

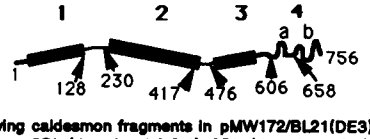

We have expressed the following caldesmon fragments in pMW172/BL21(DE3) system at 0.5 to 2.2 mg/l culture : CDh (domains 1-2-3-4), CDl (domains 1-3-4), domain 1, domain 2, domains 1-2-3, domains 3-4 (human), domain 4 and domain 4b. Tropomyosin bound tightly ($K=10^6M^{-1}$) to domains 2 and 4, weakly to domain1 and not to domain 4b. Thus caldesmon is associated with tropomyosin throughout its length in agreement with the location of caldesmon alongside tm in the thin filament from em studies. Myosin bound to domains 1 and 3-4 but not to 4. Thus myosin binds to isolated caldesmon at two separate sites in domains 1 and 3 of roughly equal affinity ($K=10^6M^{-1}$). Actin and actin-tm bound only to domain 4; 4b bound 20x weaker, thus there are actin binding sites in both domains 4a and 4b. Actin binding is enhanced by tm about 5x even in fragments (4b) which do not themselves bind to tm. Ca. Calmodulin bound to domains 4,4b, a short human fragment (626-710) and to a synthetic peptide (656-672) with affinities equal to intact caldesmon. This locates the calmodulin binding site at 659-666. Domain 4b is the smallest fragment which inhibits actin and actin.tm activation of myosin MgATPase. Inhibition is Ca.Calmodulin regulated and in the presence of tm 90% inhibition correlates with one mole of 4b bound per 14 mols actin.

M-Pos43

PHOTO-CROSSLINKING BETWEEN CALPONIN AND CALMODULIN. ((C.-L. A. Wang, S.-B. Zhuang and R. C. Lu)) Dept. of Muscle Research, Boston Biomedical Research Institute, Boston, MA 02114. (Spon. by T. L. Scott)

Interactions between calmodulin (CaM) and smooth muscle calponin (CaN) was investigated by photo-crosslinking techniques. A bacterially expressed CaM mutant, CaMQ143C, in which Gln at position 143 was replaced by a cysteine residue, was labeled with a thiol-specific photo-crosslinker, benzophenone-4-maleimide; the labeled protein was incubated with the recombinant αCaN and irradiated with UV light in the presence and absence of Ca^{2+}. In both cases a major product of the reaction had an apparent molecular weight of about 50,000, when analyzed by SDS polyacrylamide gel electrophoresis, corresponding to the covalently linked CaM-CaN complex. An additional protein adduct with a slightly higher mobility, which was not found in the absence of Ca^{2+} unless CaM was in excess, may represent a weaker, Ca^{2+}-dependent complex between CaM and CaN. The presence of a third, high molecular weight (about 64,000) crosslinking product was also evident in the presence of Ca^{2+}, presumably corresponding to the CaM_2-CaN ternary complex. Similar results were obtained when CaN was initially nicked with proteolytic enzymes prior to crosslinking. These results were consistent with the idea that each CaN has two CaM-binding sites: one is Ca^{2+}-independent, the other Ca^{2+}-dependent. Multiple CaM-binding sites of CaN have earlier been suggested by Takahashi et al., (BBRC 141, 20, 1986). Our N-terminal sequence analysis of the crosslinked products indicated that the Ca^{2+}-independent CaM-binding site is at the N-terminal region of CaN. (Supported by grants from NIH and AHA)

M-Pos44

INTERACTION OF SMOOTH MUSCLE CALPONIN WITH CALMODULIN

((F.L. Wills, W.D. M[c]Cubbin, and C.M. Kay)) MRC Group in Protein Structure and Function, Dept. of Biochemistry, University of Alberta, Edmonton, Alberta T6G 2H7.

Calponin interacts with several Ca^{2+} binding proteins in a Ca^{2+} dependent manner. In order to determine the possible relevance of these interactions in smooth muscle function it is necessary to characterize the strength and stoichiometry of the complexes formed. The interaction between calponin and calmodulin can be monitored through an acrylodan label on a cysteine of calponin. The fluorescently labelled calponin possesses the same biological function and physical behaviour in binding to calmodulin as the native calponin. This probe is very environment sensitive and responds to the calponin calmodulin interaction by the emission peak blue shifting 20 nm and by the fluorescent quantum yield increasing 3.5 times at 460 nm. The stoichiometric nature of this complex has been determined using analytical ultracentrifugation and is two calmodulins to one calponin and the interaction is Ca^{2+} sensitive with a Kd_1 of 100nM and a Kd_2 of 3mM. Calmodulin is not the only protein which interacts with calponin in this manner, but rather this interaction seems to be a general feature attributable to all hydrophobic patch exposing proteins, suggesting that it may be non-specific, occurring because of a generalized mode of interaction. Two other proteins, S-100b from bovine brain, and SMCaBP-11 from chicken gizzard, had much stronger affinities for calponin, and in particular interaction of SMCaBP-11 with calponin may be biologically relevant. In determining the nature of calponin's interaction with these Ca^{2+} binding proteins it was apparent there was no effect of Ca^{2+} upon calponin itself and physical studies could find no evidence that calponin interacts with calcium.

M-Pos45

CROSS-LINKING OF CALPONIN WITH THE CARBOXY-TERMINUS OF ACTIN

((P. Graceffa, T. Tao and R. C. Lu)) Dept. of Muscle Research, Boston Biomedical Research Institute, 20 Staniford St., Boston MA 02114.

Calponin (CaN) is a smooth muscle protein that is known to bind to actin and inhibit actomyosin ATPase activity. We have used disulfide- and photo-cross-linking techniques to study the interaction between CaN and the C-terminus of actin. Rabbit skeletal F-actin was labeled at Cys374 with 5,5'-dithiobis(2-nitrobenzoate) and mixed with a recombinant α-isoform of chicken gizzard CaN at a molar ratio of 1:3 (CaN:actin). Almost all of the CaN became disulfide cross-linked to actin within 5 min. High cross-linking yield was also obtained with a mutant CaN in which one of the three thiols, Cys238, was replaced by Ser, indicating that one of the two remaining thiols, Cys61 or Cys273, is involved in the cross-linking. When the CaN-actin cross-linked product was subjected to chymotryptic digestion an ~42 kDa product was obtained. Sequence analysis showed that this product contains actin and a C-terminal CaN fragment that begins with Thr220, indicating that it is Cys273 of CaN that is engaged in disulfide cross-linking with Cys374 of actin. A covalent cross-link between CaN and actin can also be formed via a benzophenone molety attached at Cys374 of actin. If chymotrypsin cleaved (between Tyr183 and Gly184) CaN was used only the N-terminal fragment cross-linked to benzophenone-labeled actin. Interestingly, neither chymotryptic fragment could be disulfide-cross-linked to F-actin. Taken together these results suggest that the N-terminal part of CaN interacts strongly with actin and that this interaction brings the C-terminal Cys273 region of CaN into proximity with the C-terminus of, possibly, another actin subunit. (Supported by NIH P01AR41637)

M-Pos46

PHYSICAL PROPERTIES OF CALPONIN

((W.F. Stafford III, K. Mabuchi, K. Takahashi* and T. Tao)) Dept. of Muscle Research, Boston Biomedical Research Institute, 20 Staniford St., Boston, MA 02114. *Center for Adult Diseases, Osaka, Japan.

Calponin (CaN) is a thin filament-associated smooth muscle protein that has been implicated to play a role in the regulation of smooth muscle contraction. We have used circular dichroism spectroscopy, electron microscopy, and analytical ultracentrifugation to study the physical properties of recombinant chicken gizzard αCaN. The α-helix content of αCaN was estimated from its circular dichroism spectrum to be ~21%, compared with 13% predicted by sequence analysis. αCaN melts with a single sharp transition at ~57°C. Rotary shadowed electron micrographs of αCaN reveal a composite of shapes ranging from elongated rods to collapsed coils. The lengths of the rod-shaped structures are ~19 nm. Analytical ultracentrifugation studies found αCaN to be homogeneous with a monomer molecular weight of 31.4 ± 1.0 kDa, with a $s_{20,w}$ value of 2.34S. It has a slight tendency to undergo reversible dimerization with an association constant of ~10^3 M^{-1}. Using a value of 0.366 g H_2O/g protein for the hydration and a value of 0.732 cc/g for the partial specific volume (estimated from the amino acid composition), the frictional ratio f/f_{min} was calculated to be 1.33. These data could be modelled by a prolate ellipsoid of revolution with an axial ratio of 6.32, having a length of 16.2 nm and a diameter of 2.6 nm. Taken together, our results indicate that CaN is a flexible elongated molecule whose contour length is sufficiently long to span 3 actin subunits along the length of a F-actin filament. (Supported by NIH P01AR41637)

M-Pos47

CALPONIN PHOSPHORYLATION IN VITRO AND IN INTACT MUSCLE.

((S.J. Winder, B.G. Allen[1], E.D. Fraser[1], H.-M. Kang[1], G.J. Kargacin[2] and M.P. Walsh[1].))[1]Dept. of Medical Biochemistry and [2]Dept. of Medical Physiology, University of Calgary, Alberta T2N 4N1.

Calponin, a thin filament-associated protein which has been implicated in the regulation of smooth muscle contraction, is phosphorylated *in vitro* by protein kinase C (PKC) and Ca^{2+}/calmodulin-dependent protein kinase II (CaM kinase II) and dephosphorylated by a type 2A protein phosphatase. Unphosphorylated calponin binds to actin and inhibits the actin-activated myosin MgATPase; both these properties are lost upon phosphorylation. Although both serine and threonine residues in calponin are phosphorylated, the major site of phosphorylation by either kinase is S175. Calponin is also phosphorylated when bound to the thin filament in a reconstituted actomyosin system or in washed myofibrils and results in dissociation of calponin from the thin filament. Tryptic phosphopeptide mapping indicates that the same sites are phosphorylated as in the isolated protein. Toad stomach calponin exists in at least 3 isoforms which differ in charge but exhibit the same molecular mass on SDS-PAGE. All 3 isoforms can be phosphorylated by PKC or CaM kinase II in a toad stomach homogenate as revealed by two-dimensional gel electrophoresis (NEPHGE/SDS-PAGE). Furthermore, calponin is phosphorylated in intact toad stomach smooth muscle strips metabolically labeled with $^{32}P_i$ and stimulated to contract with carbachol. These results support the hypothesis that calponin may be regulated *in vivo* by phosphorylation-dephosphorylation. (Supported by MRC Canada).

M-Pos48

CALPONIN IS PARTIALLY PHOSPHORYLATED IN ARTERIAL SMOOTH MUSCLE STRIPS.

((S.P. Driska and J.J. Cummings, Jr.)) Physiology Dept., Temple Medical School, Philadelphia, PA 19140.

To determine if calponin was reversibly phosphorylated during contraction of intact swine carotid arterial smooth muscle strips, we froze contracting and relaxed muscle strips and analyzed muscle homogenates by two-dimensional electrophoresis (non-equilibrium pH gradient electrophoresis (NEPHGE) in the first dimension, SDS in the second). This resolved calponin into 4-5 spots with the same apparent molecular weight. Identity of the spots was confirmed by Western blotting with an antibody to gizzard calponin. Densitometry of the stained gels indicated that the distribution of the calponin species was similar in contracting muscles and relaxed muscles. When tissues were incubated with ^{32}P orthophosphate, autoradiography of the gels showed ^{32}P incorporation into the most slowly migrating calponin spot, a minor spot accounting for only about 5 % of the total calponin. This spot was phosphorylated in both relaxed and contracting tissues. In summary, we detected calponin phosphorylation in smooth muscle strips, but only a small fraction of the calponin was phosphorylated, and there was no difference between contracting and relaxed tissues. Thus, our current results do not provide much support for the hypothesis that calponin phosphorylation is a regulatory mechanism. Supported by the George H. Stewart Foundation.

M-Pos49

CALPONIN PHOSPHORYLATION DURING ENDOTHELIN-1 INDUCED CONTRACTION OF INTACT SWINE CAROTID ARTERY.

((A. Rokolya and R.S. Moreland)) Bockus Research Institute, Graduate Hospital, Philadelphia, PA 19146.

Calponin is a thin filament associated, smooth muscle specific protein which has been shown in biochemical studies to inhibit actin-activated myosin ATPase activity. Phosphorylation of calponin by either protein kinase C or Ca^{2+} and calmodulin dependent protein kinase II reverses this inhibition. Although biochemical evidence has suggested a role for calponin phosphorylation in smooth muscle regulation, this has not been supported by studies using intact tissue. We addressed this question by determining if calponin is phosphorylated during endothelin-1 stimulation of intact strips of swine carotid media. Strips were incubated for 6 hours in ^{32}P, exposed to 0.3 μM endothelin-1, rapidly frozen, and homogenized. The homogenized strips were subjected to non-equilibrium pH gradient electrophoresis followed by SDS-polyacrylamide gel electrophoresis. The proteins were then transferred to nitrocellulose membranes and subjected to autoradiography. In resting tissue we could resolve four distinct calponin isoforms on amido black stained membranes which was verified by calponin antibody binding. Stimulation by endothelin-1 resulted in additional spots with increasingly acidic isoelectric points which were shown to be phosphorylated calponin by autoradiography and antibody binding. Calponin phosphorylation was demonstrable by 15 sec of stimulation, reached a maximum by 45 sec, and remained elevated for at least 30 min. These results demonstrate that calponin is phosphorylated during agonist activation of intact vascular smooth muscle and provide support for its potential role in the regulation of smooth muscle contraction. Supported in part by NIH HL 37956 and WW Smith Charitable Trust Grant H9103.

M-Pos50

BINDING OF TROPOMYOSIN TO ACTIN FILAMENTS: AN ELECTRON MICROSCOPIC STUDY ((Yasuko Mabuchi and Katsuhide Mabuchi)) Dept. of Muscle Research, Boston Biomedical Research Institute, 20 Staniford Street, Boston Mass. 02114.

Tm/F-actin complexes were rotary-shadowed for visualization and examined with the electron microscope. It was found that the way Tm binds to F-actin was quite different depending on the concentration. At 4 μg/ml F-actin and 2 μg/ml Tm, the majority of Tm bound to F-actin only at one end creating "tethered" images. On the other hand, when two proteins were mixed at 1 mg/ml F-actin and 0.26 mg/ml Tm and then diluted 200-fold just before the mixture was processed for visualization, very few tethered Tm molecules were observed. This phenomenon could be explained if Tm molecules were tightly bound along their entire length to F-actin and such Tm molecules were not visualized by rotary shadowing. When the same diluted mixture was left at room temperature for several hours, and then processed for visualization, more tethered Tm molecules were observed. This indicates that originally tightly bound Tm are dissociated from F-actin and become visible.

M-Pos51

VARIABILITY OF MYOSIN LIGHT CHAIN AND HEAVY CHAIN ISOFORMS IN SMOOTH MUSCLE AND NON-MUSCLE CELLS ((C. Subah Packer)) Dept. of Physiology and Biophysics, Indiana University School of Medicine, Indianapolis, Indiana 46202.

At least two myosin isoforms, the 200 and 204 kD heavy chains (MHC_{200} and MHC_{204}), have been found in all smooth muscles investigated. However, the non-muscle isoforms, the 196-198 and the 190 kD heavy chains (MHC_{196} and MHC_{190}) have also been reported in some smooth muscles. In addition, non-muscle (NM and smooth muscle (SM) isoforms of the 20kD myosin light chains (MLC_{20}) have been identified. The relative proportions of both the MLC_{20} and MHC isoforms in a variety of smooth muscle and non-muscle cell types and the relationship of the isoform pattern to cell function have not yet been determined. Preliminary data has been obtained from sodium dodecyl sulfate polyacrylamide gel electrophoresis (PAGE) of MHC isoforms and from urea glycerol PAGE of MLC_{20} isoforms and Western blot analyses for myosin from caudal and pulmonary arterial muscle, intestinal, tracheal and uterine muscle and from pulmonary endothelial cells. Interestingly, the vascular muscles contain equal proportions of the SM and NM MLC_{20} isoforms, while non-vascular muscles contain predominantly SM MLC_{20}. Pulmonary arterial muscle has significantly more of the NM MHC isoforms and contains both the MHC_{196} and MHC_{190} while the other smooth muscles appear to have only the MHC_{196} of the NM isoforms. Surprisingly, endothelial cells have a significant proportion of SM MLC_{20}. Apparently, the proportion of SM to NM MLC_{20} does not correlate with the proportion of MHC_{200} and MHC_{204} to MHC_{196} and MHC_{190}. However, a higher proportion of SM MLC_{20} appears to correlate with greater contractility. Supported by AHA: Indiana Affiliate. Thanks to Drs. J.T. Stull, R.S. Adelstein and D.R. Hathaway for gifts of myosin antibodies.

M-Pos52

Expression of contractile Protein Variants Along the Mesenteric Vascular Arcade. ((Hui Zou, *Paul Ratz and Michael A. Hill)) Departments of Physiology and *Pharmacology, Eastern Virginia Medical School, Norfolk, VA 23501. (Spon. DK Bartschat)

It is well established that there is a tendency toward increased contractile agonist sensitivity as artery diameter decreases. Further, spontaneous tone and control of resistance largely resides in small arterial vessels. To date, the possibility that increased reactivity of such arterial vessels relates to contractile protein isoform expression has not been examined. To test this hypothesis studies were performed on segments of sequential branch orders of rat mesenteric circulation (diam approx 150-700 μm). For comparison corresponding small veins and large arteries (abdominal aorta, femoral artery) were studied. Isoelectric variants of actin and tropomyosin were separated by two dimensional electrophoresis, stained with coomassie blue and quantitated densitometrically. Myosin isoforms were separated by one dimensional electrophoresis using 12% acrylamide with 10% glycerol. Consistent with studies performed in larger vessels actin separated into three isoelectric variants (α, β, γ); tropomyosin into two subunits (+,-); and myosin exhibited two heavy chain isoforms (SM1, SM2). Small arteries showed a significant ($P<0.01$) inverse correlation ($r=0.86$, $n=13$) between diameter and α actin content. Mesenteric arteries had significantly more α actin (57.7±0.9%) than corresponding small veins (50.0±2.0) while β actin was more abundant in the veins (26.0±2.0 c.f. 21.2±0.8). Isoelectric variants of tropomyosin appeared in similar proportions in all vessels with approximately 50% in each form. The results are consistent with the hypothesis that differences in contractile function between blood vessels may, in part, relate to differences in contractile protein expression. (Supp by NIH HL47378 and AHA)

M-Pos53

THE EFFECT OF PS AND DAG ON CA^{2+} DISSOCIATION FROM PROTEIN KINASE C. ((J. David Johnson* and John D. Walters#)) *Department of Medical Biochemistry, College of Medicine and #College of Dentistry. The Ohio State University. Columbus, OH 43210.

Protein kinase C (PKC) is known to be activated at nanomolar concentrations of Ca^{2+} in the presence of its physiological activators phosphatidyl serine (PS) and diacylglycerol (DAG). In the absence of these activators, Ca^{2+} in the mM range is required for partial activation of PKC. We have used stopped flow with the fluorescent Ca^{2+} chelator Quin to determine the rate of Ca^{2+} dissociation from purified rabbit brain PKC in the presence and absence of PS and DAG vesicles. In the absence of PS/DAG, the Ca^{2+} dissociation rate from PKC is too rapid to detect (>700/s), consistent with a low affinity of Ca^{2+} for PKC in the absence of activators. Addition of PS or DAG alone does not appear to slow Ca^{2+} dissociation from PKC. In the presence of both PS and DAG, Ca^{2+} dissociation from PKC is dramatically reduced and occurs at a rate of 0.70 ± 0.11 /s ($t_{1/2}$ = 1s) at 22° C. These first direct measurements of Ca^{2+} off-rates from PKC suggest that both PS and DAG are required to increase PKC's affinity for Ca^{2+} to the level where it can be activated by physiological $[Ca^{2+}]$.

M-Pos54

3-D DISTRIBUTION OF PROTEIN KINASE C IN SMOOTH MUSCLE CELLS; EFFECT OF ACTIVATION. ((E.D.W. Moore, G.A. Meininger[1] and F.S. Fay)) Biomed. Imaging Group, U. Mass. Med. Center, Worcester MA, 01605; [1]Dept. of Med. Physiol. Texas A & M Univ., College Station, TX, 77843. (Spon. by D. Gordon)

We have examined the 3-D distribution of protein kinase C (PKC) in smooth muscle. Cells were enzymatically dissociated from the stomach of the toad *Bufo marinus*, seeded on poly-L-lysine coated cover slips and fixed with paraformaldehyde; PKC was localized using indirect immunofluorescence. A series of 2-D images were acquired through focus at 0.25 μm intervals, and reconstructed into a 3-D image using a deconvolution algorithm based on regularization theory. At the cell periphery, PKC was organized into strands 0.5 μm wide which ran roughly parallel to the cell's long axis; staining was diffuse throughout the rest of the cell. After a 1 min. incubation with 10^{-4} M acetylcholine, PKC organized into strands throughout the cell. Similar changes in the distribution of PKC were seen following activation for 10 min. with 1 μM phorbol ester. The basis for the cortical and cytosolic organization have not been determined. The membrane however has two functional macrodomains (Moore *et al.* A.N.Y.A.S., 639, 543-549, 1991), one containing vinculin and the other the Na^+/K^+ pump and Na^+/Ca^{2+} exchanger. These domains are also organized into strands roughly 0.5 μm wide; a similarity suggesting that PKC is located near one of these macrodomains. (Supp. by AHA 13-536-912 to EDWM, HL33324 and Est.Inv.Awd. to GAM, and HL14523 to FSF).

M-Pos55

PHOSPHOLIPASE C γ1 AND PROTEIN KINASE C α IN RAT TAIL ARTERY. ((E.F. LaBelle and H.Gu)), Bockus Research Institute, Graduate Hospital,Philadelphia,PA 19146. (spon. by E. Murer)

In order to determine the isoforms of phospholipase C and protein kinase C that are responsible for force development and maintenance in vascular smooth muscle, we homogenized rat tail artery at liquid N_2 temperature in sucrose solution, subjected the extract to centrifugation in order to separate cytosol from membranes, and separated the proteins by SDS PAGE. The proteins were transferred to nitrocellulose filters by Western blotting, and the filters incubated with monoclonal antibodies to either phospholipase C γ1 (PLC γ1) or protein kinase C α (PKC α), and then treated with secondary antibodies directed against mouse IgG and conjugated to alkaline phosphatase. After exposure of the filters to alkaline phosphatase substrate, purple bands indicated the presence of PLC γ1 in rat tail artery cytosol and also the presence of PKC α in rat tail artery membranes. The MW of each isoform was the same as we observed using homogenates of rat brain as standards: 145kD for PLC γ1 and 78kD for PKC α. We are currently investigating the ability of norepinephrine to either phosphorylate, activate, or translocate these isoforms into the plasma membrane or the nucleus. We are also looking for other isoforms of either PLC or PKC using monoclonal antibodies and similar procedures.(Supported by NIH Grant HL 37413).

M-Pos56

CLONING OF SMOOTH MUSCLE CaM KINASE II ISOFORMS.

Z-H Lucy Zhou and Mitsuo Ikebe, Dept. of Physiology and Biophysics, Case Western Reserve Univ., Cleveland, OH 44106

CaM kinase II is a member of CaM-dependent protein kinases originally found in brain. CaM kinase II was also isolated from smooth muscle recently, and it is thought that this kinase plays a role in modulating Ca^{2+} signalling and contractile apparatus of smooth muscle. In the present study, we cloned smooth muscle CaM kinase II isoforms from rat aorta. The cDNA library was screened using the brain CaM kinase II cDNA of δ isoform and several cDNA clones were obtained. One of them consisted of 1.7 kb showed high homology with the γ isoform of the brain kinase. The nucleotide sequence in the 5'-half of the molecule was completely identical to the brain γ isoform, however, the unique region resided at the end of the calmodulin binding domain, with only 40% homology in nucleotides and 34% homology in amino acids to the corresponding region of the brain isoform. By comparing the sequence of rat isoform with the brain isoform, it was revealed that nucleotides in the brain isoform were deleted from the smooth muscle isoform and a unique sequence was inserted instead. In addition, analysis of the 5'-sequence of smooth muscle cDNA clone raised the possibility of a different transcription initiation site. Another cDNA clone containing a partial sequence of the brain δ isoform was also obtained. However, this clone also contained unique sequence. Our results suggest that smooth muscle isoforms are produced by alternative splicing of γ and δ CaM kinase II genes(supported by NIH and AHA).

M-Pos57

CHARACTERIZATION OF Ca^{2+}/CALMODULIN-DEPENDENT PROTEIN KINASE II ACTIVITY FROM A SOLUBLE FRACTION OF ARTERIAL SMOOTH MUSCLE

((Harold A. Singer, Charla Sweeley, and Charles M. Schworer))Weis Center for Research, Geisinger Clinic, Danville, PA 17822

Ca^{2+}/calmodulin dependent protein kinase II (CaM-kinase II) has been implicated in the regulation of smooth muscle contractile activity by virtue of its ability to phosphorylate and modulate the functional activity of smooth muscle contractile proteins and associated regulatory proteins *in vitro*. Previous reports of CaM-kinase II in smooth muscle have described an activity which tightly associates with an insoluble myofibrillar fraction and co-purifies with and phosphorylates caldesmon. In this study, we have documented the partial purification of an abundant protein kinase activity from a soluble fraction of swine carotid arterial smooth muscle, which has the following properties: 1.) Ca^{2+}/calmodulin-dependent phosphorylation of autocamtide-2, a peptide substrate based on the conserved autophosphorylation sequence of the known CaM-kinase II subunits isolated from rat tissues, 2.) Ca^{2+}/calmodulin-dependent autophosphorylation resulting in the generation of activator-independent kinase activity, 3.) a native size of 650 kDa, 4.) subunit immunoreactivity with antipeptide antibodies based on conserved sequences of rat brain CaM-kinase II isozymes and lack of cross-reactivity with monoclonal antibodies recognizing the α- or β-subunits. These properties identify this kinase activity as a smooth muscle isozyme(s) of CaM-kinase II, composed of two subunits with apparent sizes of 54 and 58 kDa.

M-Pos58

SMOOTH MUSCLE CALDESMON PHOSPHATASE IS SMP-I, A TYPE 2A PROTEIN PHOSPHATASE.

((M.D. Pato[1], C. Sutherland[2], S.J. Winder[2] and M.P. Walsh[2].))[1]Dept. of Biochemistry, University of Saskatchewan, Saskatoon, Saskatchewan S7N 0W0 and [2]Dept. of Medical Biochemistry, University of Calgary, Calgary, Alberta T2N 4N1.

Caldesmon (CaD) phosphatase was identified in chicken gizzard smooth muscle using as substrates CaD phosphorylated at different sites by PKC, CaM kinase II and cdc2 kinase. Most (~90%) of the CaD phosphatase activity was recovered in the cytosolic fraction. A single major CaD phosphatase activity was detected at each stage of purification which copurified with calponin phosphatase and myosin LC_{20} phosphatase. The purified enzyme consisted of 3 subunits of 60, 55 and 38 kDa and was identified by Western blotting as SMP-I, a type 2A protein phosphatase. Consistent with the conclusion that SMP-I is the major CaD phosphatase of smooth muscle, purified SMP-I from turkey gizzard dephosphorylated all 3 phosphorylated forms of CaD whereas SMP-II, -III and -IV were relatively ineffective. The relative rates of dephosphorylation of the 3 phosphorylated CaD species and calponin were: CaD (CaM kinase II): CaD (PKC): CaD(cdc2): calponin (PKC) = 1:5:7:74. We suggest therefore that CaD phosphorylation *in vivo* can be maintained following kinase inactivation due to slow dephosphorylation by SMP-I while calponin and myosin are rapidly dephosphorylated by SMP-I and SMP-III/SMP-IV, respectively. This may have important functional consequences in terms of the contractile properties of smooth muscle. (Supported by MRC Canada).

M-Pos59

CHARACTERIZATION OF TURKEY GIZZARD MYOSIN PHOSPHATASES.

((G. T. Tulloch and M. D. Pato)) Department of Biochemistry, University of Saskatchewan, Saskatoon, Saskatchewan, Canada S7N 0W0.

Two myosin phosphatases, termed Smooth Muscle Phosphatase (SMP)-III (M_R=40, 000) and -IV (M_R=58,000 and 40, 000), have been purified from turkey gizzards. Classification of these enzymes with respect to their sensitivity to heat stable Inhibitor-2 and activities toward phosphorylase kinase revealed that they exhibit properties of Type 1 and 2 protein phosphatases (PP). Like other PP2, SMP-III and -IV are not inhibited by the Inhibitor-2. But SMP-IV dephosphorylates the β-subunit of phosphorylase kinase, a property of PP1, while SMP-III is inactive toward this protein. Furthermore, SMP-III and -IV cross-react with polyclonal and monoclonal antibodies against PP1. No cross-reativity was observed with PP2A1 and PP2C polyclonal antibodies. Time courses of tryptic digestion of SMP-III and -IV showed progressive decrease in size of their catalytic subunits from 40,000 Da to 38,000 and finally to a 35,000 Da fragment. Proteolysis of these enzymes resulted in stimulation of their activities toward heavy meromyosin and myosin light chains, increased sensitivity to the heat stable inhibitor-2 and activation of SMP-III toward the β-subunit of phosphorylase kinase. Thus, proteolysis of SMP-III and -IV by trypsin altered the properties of these enzymes to those of typical Type 1 Protein Phosphatases. Kinetic properties of the proteolytic products were studied. (*Supported by the Medical Research Council of Canada*).

M-Pos60

MYOSIN LIGHT CHAIN PHOSPHATASE ACTIVITY IN CANINE TRACHEAL SMOOTH MUSCLE.

((X. Liu, A.J. Halayko, K. Rao & N.L. Stephens)) Dept. of Physiol., Univ. of Manitoba, Winnipeg, Manitoba, Canada R3E 0W3.

We have reported that myosin light chain phosphorylation (MLC_{20}-p) is increased by 30-40% in contracting airway smooth muscle (SM) from ragweed sensitized dogs. Myosin light chain kinase (MLCK) activity is increased also and may be responsible for the elevated shortening velocity in SM from these animals. It is not known if modulation of myosin phosphatase activity contributes to enhanced MLC_{20}-p in sensitized canine SM. We describe a myosin phosphatase assay which can be carried out on tissue and cell homogenates of airway SM. Homogenates were prepared by suspending, frozen, pulverized tracheal SM in: imidazole (40mM), KCl(60mM), $MgCl_2$(1mM), $CaCl_2$(0.1 mM) containing protease inhibitors. MLC_{20}-p was initiated with Mg^{2+}-ATP (1mM), maximum MLC_{20}-p (~40%) was reached after 45s and was maintained for over 5 min. The relative state of MLC_{20}-p was estimated by immunoblot assay. Myosin phosphatase activity was estimated by the rate of decline in MLC_{20}-p after adding singly, MLCK inhibitor (MLCK-I, a synthetic pseudosubstrate domain undeca peptide), EGTA, trifluoperazine (TFP) or combinations of these. Times for dephosphorylation to 50% of maximally phosphorylated MLC_{20} and to basal phosphorylation levels are listed in the table below. In the presence of okadaic acid (5nM), no MLC_{20} dephosphorylation was seen 30s after addition of MLCK inhibitors, and <20% dephosphorylation was seen after 5 min. This effect was similar in control and sensitized homogenates suggesting that dephosphorylation of MLC_{20}-p is due to similar populations of myosin phosphatases. This assay measures myosin phosphatase activity in tissue homogenates and permits its use in the assessment of the enzyme in populations of cultured SM cells. Application of this assay indicates that, in ragweed sensitized airway SM, the increase in maximum velocity of shortening we previously reported, is not contributed to by changes in myosin phosphatase but is due to increased MLCK activity that we have also, already reported. (Supported by the National Centres of Excellence of Canada and the Medical Research Council of Canada.)

Treatment (mM)	Dephosphorylation Time (s) 50% Max.	Basal
MLCK-I(0.2)	7	145
TFP(0.2)	18	175
EGTA(1)	17	160
MLCK-I(0.2) /EGTA(1)	<5	5
MLCK-I(0.2) /TFP(0.2)	<5	5

M-Pos61

AFFINITY LABELLING OF SMOOTH MUSCLE MYOSIN LIGHT CHAIN KINASE BY ρ-FLUOROSULFONYL BENZOYL ADENOSIN (FSBA)

Hideyuki Komatsu and Mitsuo Ikebe Department of Physiology and Biophysics, Case Western Reserve University, Cleveland, OH 44106

Smooth muscle myosin light chain kinase (sm MLCK) is a member of the calmodulin dependent protein kinases which phosphorylate the regulatory light chain of smooth muscle myosin so as to initiate contraction. In the present study, we affinity labelled the adenine binding site of MLCK by using FSBA and determined the FSBA binding site. It was reported recently that FSBA is stoichiometrically incorporated in MLCK[1]. We synthesized ^{14}C-labelled FSBA in which ^{14}C is incorporated in the acetyl carbon because if ^{14}C is incorporated in the adenine moiety the ^{14}C label can be removed from the labelled amino acid residues in the acidic conditions during the peptide isolation steps. FSBA inhibited sm MLCK activity and ^{14}C-FSBA was stoichiometrically incorporated into sm MLCK. Both inhibition of sm MLCK activity and incorporation of ^{14}C-FSBA were abolished by addition of excess ATP suggesting that the modification is specific. The labelled sm MLCK was proteolyzed completely by α-chymotrypsin and the produced peptides were purified by DEAE 5PW and C-18 reverse phase columns. The isolated ^{14}C labelled peptides were subject to sequencing analysis and the sequence of AGXF was obtained where X is the labelled amino acid. By comparing with the known sequence of sm MLCK, the labelled residue was identified as lysine-548 which is conserved among various protein kinase. (Supported by NIH and AHA)

1) Kenelly et al., Biochemistry (1992) 31, 5394-5399

M-Pos62

DEPHOSPHORYLATED SMOOTH MUSCLE MYOSIN MOVES ACTIN FILAMENTS AT REDUCED VELOCITY IN AN *IN VITRO* MOTILITY ASSAY ((J.R.Haeberle))

Department of Physiology & Biophysics, The University of Vermont, Burlington, VT, 05405. (Spon. by B.B.Hamrell).

A previous investigation of the effects of caldesmon on actin filament movement in an *in vitro* motility assay demonstrated that relatively high concentrations of reducing agent were required (i.e. 10 mM DTT) to prevent oxidation of caldesmon (Haeberle *et al.*, J.Biol.Chem. 267, 23001, 1992). An additional effect of maintaining reducing conditions in the motility assay is that freshly prepared dephosphorylated smooth muscle myosin moves actin filaments at 0.5 μm/sec compared to 2.5 μm/sec for thiophosphorylated myosin (32°C, 80 mM KCl). After as little as 1 wk storage at -20° C in 50% glycerol, velocity is reduced to <0.3 μm/sec and many filaments do not move at all. The velocity can be restored to 0.5 μm/sec by inclusion of 50 mM DTT in the motility buffer. By analyzing a wide range of myosin-loadings on urea/glycerol gels, it can be shown that the amount of phosphorylated 20,000 dalton light chain is <0.2% of the total. Further evidence that this is not a small amount of contaminating, unregulated myosin comes from studies in which the actin-binding protein calponin is added to the motility buffer (see adjoining abstract). While calponin has no effect on the velocity of fresh myosin, it increases the velocity seen with stored myosin to 0.5 μm/sec and promotes motion of essentially all filaments. The combination of 1 μM calponin and 50 mM DTT results in motion of essentially all filaments at 0.5 μm/sec. These results are consistent with the notion that oxidation of a small number of myosin molecules can prevent motion of dephosphorylated myosin by mechanically loading the filaments. These results suggest that restoration of motion with 50 mM DTT is due to elimination of loading, whereas, the addition of calponin causes recruitment of addition slow-cycling cross bridges.

M-Pos63

THE EFFECT OF CALDESMON ON MYOSIN-ACTIN INTERACTION IS MEDIATED THROUGH TROPOMYOSIN. ((Kurumi Y. Horiuchi and Samuel Chacko)) Dept. of Pathobiology, University of Pennsylvania, Philadelphia, PA 19104

Caldesmon, a component of the thin filament in smooth muscle, inhibits actin-activated ATPase activity of myosin. Although inhibition of actin activation by caldesmon occurs in the absence of tropomyosin, there are several reports showing that caldesmon inhibition is modulated by tropomyosin. Experiments were carried out to determine if the effect of caldesmon on myosin-actin interaction is mediated through tropomyosin. Binding of myosin heads to actin releases the bound caldesmon from actin filament. On increasing the rigor-bonds utilizing skeletal S1 in the absence of ATP, caldesmon bound to actin filament was completely released when 5 out of 7 actin monomers were saturated with rigor-bonds. In the presence of tropomyosin, complete detachment of caldesmon from actin filament requires a 1:1 saturation of actin monomers with rigor bonds, indicating that the affinity for caldesmon to actin filament is increased in the presence of tropomyosin. Hence, it is likely that caldesmon in the intact muscle may not detach from thin filament, since thin filaments contain bound tropomyosin. In another experiment, the effect of caldesmon on the actin-activated ATPase of heavy meromyosin was measured in the presence of rigor-complexes on tropomyosin-actin. Rigor complexes, produced with NEM-treated S1, cooperatively turn on the acto-HMM ATPase in the presence of tropomyosin. This effect is abolished by the presence of caldesmon at a caldesmon to actin molar ratio of 1:7. Similar result was obtained with a 38-kDa C-terminal fragment of caldesmon which retains full actin- and tropomyosin-binding region, but with a shorter molecular length. This implies that the functional effect of caldesmon on actin filament does not require the entire caldesmon molecule; one caldesmon (or even actin-binding fragment) is able to regulate 7 actins mediated through one tropomyosin. Supported by NIH grants DK 39740 & HL 22264.

M-Pos64

VARIABLE EXPRESSION OF MYOSIN HEAVY CHAINS WITH DEVELOPMENT IN MOUSE SMOOTH MUSCLE TISSUES. ((T.J. Eddinger)) Biology Department,Marquette University, Milwaukee, WI 53233

Developmental expression of myosin heavy chains (MHC) in mouse uterus, aorta, bladder and stomach was determined using tissue homogenates and high resolution polyacrylamide gel electrophoresis. In the mouse uterus, two smooth muscle (SM) and two non-muscle (NM) MHC's can be resolved and identified with isoform-specific antibodies. Both SM MHC's show an increase in relative content with increasing age, while the NM MHC's show a decrease. The NM1 MHC shows a significant decrease in relative content from 10- to 20-day animals, while the decrease in NM2 MHC relative content occurs later in development and takes place over a longer time span (day 20 to day 60). In addition, the SM1:SM2 ratio remains unusually high in the uterus, even in the adult animals (3.4 at 150 days). The mouse aorta shows a significant increase in the SM MHC's and a significant decrease in the NM MHC from day 10 to day 30, which is similar to data reported for rat aorta. While both the bladder and stomach contain relatively small amounts of NM MHC's (approximately 10% or less), these quantities do show decreases with development. The SM1:SM2 ratio for the aorta, bladder and stomach also start out high, but tend towards 1.0 in the 150-day animals. The differences in the time course of developmental expression of the NM MHC's, in addition to the developmental regulation of expression of the SM MHC's in mouse uterus, are consistent with hypotheses of unique regulation and functional roles for these isoforms. Supp. by AHA Grant #91-GA-22.

M-Pos65

MYOSIN HEAVY CHAIN (MHC) ISOFORMS ARE REGULATED DIFFERENTLY IN MYOMETRIUM (MYO) AND UTERINE ARTERY SMOOTH MUSCLE (UA) IN OVINE PREGNANCY AND THE PUERPERIUM. ((CR Rosenfeld and KE Kamm)) Depts of Peds and Physiol, UT Southwestern Med Ctr, Dallas, TX 75235.

UA MHC SM1/SM2 is >2 in the last 2wks of ovine pregnancy and <2 in the puerperium, changes not seen in renal or carotid arteries. It is unclear when in pregnancy this occurs and if it occurs in other smooth muscles. We studied the ontogeny of these changes in UA as well as bladder and MYO. Tissues obtained from pregnant (P;n=11;88-139d;term=145d), postpartum (PP;n=9;5-42d) and non-pregnant (NP;n=6) ewes were analyzed by SDS-PAGE for protein contents and MHC isoforms with 3-20% and 4% polyacrylamide gels, respectively. There were no changes in bladder MHC isoforms for P+PP+NP by linear regression analysis. Whereas, UA SM1 (%MHC) fell during the puerperium (R=-0.43,p<0.03) and SM2 rose (R=0.41,p=0.04), the opposite occurred in MYO, SM1 rose (0.50,p=0.01), SM2 fell (R=-0.59,p<0.01), and SM1/SM2 rose (R=0.57,p<0.01). Analyzing MYO MHC isoforms as P, early PP (<30d), late PP and NP, SM1 (%MHC) values were 51±8(SD), 45±6, 59±7 and 68±11 (p<0.001), respectively; SM2(%MHC) were 48±8, 52±3, 36±3, and 28±8 (p<0.001), respectively. Western analysis of 2 nonmuscle MHC isoforms showed no brain (embryonic) MHC isoform in any tissue and <1% platelet MHC. MYO and UA MHC isoforms are regulated differentially in ovine pregnancy, possibly reflecting local differences in growth, function and/or the endocrine milieu. MYO may provide a model for study of functional aspects of smooth muscle MHC isoforms.

M-Pos66

MYOSIN FILAMENT STRUCTURE IN VERTEBRATE SMOOTH MUSCLE. ((Jun-Qing Xu, Jean-Marie Gillis* and Roger Craig)) Dept. of Cell Biology, Univ. of Mass. Medical School, Worcester, MA 01655 and *Département de Physiologie, Université Catholique de Louvain, Bruxelles, Belgium. (Spon. by C. Scheid.)

The in vivo structure and state of assembly of myosin filaments in vertebrate smooth muscle are controversial. We are using freeze-substitution to preserve the native structure of the contractile apparatus of guinea pig taenia coli and rat anococcygeus muscles rapidly frozen under physiological conditions. Myosin filaments are generally found in the relaxed state, in agreement with Somlyo et al (Nature 294, 567-570, 1981) and Tsukita et al (Eur. J. Cell Biol. 28, 195-201, 1982), although the number of filaments is variable, and sometimes few or no filaments are seen. The lower densities of filaments suggest that in some cells not all of the myosin is filamentous, in agreement with Gillis et al (J. Muscle Res. Cell Motil. 9, 18-28, 1988). Significant amorphous background staining in these cases is suggestive of the presence of non-polymerized myosin. We are currently preparing antibodies to test whether the amorphous material is indeed myosin. The myosin filament backbone in transverse section most commonly shows a square profile, consistent with the cross-sectional appearance of synthetic side-polar smooth muscle myosin filaments (Craig and Megerman, J. Cell Biol. 75, 990-996, 1977), but not with the profile of the bipolar, helical myosin filaments found in striated muscle. The myosin filaments in longitudinal sections and in negatively stained preparations have a structure suggestive of a side-polar crossbridge arrangement, but preservation is not yet adequate to define the crossbridge polarity unequivocally. A side-polar arrangement would be a significant factor in the ability of smooth muscle to shorten by large amounts. (Supported by NIH grant AR34711.)

M-Pos67

QUANTITATION OF FOLDED MONOMERIC MYOSIN IN RELAXED AND CONTRACTED SMOOTH MUSCLE CELLS BY IMMUNOFLUORESCENCE

((A. Horowitz[1], K.M. Trybus[1], D. Bowman[2], and F.S. Fay[2])), [1]Rosenstiel Res. Center, Brandeis University, Waltham, MA 02254; [2]Dept. of Physiol., Biomed. Imaging Group, Univ. Mass. Med. Center, Worcester, MA 01655

Dephosphorylated smooth muscle myosin *in vitro* forms an assembly-incompetent monomer, which unfolds and assembles into filaments upon phosphorylation. Filaments are clearly present in relaxed smooth muscle cells, but a pool of folded monomers could contribute to maintaining the relaxed state. Cryosections labeled with monoclonal antibody 10S.1, which has 100-fold higher affinity for the folded than the extended monomer (Trybus and Henry, JCB 109:2879, 1989) suggested that this structural state exists in relaxed gizzard tissue (Trybus *et al.*, JCB 115:332a, 1991). Here these findings are extended by using digital imaging microscopy to quantitate the amount of folded myosin in relaxed and contracted tissue. Unfixed, cryosectioned gizzard tissue was first reacted with either Ab 10S.1, Ab S2.2 (which reacts preferentially with extended myosin), or a non-specific antibody, and detected with a secondary antibody conjugated to Texas Red. The tissue was then double-labeled with a conformation-independent antibody (Ab LMM.1) directly conjugated to fluorescein. The intensity of the Texas Red/fluorescein fluorescence was determined, and the value obtained with Ab S2.2 normalized to 1. In relaxed tissue, the value obtained with Ab 10S.1 was 0.38, compared to 0.08 with the control Ab. This value does not necessarily imply a large pool of folded monomer, since the reactivity of Ab S2.2 with filamentous myosin is limited by epitope accessibility. Similar approaches are being applied to phosphorylated, contracted gizzard tissue to see if the monomeric pool is recruited to assemble upon activation.

M-Pos68

SUBCELLULAR REDISTRIBUTION OF MAP KINASE PROVIDES LINK BETWEEN PROTEIN KINASE C AND CONTRACTILE ACTIVATION? ((R.A. Khalil and K.G. Morgan)) Harvard Medical School, Beth Israel Hospital, Boston, MA 02215.

We have previously shown that translocation of the Ca^{2+}-independent protein kinase C (PKC) isoform ϵ-PKC to the surface membrane is involved in phenylephrine (PE)-induced contraction of ferret aorta smooth muscle. However, the signalling pathway between membrane-associated PKC and the contractile proteins is uncertain. Here, we hypothesized a PKC-initiated kinase cascade. We used immunofluorescence and digital imaging microscopy to localize the PKC substrate MAP kinase in ferret aorta cells. In resting cells, MAP kinase was homogeneously distributed in the cytosol with the nuclear region consistently unstained. PE caused an increase in the relative amount of MAP kinase staining at the surface membrane reaching a peak prior to peak cell contraction. Coincident with peak cell contraction, MAP kinase redistributed back to the cytosol in the vicinity of contractile filaments. The PE-induced redistribution of MAP kinase was completely prevented by the PKC inhibitors staurosporine and calphostin C. In contrast with PE, membrane depolarization by 66 mM KCl to activate other, Ca^{2+}-dependent, kinases did not change the distribution of MAP kinase. The PE-induced Ca^{2+}-independent but PKC-dependent transient redistribution of MAP kinase suggests a role for MAP kinase in the signal transduction cascade between translocation of ϵ-PKC to the surface membrane and Ca^{2+}-independent contraction of smooth muscle. Support: NIH HL31704, HL42293 & AHA

M-Pos69

DIFFERENTIAL REGULATION OF PROTEIN KINASE C ISOZYMES BY GONADAL STEROIDS IN RAT UTERUS AND HEART. ((A. Kulick and A.L. Ruzycky)) Dept. Obstetrics, Gynecology & Reproductive Sciences, University of Pittsburgh, Pittsburgh, PA.

Gonadal steroids are important regulators of uterine contractility during pregnancy. Activation of protein kinase C (PKC) is one mechanism by which smooth muscle contractions are expressed. PKC activation results in the translocation of inactive PKC from the cytosol to the cell membrane. It is now recognized that PKC exists as a family of at least 7 different isozymes, differing in cofactor requirements for activation and substrate specificity. We examined whether 17β-estradiol and progesterone affected the expression of membrane-associated (activate) PKC isozymes and whether this effect was tissue specific. Rat uterine smooth muscle and heart ventricles were obtained from ovariectomized non-pregnant animals (OVX) treated with 17β-estradiol (E2; 4 days, 200 μg/kg s.c.) or 17β-estradiol (8 days, 200 μg/kg s.c.) and progesterone (E2P4; last 4 days, 20 mg/kg). Tissues were pooled from 10 animals (per treatment group). Cell membranes were prepared in the presence of protease inhibitors at 4°C and frozen at -80°C until use. Immunoblot analysis of subcellular membrane fractions was performed using isozyme-specific antisera with atleast three separate determinations. E2 treatment significantly increased membrane levels of all PKC isoforms to different degrees (20-137 %) in the uterus. However, in heart only PKC-α was increased and to a much smaller degree than in the uterus (14±3 % vs 80±10 %, mean±SEM respectively). E2P4 treatment compared to OVX increased all PKC isoform levels in the uterus as well. However, PKC-δ, −α, and −β1 levels were decreased relative to levels observed with E2 treatment. In heart, only PKC-δ was affected with E2P4 treatment (increased 18±1%). These results indicate that: 1) Estrogen and progesterone affect PKC isoform expression in tissue-specific manner, and 2) In the uterine smooth muscle, gonadal steroids increase PKC levels in an isozyme specific fashion.

M-Pos70

IMAGING OF CALPONIN DURING CONTRACTILE ACTIVATION OF FERRET PORTAL VEIN CELLS ((C.A. Parker+, W.E. Butler+, K. Takahashi**, T.C. Tao* and K. G. Morgan+; SPON: D.R. Rigney)) +Harvard Medical School, *Boston Biomedical Research Institute Boston, MA 02215, **Center for Adult Diseases, Osaka, Japan

Calponin (CaN) is a thin filament-associated protein that has been implicated to play an auxiliary regulatory role in smooth muscle contraction. We have used immunofluorescence digital and optical confocal microscopy to determine the cellular distribution of CaN in single cells freshly isolated from the ferret portal vein. In resting cells CaN is distributed throughout the cytosol and is excluded from the nuclear area of the cell. It can be seen to run along bundles of myofilaments. The ratio of surface membrane-associated CaN versus cytosol-associated CaN was found to be $R=0.90\pm0.03$ ($n=12$). Upon depolarization of the cell with 96mM K+ the distribution of CaN did not change from that of a resting cell, $R=0.94\pm0.07$ ($n=4$). Upon stimulation with phenylephrine, the cellular distribution of CaN changed from a primarily cytosolic one to one that is primarily surface membrane-associated, $R=1.54\pm0.11$ ($n=8$) $p=0.0007$. Phenylephrine is known to activate PKC-α and to increase $[Ca^{2+}]_i$ in these cells (Biophys. J. 61:A159,1992, J. Physiol. 351:155, 1984). Thus our results suggest that the physiological function of CaN is to mediate agonist activated contraction via a protein kinase C pathway. Support: NIH HL42293, AR41637 and AHA.

M-Pos71

MAPPING CALMODULIN BINDING IN LIVING CELLS BY FLUORESCENCE ANISOTROPY RATIO IMAGING ((A.H. Gough and D.L. Taylor)) Center for Light Microscope Imaging & Biotechnology and Dept. of Biological Sciences, Carnegie Mellon University, Pittsburgh, PA.

Calmodulin is a calcium transducer that activates key regulatory and structural proteins through calcium-induced binding to the target proteins. Steady state fluorescence anisotropy (SSFA) is very sensitive to these interactions. We have implemented SSFA in an imaging system in order to map these interactions in living cells under controlled conditions. Because imaging SSFA in cells with high spatial resolution requires more sensitivity than comparable *in vitro* measures, several fluorescent analogs of calmodulin are compared specifically with respect to fluorophore brightness as well as sensitivity to viscosity and binding interactions. SSFA images of fluorescein calmodulin in serum-deprived Swiss 3T3 cells show that a majority of the calmodulin remains unbound (fraction bound, f_B<10%) under conditions of low free calcium. Furthermore, serum stimulation of these cells, which results in a transient increase in free calcium, leads to calmodulin binding (maximum f_B ~95%) which is correlated with the time course of the elevation and decline of the free calcium ion concentration. The physiological implications of this, and other results, will be described. These results demonstrate the utility of SSFA imaging for mapping interactions of proteins and other macromolecules in living cells. Furthermore, these results are used to explore the potential and limitations SSFA for detecting molecular interactions *in vitro* and *in vivo*. (Supported by NSF DIR-8920118 and Council for Tobacco Research-USA 2044A).

EXCITATION-CONTRACTION COUPLING I

M-Pos72

STRUCTURAL CORRELATES OF EXCITATION-CALCIUM RELEASE (ECR). ((J.R. Sommer, P. Ingram, R. Nassar)) Depts. Path. and Cell Biol., Duke Univ. and VA Med. Centers, and Research Triangle Institute, Durham, NC 27705, and Research Triangle Park, NC; 27709.

Preliminary results of electron probe X-ray microanalysis (EPXMA) show (1) a 0.3 to 0.7 ms interval between an electrical stimulus and Ca release from junctional SR (JSR) in single intact frog skeletal muscle cells quick-frozen at known time intervals following field stimulation (better than 0.1 ms time resolution) and, (2) that by 1 ms, notable amounts of Ca appeared to have returned. Methods: Nassar et al. Scanning EM 1986, I, 309; Nassar and Sommer, Scann. Microsc. 6:745, 1992; LeFurgey et al. J.Micros.164:191,1992. Discussion: The ECR time happens to coincide with and, thus, might be verified independently by, a numerical increase of E-face pits in freeze-etch replicas of JSR and free SR (FSR = smooth SR free of differentiation) reported earlier (Sommer et al. EMSA 1984, p.300). Such an increase may be the result of freeze-cleavage planes being favored at boundaries between membrane lipids and channel proteins altered momentarily during ECR, and captured by quick-freezing. Analogous time-dependent conformational changes in calsequestrin, varying between exposure or burial of polar groups to which heavy metal stains used in electron microscopy (EM) can bind, could account for the consistent marked differences in electron-density of granular material inside the JSR, between muscle fibers quick-frozen at rest or in tetanus (see Nassar et al., above). Such differences are never seen after conventional fixation for EM. The initial fast return of Ca to the JSR, measurable uniquely with EPXMA, suggests rebinding to high affinity sites as they become reestablished on the cytoplasmic side of JSR during ECR: EPXMA measures total Ca, and cannot distinguish between Ca on the outside or inside of the JSR. (Supported by NIH grant # HL-12486, HL20749 and the VA Research Service)

M-Pos73

THE EFFECT OF WARM BLOOD CARDIOPLEGIA ON INTRACELLULAR ELEMENTAL CONTENT OF HUMAN ATRIAL TISSUE. ((Christine S. Moravec, Wendy E. Sweet and *Robert W. Stewart)) Depts of Cardiovascular Biology & *Thoracic and Cardiovascular Surgery, Cleveland Clinic Foundation, Cleveland, OH

Electron probe microanalysis (EPMA) was used to investigate the effects of warm (37°C) blood cardioplegia (CP) on intracellular elemental composition of human atrial tissue. Two pectinate muscles were removed from the right atrial appendage during open heart surgery, before and after exposure to CP. Muscles were mounted in a tissue bath containing 37°C bicarbonate buffer. Isometric contraction and relaxation were recorded at L_{max}. Muscles were frozen during relaxation, using a computerized rapid freezing device, as previously described (Moravec & Bond, Am J Physiol 1991). EPMA was performed on freeze dried cryosections cut from the surface of the frozen muscles. X-ray spectra were collected in scanning mode from each of 10 cells per muscle. All elemental concentrations are expressed as mmol/kg dry wt ± SEM. Elemental composition of the cell was compared between each pair of muscles. Contractile data indicated no significant effect of CP on muscle contraction or relaxation. EPMA on paired muscles taken from the first heart (30 Abands from 10 cells per muscle) revealed an increase in cytoplasmic K (849.8 ± 22.3 (SEM) mmol/kg dry wt in control vs 996.9 ± 22.9 mmol/kg dry wt in CP treated), Cl (193.2 ± 10.6 mmol/kg dry wt in control vs 265.9 ± 10.8 mmol/kg dry wt in CP treated) and Ca (1.75 ± 0.3 mmol/kg dry wt in control vs 2.76 ± 0.4 mmol/kg dry wt in CP treated) following CP treatment. There were no changes in intracellular Na, Mg, or P following CP. These initial results suggest that intracellular concentrations of K, Cl and Ca in human atrial cells are affected by CP, while Na Mg and P remain unchanged. The fact that these changes were measured after stabilization in a tissue bath suggests that the effects of CP on intracellular ion movement are long term rather than acute.

M-Pos74

HIGH TEMPERATURE DEPENDENCE OF CHARGE MOVEMENT REPRIMING.

((A. Gonzalez, C. Caputo)) CBB. IVIC. Caracas. Venezuela.

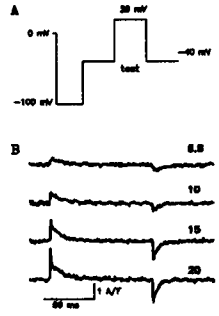

Repriming is a voltage dependent phenomenon occurring at the level of the voltage sensor for contractile activation. We have studied the effect of temperature on intramembrane charge movement (Q) repriming in the cut fiber (L. insularis) preparation using the triple vaseline gap voltage clamp technique. The solutions were (mM): Internal, Ca-aspartate, 110; EGTA, 15; ATP-Mg, 5; Phosphocreatine, 5; Hepes, 5, Ca, 0.79 and Glucose, 5; external : TEA-methanesulphonate, 110; Mg, 10; 3-4 DAP,1; TTX, 0.001; Hepes, 10. Repriming was studied using the protocol shown in the figure (A) designed to avoid contamination from charge 2. The change in temperature from 6 to 20 °C did not affect the voltage distribution of Q_β and Q_γ. However the charge appearing after a short period of repriming was clearly influenced by temperature as it is shown in B. The Q_{10} of the repriming process in 4 fibers was 4.7 (0.3). This result agrees with the high temperature dependence of the contractile repriming. Since Q_γ and Q_β do not show such dependency, it is possible that repriming may be related to the coupling of the voltage sensor with some other structure or molecules that modulate its function as it has been proposed in the mechanical hypothesis or in the Ca-induced feedback. Supported by CONICIT Grant # S1-2148.

M-Pos75

EFFECT OF La^{3+} ON CHARGE MOVEMENT REPRIMING IN FROG SKELETAL MUSCLE.

((C.Caputo,P.Bolaños and A.Gonzalez)).CBB. IVIC. Caracas, Venezuela.

Contractile activation and inactivation are expressed at molecular level by intramembranous charge movement Q_γ and Q_β respectively. Recovery from inactivation (repriming) being linked to the interconversion of Q_β to Q_γ (Brum and Rios 1988). We have studied the effect of La^{3+} (50 μM) on charge movement repriming, since this ion is known to improve contractile repriming (Caputo and Bolaños, 1989). We used a pulse protocol designed to measure only Q_γ. It comprised a prepulse to a negative potential, where repriming occurred, followed by a pedestal to -40 mV in order to avoid Q_β and finally the test pulse. The control pulse protocol was the same, but not allowing for repriming. Single cut frog skeletal muscle fibers (Leptodactilus insularis) were used with the triple vaseline gap technique. The cut ends, briefly saponinized (0.005 %), were bathed in a solution containing, in mM: Ca-Aspartate, 110; EGTA, 15; $Ca(OH)_2$, 0.78; ATP-Mg, 5; Phosphocreatine, 5; $Mg(OH)_2$, 0.5; Hepes, 5. The external solution contained (mM): TEA-Methanesulfonate, 110; $Mg(OH)_2$, 10; 3-4 Diaminopiridine, 1; TTX, 0.001; Hepes, 10. La^{3+} did not affect the voltage distribution of charge in depolarized (0 mV) fibers nor the voltage dependence of charge repriming. In three fibres the repriming time course could be fitted by the sum of two exponential with τ_1 = 6.4 and τ_2 = 30.1 s. Lanthanum speeds up the time course of repriming: τ_1 = 0.8 and τ_2 = 19.1 s, without changing the maximum charge reprimed. This effect suggests that La^{3+} binds preferentially over Mg^{2+} on an external site on the voltage sensor, modulating the time dependent steps of repriming. The same site could modulate also inactivation of the voltage sensor.
Supported by CONICIT Grant # S1-2148.

M-Pos76

T-SYSTEM VOLTAGE CHANGES, CHARGE MOVEMENT, AND INTRINSIC OPTICAL SIGNALS RECORDED IN THE PRESENCE OF BAPTA.

((K. Polakova and J.A. Heiny)) Dept. of Physiology & Biophysics, Univ. of Cincinnati, Cincinnati, OH 45267-0576

We examined the effect of SR depletion on the T-system nonlinear potential change (Heiny & Jong, *J Gen Physiol* 95:147-175, 1990) recorded optically from single voltage-clamped frog fibers. To deplete the SR, we used high concentrations of the fast intracellular Ca buffer BAPTA in combination with a repetitive suprathreshold pulse protocol. The intrinsic optical signal (Rios et al, *Biophys J* 41:396a, 1983), recorded at a wavelength beyond the absorption spectrum of the potentiometric dye, was used as a monitor of Ca release. BAPTA was applied at a concentration of 10-20 mM in the end pools and diffused slowly into the central pool where its concentration did not reach equilibrium during a 2-3 hour experiment. The BAPTA concentration in the central pool was estimated using a model of 1-dimensional diffusion down a cylinder and published apparent myoplasmic diffusion coefficient for the closely similar compound FURA-2 (Baylor & Hollingworth, *J Physiol* 403: 151-192,1988). When BAPTA reached an estimated concentration of 2-3 mM in the central pool, we applied repetitive suprathreshold pulses at 0.1 Hz to empty Ca from the SR. With this protocol, we could completely eliminate the intrinsic signal after an average of 6 pulses, suggesting that BAPTA irreversibly binds the released Ca during the pulse intervals used. This protocol significantly reduced or eliminated the nonlinear component of the T-system potential change. However, charge movement, recorded simultaneously, was also altered by this protocol. These findings are being analyzed in terms of feedforward or feedback models of E-C coupling. (Supported by NIH and AHA)

M-Pos77

CALIBRATION OF TRANSVERSE TUBULE MEMBRANE POTENTIAL USING THE POTENTIAL-SENSITIVE DYE DiSC3(5).

((James W. Kramer and Adrian M. Corbett.)) Department of Physiology and Biophysics, Wright State University, Dayton, OH 45435

Membrane potential changes associated with altered K^+ gradients were studied in isolated transverse tubule vesicles from rabbit skeletal muscle. The vesicles were equilibrated in either a 100mM K-Propionate or a 4mM K-Propionate solution containing 2mM $MgCl_2$, 1mM Na-azide, 36mM Imidazole, and 2.5μM final DiSC3(5) (3,3'-Dipropylthiadicarbocyanine iodide). Vesicles equilibrated with 100 mM K-propionate were diluted into TEACl solutions to produce lower extravesicular [K^+] (resulting in depolarization) while vesicles equilibrated with 4 mM K-propionate were diluted into K-propionate solutions to produce higher extravesicular [K^+] (resulting in hyperpolarization). A constant dye/protein ratio was maintained for all dilutions. Membrane potential changes were measured by changes in DiSC3(5) fluorescence. Dilution of transverse tubules into either depolarizing or hyperpolarizing solution was compared to a non-depolarizing solution to determine the percent change in fluorescence in the presence of valinomycin. The percent change in fluorescence varied linearly with the log of extravesicular [K^+]. The slope obtained for 100 mM luminal [K^+], under depolarizing conditions, was -15.52 while the slope obtained for 4 mM luminal [K^+], under hyperpolarizing conditions, was -10.89. According to these experiments, the presence of valinomycin was needed to achieve a full membrane potential change. Depolarization-induced calcium release experiments, using isolated triads, were performed in the presence of valinomycin. This resulted in a voltage dependence of calcium release that was steeper and shifted to the right compared to previous studies (Kramer & Corbett, 1992, Biophysical J. 61:A24). This work was supported by NSF Biological Instrumentation Grant DIR-8812094.

M-Pos78

T-TUBULE - MEDIATED SR CA^{2+} RELEASE FROM RABBIT SKELETAL MUSCLE HOMOGENATES IS NOT INHIBITED BY BAPTA.

((Kristin Anderson and Gerhard Meissner)). Dept. of Biochemistry & Biophysics, Univ. of North Carolina, Chapel Hill, NC 27599. (Spon. by H. Xiong)

In skeletal muscle excitation-contraction coupling, the role of Ca^{2+} in mediating sarcoplasmic reticulum (SR) Ca^{2+} release is not well understood. We have investigated the effects of Ca^{2+} on transverse (T)-tubule - mediated Ca^{2+} release from rabbit skeletal muscle homogenates using a rapid filtration protocol. Homogenates were added to an active SR $^{45}Ca^{2+}$ loading medium which was designed to result in the establishment of a T-tubule membrane potential. The homogenates were then placed on filters and washed with a medium which was expected to result in T-tubule "depolarization". A small amount of T-tubule depolarization-induced Ca^{2+} release (~10% in 50 ms) was observed in the presence of 1 mM BAPTA, which could be inhibited by prior incubation of homogenates with 1 μM PN200-110. This result indicates that muscle homogenates contain functional T-tubule - SR junctional complexes and that Ca^{2+} is not required for T-tubule - mediated SR Ca^{2+} release.

M-Pos79

GTPγS REMOVES D600 BLOCK IN MECHANICALLY PEELED RABBIT SKELETAL FIBERS.

((L.Carney-Anderson and S.K. Donaldson)) U of MN, Minneapolis, MN 55455. (Spon. by D. Levitt)

G proteins located in the transverse tubules (TT) of skeletal muscle may physically interact with the dihydropyridine receptor (DHPR), the voltage sensor of excitation-contraction (EC) coupling. In this study, using the mechanically peeled rabbit skeletal fiber preparation (sarcolemma removed, TT sealed/polarized), GTPγS, a nonhydrolyzable G protein activator, augments TT depolarization-induced tension transients at a concentration of 50μM. This GTPγS augmentation is blocked by 500μM GDPβS, a G protein specific inhibitor, suggesting involvement of a G protein which might act through a DHPR mechanism. To reveal a direct, physical interaction between the DHPR and G protein, the peeled fiber was put into a D600-blocked state and GTPγS (50μM) was added to the bath. GTPγS removed the D600 block of EC coupling despite the continued presence of bath D600. Preliminary results indicate that GDPβS (500μM) can also reverse a D600 block. These findings show that when stimulatory or inhibitory GTP analogues are bound to a G protein, they reverse the EC coupling blocking action of D600; this suggests a physical interaction of a G protein and the DHPR. Supported by USPHS, NIH (AR 35132) and MDA grants.

M-Pos80

CONTRACTILE THRESHOLD IN MUSCLES AND MYOTUBES FROM NORMAL AND MALIGNANT HYPERTHERMIC NEONATAL PIGLETS.

((E.M. Gallant and R. Jordan)) University of Minnesota, St. Paul, MN 55108.

Studies where conducted with muscles from neonatal piglets that were homozygous for Arg^{615} (normal (N)) or homozygous for Cys^{615} (malignant hyperthermic (MH)) ryanodine receptor alleles, and with heterozygotes (H). Contractile activation threshold was evaluated in cultured myotubes and in bundles of intact muscle cells in order to determine whether the lower than normal threshold characteristic of adult MH and H muscles (AJP 262:C422, 1992) was expressed in immature muscles. Strength-duration relationships for myotubes were determined using whole cell patch clamp techniques with membrane potential held at -80 mV and myotubes subjected to square pulses of various strengths and durations. External solutions contained 3 μM TTX and no added Na^+ or K^+. Threshold was determined by observing the cell for contraction on a high resolution video monitor. Rheobase values (threshold for long pulses, i.e., 300 msec) were -5.8$\pm$1.1 mV for N, -15.5$\pm$3.4 mV for H and -22.6$\pm$2.6 mV for MH myotubes. Similarly the threshold for K-contractures in intact cell bundles from N muscles (40 mM K^+) was higher than in H (25 mM) or MH (15 mM) muscles ($P<0.03$) in solutions with constant $[K^+]x[Cl^-]$. Thus the enhanced sensitivity to depolarization which is characteristic of MH and H adult muscle cells was also expressed in myotubes and piglet muscles. Therefore, these developmentally immature preparations are likely to express other differences associated with adult MH muscles. (Supported by American Heart Assn and NIH AR-27410 grants.)

M-Pos81

PEAK CALCIUM RELEASE IS SUPPRESSED BY HIGH AFFINITY CALCIUM BUFFERS APPLIED FROM THE CUT ENDS OF FROG SKELETAL MUSCLE FIBERS.

((L. Csernoch, V. Jacquemond, M.F. Schneider)) Dept. Biochem., UMAB, Baltimore, MD 21201

Calcium transients ($\Delta[Ca^{2+}]$) were recorded simultaneously at high and low sensitivity using the dyes Antipyrylazo III and fura-2 in Rana pipiens single fibers voltage clamped in a double vaseline gap. The rate of release of calcium (R_{rel}) from the sarcoplasmic reticulum (SR) was calculated from $\Delta[Ca^{2+}]$. To minimize errors due to possible incorrect scaling of the calcium bound to fast buffers R_{rel} was corrected for depletion of calcium in the SR and normalized to the calculated SR calcium content. High affinity calcium buffers, fura-2 or BAPTA, were applied at the cut ends in millimolar concentrations and reached the voltage clamped segment by diffusion. $\Delta[Ca^{2+}]$ was suppressed and R_{rel} lost its peak as the concentration of the applied buffer increased at the site of the measurement, whereas the steady level of R_{rel} showed no significant changes. In 4 fibers in which 1.1-1.6 mM fura-2 markedly suppressed peak R_{rel} the steady level was 0.49 $\pm$ 0.04 % ms^{-1} (mean $\pm$ S.E.), equal to control values (0.56 $\pm$ 0.06 % ms^{-1}, n=5) from other fibers with low internal buffering. The degree of suppression of peak R_{rel} was similar in these diffusion experiments to that reported earlier for microinjection of comparable buffer concentrations. When the concentration of fura-2 or BAPTA exceeded about 2 mM at the voltage clamped segment the peak of R_{rel} was completely lost. Supported by NIH and MDA.

M-Pos82

CALCIUM UPTAKE PROPERTIES OF SR VESICLES STUDIED AT SUB-μM $[Ca^{2+}]$ USING FURA-2 AS BUFFER/INDICATOR.

((M. Y. Ho, M.F. Schneider)) Dept. Biochem., UMAB, Baltimore, MD 21201

Calcium uptake of rabbit skeletal SR vesicles (100 μg protein/ml) in (mM) 100 KCl, 5 $MgCl_2$, 20 HEPES (pH 7.0) and 2 ATP plus ATP regenerating system was monitored at sub-μM $[Ca^{2+}]$ using fura-2 (10μM). If fura-2 is <75% saturated virtually all of the Ca outside the SR ($=Ca_T$) is Ca-fura, so the net rate of Ca uptake by the vesicles ($=-dCa_T/dt$) is given by -dCa-fura/dt plus a small contribution from $-d[Ca^{2+}]/dt$. After Ca_T increments of 1 to 5 μM Ca-fura and $[Ca^{2+}]$ returned to pre-addition levels along a 2 exponential time course. $-dCa_T/dt$ was calculated as the derivative of a 2 exponential fit to Ca_T and was plotted as a function of the $[Ca^{2+}]$ measured at the same point in time. At a given $[Ca^{2+}]$, the observed $-dCa_T/dt$ was considerably lower after a 5 μM Ca addition than after a 1 μM addition. This was not due to greater accumulated intravesicular Ca since the 1 μM addition was made after a 5 μM addition. The eqn $-dCa_T/dt = A[Ca^{2+}]^n - L$, which applies to the low $[Ca^{2+}]$ range of a cooperative Ca uptake system acting against a constant leak (L), gave a good fit to the data for Ca_T increments of 1-5 μM using a value of n near 4, consistent with pump molecules acting as functional dimers since each molecule binds 2 Ca ions. The high power $[Ca^{2+}]$ dependence of uptake detected in muscle fibers (J Physiol 441:639, 1991) is thus also seen in the net uptake properties of vesicles at sub-μM $[Ca^{2+}]$ under conditions where uptake can be monitored at different SR contents. Supported by NIH.

M-Pos83

DETECTION OF CA^{2+} TRANSIENTS IN SKELETAL MUSCLE FIBERS USING THE LOW AFFINITY DYE CALCIUM-GREEN-5N.

((J. Vergara and A. Escobar)) Dept. of Physiology, UCLA School of Medicine.

Calcium transients elicited either by electrical stimulation or flash photolysis of DM-nitrophen were recorded from frog single skeletal muscle fibers using the fluorescent dye Calcium-Green-5N. The Ca-binding properties of this dye were characterized in cuvette calibrations at 0.1 M ionic strength (17 °C) and yielded a K_d of 85 μM and exponential responses to flash photorelease of Ca^{2+} ions with a predominant time constant of about 30 μs. Flash photolysis Ca^{2+} transients (FP-transients) in DM-Nitrophen-loaded muscle fibers had early exponential components comparable to those recorded *in-vitro* but they were usually followed by secondary components of Ca^{2+} released by the SR. Ca^{2+} transients generated by action potential stimulation of the fibers (AP-transients) reported peak values of 10-20 μM, far below the levels of saturation of the dye by Ca^{2+}. In spite of this, when FP-transients were elicited in superposition with AP-transients, the resulting Ca^{2+} signals showed evidence of non-linear interactions that rule out the possibility of independent processes. Specifically, AP-transients were associated with an increase in the buffer capacity of the fiber that resulted in dampening of the FP-transients, and FP-transients could release Ca^{2+} from the same pool of AP-transients. (Supported by USPHS AR-25201 and MDA)

M-Pos84

EFFECT OF 0-6 mM FURA-2 ON ACTION-POTENTIAL STIMULATED Ca RELEASE FROM SARCOPLASMIC RETICULUM (SR) OF FROG CUT MUSCLE FIBERS.

((P.C. Pape, D.-S. Jong, W.K. Chandler, & *S.M. Baylor)) Dept. of Cellular and Molecular Physiology, Yale Univ. School of Medicine, New Haven, CT 06510 and *Dept. of Physiology, Univ. of Pennsylvania, Philadelphia, PA 19104.

Stretched fibers from *Rana temporaria* were mounted in a double Vaseline-gap chamber with a K-glutamate internal solution and a Ringers external solution (~14°C). PDAA, a low affinity Ca indicator, was added to the end pools where it could diffuse into the fiber to monitor changes in myoplasmic free [Ca], Δ[Ca], at the optical recording site (Hirota et al., 1989). When [PDAA] had reached about 3 mM, 4 or 8 mM fura-2, a high affinity Ca indicator, was added to the end pools. Δ[Ca] and SR Ca release were monitored after action potential stimulation as fura-2 diffused into the fiber. The rate of SR Ca release, $d\Delta[Ca_T]/dt$, was taken to be equal to the rate of Ca binding to intrinsic myoplasmic sites, calculated from Δ[Ca] (Baylor et al., 1983), plus d[Cafura-2]/dt. The mean peak value of $d\Delta[Ca_T]/dt$ was 138 μM/ms with 0 mM fura-2, 155 μM/ms with 0.5-2 mM, 147 μM/ms with 2-4 mM, and 77 μM/ms with 5-6 mM. The increase in $d\Delta[Ca_T]/dt$ from 0 to 4 mM fura-2 is qualitatively consistent with the results of Baylor and Hollingworth (1988) and Hollingworth et al. (1992) who suggested that it is due to a reduction in Ca-dependent inactivation of SR Ca release. The decrease from 4 to 6 mM may be due to a reduction in Ca-induced Ca release (Jacquemond et al., 1991) or some pharmacological effect of the large fura-2 concentration. *Supported by NIH grant AR-37643.*

M-Pos85

EFFECT OF 0-8 mM FURA-2 ON SR Ca RELEASE IN VOLTAGE-CLAMPED FROG CUT MUSCLE FIBERS.

((D.-S. Jong, P.C. Pape, W.K. Chandler & *S.M. Baylor.)) Dept. of Cellular and Molecular Physiology, Yale Univ. School of Medicine, New Haven, CT 06510 and *Dept. of Physiology, Univ. of Pennsylvania, Philadelphia, PA 19104.

The experimental method was similar to that used in the preceding abstract except for the use of a Cs-glutamate internal solution and a TEA-methanesulfonate external solution. Trace 0 shows the estimated rate of SR Ca release, after correction for SR Ca depletion, with [fura-2] = 0 mM. The decline after the peak is attributed to Ca-dependent inactivation of SR Ca release. Jacquemond et al. (1991) obtained a qualitatively similar response with 0 mM fura-2 and found that 2-3 mM fura-2 removed the transient component without affecting the smaller steady level. They proposed that the transient component depends on Ca-induced Ca release, which is blocked by fura-2. In our experiments (see figure), fura-2 increased the rate of SR Ca release, consistent with a reduction in Ca-dependent inactivation of SR Ca release. *Supported by NIH grant AR-37643.*

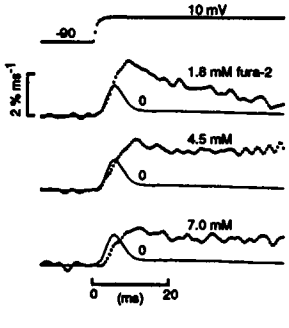

M-Pos86

Ca^{2+} MODULATION OF SR Ca^{2+} RELEASE IN MAMMALIAN SKELETAL MUSCLE FIBERS. ((Osvaldo Delbono and Enrico Stefani)). Dept. of Molecular Physiology and Biophysics, Baylor College of Medicine, Houston, TX, 77030.

Intracellular Ca^{2+} transients were recorded using the double Vaseline gap technique and Mag-Fura-2 (400 μM), Fura-2 (50 μM) as Ca^{2+} indicators, in rat extensor digitorum longus fibers. Double pulse protocols varying the first pulse duration, the interpulse time, the conditioning pulse duration and amplitude were used in order to set the myoplasmic Ca^{2+} concentration ($[Ca^{2+}]_i$) at different values. The figure shows that shorter interpulse time (30 ms) abolish the first sharp and initial component of the calculated Ca^{2+} release (dCa_{rel}/dt) compared to control (1000 ms). This phenomenon was more pronounced with longer conditioning pulses.

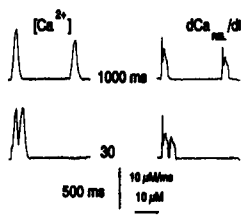

Another maneuver to study the myoplasmic $[Ca^{2+}]_i$ conditioning of Ca^{2+} release from the SR was the use of high intracellular Ca^{2+} buffers concentrations. Fura-2, 50 μM and Br_2BAPTA (1,2-bis-(2-amino-5-bromo-phenoxy)ethane-N,N,N',N'-tetraacetic acid) 4 mM, preclude major myoplasmic $[Ca^{2+}]_i$ increments in response to fiber depolarization. In this conditions, the steady state Ca^{2+} release was not modified while the first component was abolished. This is in agreement with observations in amphibian (Csernoch *et al.* Biophys. J. (1992) 61, A23). Supported by MDA and NIH grants.

M-Pos87

DETERMINATION OF RESTING FREE CALCIUM IN BARNACLE MUSCLE USING MODIFIED AEQUORINS AND IMAGE-ENHANCEMENT DURING CALCIUM BUFFER INJECTIONS. ((E.B. Ridgway and A.M. Gordon)) Dept. Physiol., Med. Coll. Va, Richmond, VA 23298; and Dept. Physiol. & Biophys., U.W. Med. Sch., Seattle, WA 98195.

The resting free calcium level is an important parameter for interpreting calcium transients, and modeling the relationships between calcium transients and force during contraction. We injected modified aequorins (recombinant, and hch-, kindly provided by O. Shimomura, Woods Hole), which after a 30 min. diffusion give reasonable resting glows. Subsequent injection of calcium (strongly buffered (10 mM) with either EGTA or BAPTA) causes the resting glow to increase, decrease, or remain unchanged depending on the free calcium level in the injection buffer mixture. This null method is inherently accurate, but mechanical artifacts on injection (almost always due to damage, or swelling) substantially reduce the accuracy when total light emission is measured. We therefore resorted to image-intensified video-microscopy of the injected region during injection, followed by video processing (Image-1) of artefact-free regions, to greatly improve the consistency of the null method. We found the resting free calcium level in the lateral depressor fibers of freshly dredged barnacles to be 335±46 nM (±SD) under conditions of hch-aequorin and BAPTA buffers. Recombinant-aequorin gave essentially the same result while EGTA buffers yielded slightly lower values. Supported in part by NSF grant DCB-8904377 and NIH grant NS-08384.

M-VCR1

SPLOTCHY AND NON-HOMOGENOUS Ca RELEASE IN ISOLATED FROG SKELETAL MUSCLE FIBERS. ((M. Rozycka, H. Gonzalez-Serratos and W.F. Goldman)) Departments of Biophysics and Physiology, University of Maryland School of Medicine, Baltimore, MD 21201

During normal contractions in skeletal muscle cytosolic calcium gradients should be seen only briefly as calcium diffuses from sarcoplasmic reticulum (SR) calcium-release sites[1]. Over longer periods $[Ca^{2+}]_i$ gradients have been reported in heart muscle cells during propagated waves of elevated $[Ca^{2+}]_i$[2] and in diverse isolated or cultured cells. These long-term $[Ca^{2+}]_i$ fluctuations arise because intracellular calcium sources contain calcium-release channels controlled or influenced by $[Ca^{2+}]_i$. In skeletal muscle, however, where calcium release is controlled by voltage across the tubular membrane, and is assumed not to depend on $[Ca^{2+}]_i$, Ca gradients are limited to the sub-millisecond time-scale[1], and have not been resolved experimentally. We have examined the spatial distribution of $[Ca^{2+}]_i$ during tetanic stimulation in isolated frog skeletal muscle cells using fluorescence imaging methods. We have found a new and completely unexpected pattern of Ca release in skeletal muscle cells during steady-state tetanic contractions; more Ca is released towards the center of the fibers, and within this gradient there are spots of very significant and slow fluctuations of intracellular calcium release. These patterns are not caused by either movement or photon noise. Our findings could be explained if the calcium release process in skeletal muscle is influenced significantly by either $[Ca^{2+}]_i$, or the SR calcium content, like cardiac muscle, and suggests that the control of skeletal muscle SR Ca release can include the established voltage-dependent plus a cardiac-like process of calcium-induced Ca release and a Ca release inhibition by Ca. (Supported by NIH Grant R01 NS17048). [1]Biophys. J. 45:913 (1984). [2]Circ. Res. 65:115 (1989).

M-VCR2

CALCIUM TRANSIENTS IN DYSGENIC MYOTUBES *IN VITRO*. ((B.E. Flucher, S.B. Andrews, S. Haynes and J.A. Powell)) Lab. of Neurobiology, NINDS, NIH, Bethesda, MD 20892 and Dept. of Biological Sciences, Smith College, Northampton, MA 01063. (Spon. T.S. Reese)

Muscular dysgenesis (*mdg*)—a mutation in the gene of the α_1 subunit of the skeletal muscle dihydropyridine receptor—is characterized by a lack of excitation-contraction coupling, slow (L-type) calcium conductances and the movement of intramembrane charges associated with voltage sensing. Comparison of calcium transients, i.e., rapid changes in free cytoplasmic calcium levels, in normal and dysgenic myotubes using the fluorescent calcium indicators fluo-3 and indo-1 shows that dysgenic cultures express two of the three types of calcium transients found in normal cultures. Dysgenic myotubes generate spontaneous localized calcium transients (fast localized transients, FLTs) and propagated calcium waves but do not respond to electrical stimulation with a calcium transient. Calcium waves are propagated at the normal rate of approximately 35 μm/s. They can be stimulated with 2 mM caffeine but, unlike waves in normal myotubes, they can also occur spontaneously. FLTs appear qualitatively similar in dysgenic and normal myotubes; however, they occur more frequently in the mutant cultures. Since FLTs and calcium waves are independent of extracellular calcium, they may represent spontaneous and calcium-induced calcium release from sarcoplasmic reticulum (SR), respectively. Thus, the uncoupling of excitation and calcium release in dysgenic myotubes does not inhibit membrane potential-independent modes of calcium release from the SR. The increased spontaneous release activity as well as the occurrence of spontaneous calcium-induced calcium release events may result from altered resting levels of calcium. The observed periodic fluctuations of cytoplasmic calcium concentrations may serve as regulatory signals during muscle development in normal and dysgenic myotubes alike. (Supported by a grant from MDA to JAP)

M-Pos88

CHLORIDE-DEPENDENCE OF Ca^{2+}-INDUCED Ca^{2+} RELEASE IN JUNCTIONAL SR VESICLES OF RABBIT SKELETAL MUSCLE. ((M. Sukhareva and R. Coronado.)) Department of Physiology, University of Wisconsin Medical School, Madison, WI 53706.

Ca^{2+}-induced Ca^{2+} release (CICR) from SR vesicles was studied in the presence of different anions using the fast-filtration technique. SR were passively loaded with 5 mM $^{45}Ca^{2+}$ (70 nmoles/mg) and release was induced by 1 μM buffered free Ca^{2+}, pH 7.2. In the absence of Cl^- (150 mM K-gluconate in and out of the SR; curve 1), CICR was incomplete and about 3 times slower than that in the presence of Cl^- (150 mM Choline-Cl in and out; curve 4). When Cl^- was present only inside (150 mM K-gluconate out, 150 mM Choline-Cl in; curve 2) or only outside (150 mM Choline-Cl out, 150 mM K-gluconate in; curve 3), CICR was less than when Cl^- was present on both sides. Ruthenium red blocked >90% of CICR in all solutions. Other anions activated CICR, in the following ranking order: Cl^->SO_4^{2-}>Br^->HEPES$^-$>SCN^->Methane sulfonate$^-$>Gluconate$^-$>I^->Acetate$^-$. Our data suggest a component of Cl^--induced SR Ca^{2+} release observed in isolated triad and skinned fiber preperations may be due i) to a direct effect of Cl^- on the activity of the ryanodine receptor or ii) to the presence of a secondary Ca^{2+} efflux channel sensitive to anions (Supported by NIH, MDA, and AHA.)

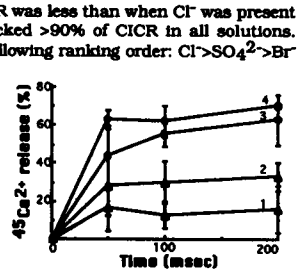

M-Pos89

EVIDENCE FOR A Ca^{2+}-DEPENDENT NEGATIVE CONTROL MECHANISM FOR Ca^{2+}-INDUCED Ca^{2+} RELEASE IN CRAYFISH MUSCLE FIBERS. ((S. Gyorke and P. Palade)) Dept. Physiology and Biophysics, Univ. Texas Medical Branch, Galveston, TX 77550.

Ca^{2+} dependent inactivation of the Ca^{2+} release has been suggested as an essential negative control mechanism which counters the intrinsically assumed positive feedback of Ca^{2+}-induced Ca^{2+} release (CICR) in heart (Fabiato, 1985). The experimental demonstration of this negative control mechanism in cardiac myocytes however has been controversial. We have been studying CICR in crayfish cut muscle fibers using the triple vaseline voltage clamp technique and rhod-2 (J. Physiol. 456, 443, 1992). Three experimental approaches were used to define a negative control mechanism for CICR in crayfish muscle fibers. 1) Preelevations of $[Ca^{2+}]$ induced by conditioning depolarization or photolytic liberation of Ca^{2+} from DM-nitrophen (caged Ca^{2+}) depressed the rate of Ca^{2+} release during a subsequent test pulse. 2) When the rate of I_{Ca} onset was varied by applying voltage ramps with different slopes, currents with fast onset elicited bigger Ca^{2+} release than currents with slower onset, even though the amplitude of the currents was the same. 3) Sustained steps of I_{Ca}, obtained by diffusion out the cut ends of metabolic factors promoting I_{Ca} inactivation, caused only transient releases of Ca^{2+} from the SR. The early cessation of the release was not due to a depletion of Ca^{2+} from the SR since caffeine dramatically potentiated the amplitude of the Ca^{2+} transients. These results provide evidence for the existence of a Ca^{2+}-dependent negative control mechanism for CICR in crayfish muscle. (Supported by AHA).

M-Pos90

EXTRASYSTOLIC POTENTIATION OF CONTRACTION IN GUINEA PIG LEFT VENTRICULAR MYOCYTES IN THE ABSENCE OF INCREASED PEAK FREE CALCIUM. ((F.M. Siri, C. Nordin, R. Aronson and E.H. Sonnenblick)) Albert Einstein College of Medicine, Bronx, N.Y. 10461.

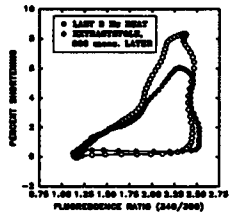

We sought to define the extent to which changes in free cytosolic calcium (Fura2-AM) underly the contractile potentiation seen in extrasystoles triggered at varying delays after steady-state 3 Hz drive (37°C) in single guinea pig left ventricular myocytes (n=8). Maximal potentiation ($P<0.01$) was produced with a delay of 800 msec. (Figure: group averages, 4 msec. data points). This occurred despite a small but significant decrease in the peak of the fluorescence transient ($P<0.01$) and no significant change in diastolic cell length. Although integrated peak area (ratio units x seconds) increased significantly in the extrasystole (2.76±0.40 vs. 2.36±0.36, mean±SD, $P<0.01$), it remained high in two subsequent beats 2 and 4 seconds later (2.91±0.33 and 2.80±0.32, respectively) despite progressive decreases in both the peak of the fluorescence transient (2.36±0.25, 2,22±.0.25) and percent cell shortening (7.39±2.12, 6.15±1.89). Thus, although changes in free calcium parallel the contractile decay in subsequent beats, potentiation of myocyte shortening in the extrasystolic beat is not attibutable to altered cell length or to altered peak free calcium. This raises the possibility that acute changes in myofilament calcium-responsiveness may be involved.

M-Pos91

VOLTAGE-DEPENDENCE OF CONTRACTION IN ISOLATED RAT VENTRICULAR MYOCYTES. ((R.A. Bouchard, R.B. Clark, W.R. Giles)) Dept. Medical Physiology, University of Calgary, Alberta, Canada T2N 4N1

Activation of contraction was studied in single rat ventricular cells. Contraction measured as unloaded cell shortening was recorded simultaneously with membrane voltage and current. At a fixed holding potential of -80 mV, a bell shaped shortening-voltage (S-V) relation was obtained in the presence of TTX (2×10^{-6} M) and 4-AP (3×10^{-3} M) to block Na and K currents, respectively. The voltage dependence of contraction was very similar to that of L-type Ca current, I_{Ca}, in these cells; and both I_{Ca} and contraction were blocked completely by Cd or verapamil. Removal of TTX resulted in significant activation of contraction at potentials negative to the threshold for activation of I_{Ca} (-70 to -40 mV). Two-microelectrode experiments showed that in this voltage range there were large deviations of membrane potential from the applied clamp potential, suggesting that voltage 'escape' allowed sufficient depolarization to activate I_{Ca}. Contraction at these test potentials was suppressed completely by Cd or verapamil or depolarization of the holding potential to -40 mV; or by substitution of external Na with Cs (but not Li). Deletion of 4-AP from the superfusate resulted in a plateau on the S-V curve at test potentials between +20 and +80 mV. Contraction in this voltage range was accompanied by large transient outward K current, I_t. Two microelectrode experiments again showed significant voltage escape during activation of I_t. Contractions positive to +20 mV were suppressed by Cd or verapamil or by depolarization of the holding potential, but were insensitive to TTX or changes in external Na, pipette Na, an inhibitory peptide (XIP) to the cardiac Na/Ca exchanger. These results demonstrate that activation of contraction in rat ventricular cells depends exclusively on Ca influx through L-type Ca channels. (Supported by AHFMR, CHF and MRC).

M-Pos92

REGULATION OF UNLOADED CELL SHORTENING BY SARCOLEMMAL Na/Ca EXCHANGE IN ISOLATED RAT VENTRICULAR CELLS. ((R.A. Bouchard, R.B. Clark, W.R. Giles)) Dept. Medical Physiology, University of Calgary, Alberta, Canada T2N 4N1

Regulation of cell shortening and relaxation by sarcolemmal Na/Ca exchange was investigated in rat ventricular myocytes. Contraction was measured simultaneously with membrane current and voltage using the whole-cell voltage clamp technique and a video edge detection device. Peak shortening was strongly dependent on diastolic membrane potential between -140 and -50 mV. This voltage-dependence was abolished completely when an inhibitory peptide to the cardiac Na/Ca exchange (XIP, 2×10^{-5} M) was present in the recording pipette. Rapid (<1 s) changes of external Na had marked effects on action potential configuration but did not change the magnitude of contraction at a fixed level of Ca loading, suggesting that Na/Ca is not required for activation of contraction. Depolarizations to test potentials between -70 and +70 mV resulted in a bell-shaped shortening-voltage (S-V) relation. Contractions in this voltage range were suppressed by Cd or verapamil but were unaffected by TTX, 1.5×10^{-6} M or reduction of external Na with Li or Cs. Changes in pipette Na between 8-13 mM or inclusion of XIP in the recording pipette had no effect on the shape of the S-V curve, suggesting that the voltage-dependence of contraction was resulted from Ca influx through Cd-sensitive Ca channels. The effect of changing the rate of repolarization on cell shortening was studied by applying a series of ramp waveforms immediately following depolarizations which activated contraction. Slowing repolarization had no immediate effect on contractions at a fixed level of Ca loading, thereafter twitch amplitude increased in a beat-dependent manner. These inotropic changes developed fully during the first test contraction in the presence of caffeine and were markedly reduced with XIP in the recording pipette, suggesting that they were due to time-dependent changes in loading and release of Ca from intracellular stores. (Supported by AHFMR, CHF and MRC).

M-Pos93

8-BROMO CYCLIC GMP DECREASES MYOFILAMENT CALCIUM RESPONSIVENESS IN RAT MYOCYTES. ((*A.M.Shah, H.Spurgeon & E.G.Lakatta))GRC/NIA,NIH,Baltimore,MD 21224 & *UWCM,Cardiff,UK.

There are conflicting data on the myocardial actions of cGMP. We studied the effect of 8-bromo cGMP (8bcGMP, 1-100 μM) on cell length (CL) and indo-1 fluorescence (410:490nm ratio, R) in adult rat ventricular myocytes (HEPES buffer, 1 mM Ca^{2+}, 0.5 Hz, 25°C). 8bcGMP (50 μM) increased steady-state diastolic CL by 0.9±0.4 μm (mean,SE), decreased time to peak twitch shortening by 17.1±1.3% and decreased extent of shortening by 17.3±5.8% (all $p<0.05$; n=7), but caused no significant change in peak shortening velocity, diastolic and peak systolic R or time to peak R (bold lines, fig). In the CL vs. $[Ca^{2+}]_i$ phase-plane diagram, 8bcGMP shifted the terminal trajectory during twitch relaxation to the right. 8bcGMP effects were inhibited by KT 5823 (1 μM), which inhibits cGMP protein kinase (PKG), or in the presence of isoprenaline (3 nM). 8bcGMP had no effect on pH_i in SNARF-loaded myocytes (n=4). These data indicate that 8bcGMP decreases relative myofilament response to Ca^{2+} in rat cardiac myocytes probably via activation of PKG. This action is independent of changes in pH_i but may involve a cyclic AMP-sensitive mechanism.

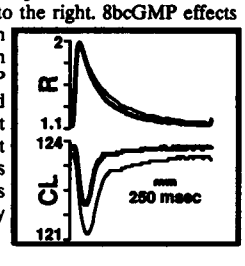

M-Pos94

DIFFERENTIAL EFFECTS OF COCAINE AND COCAETHYLENE ON INTRACELLULAR CALCIUM AND MYOCARDIAL CONTRACTION IN CARDIAC MYOCYTES. ((Z.H. Qiu and J.P. Morgan)) Department of Medicine, Harvard Medical School, Boston, MA 02215.

Isolated ferret cardiac myocytes were used to investigate the influence of cocaine (COC) and cocaethylene (CET) on the intracellular Ca^{2+} transient indicated by the indo-1 405/480 nm ratio signal, and peak cell shortening. Both COC and CET produced significant decreases in peak intracellular Ca^{2+} and peak cell shortening in a dose-dependent manner. Of interest, (1) the minimally effective dose of CET was tenfold lower (10^{-8} M vs 10^{-7} M) than that of COC; (2) the log EC_{50} of CET was $\sim 2 \times 10^{-6}$ M, which was tenfold lower than that of COC ($\sim 2 \times 10^{-5}$ M); and (3) 1×10^{-4} M CET decreased the contraction amplitude by 71 ± 7%, while the same concentration of COC decreased the amplitude only by 55 ± 5%, indicating that CET is more potent than COC. The negative inotropic effects of either COC or CET could be reversed by norepinephrine (~ 5 μM) or calcium. In contrast to COC, CET shifted the peak $[Ca^{2+}]_i$-peak shortening relationship downward, indicating that CET decreased myofilament Ca^{2+}-responsiveness. These data indicate that both COC and CET act directly on cardiac myocytes to produce a negative inotropic effect that is due to decreased Ca^{2+} availability. In contrast to COC, CET produces more potent inhibition by an additional action to decrease myofilament Ca^{2+}-responsiveness. (Supported by NIH grant DA-06306).

M-Pos95

EXCITATION CONTRACTION COUPLING IN AGED HEART. ((S.E. Howlett and J. Bobet)) Dalhousie University, Halifax, Nova Scotia B3H 4H7 and University of Alberta, Edmonton, Alberta T6G 2H9.

Force-interval (FI) curves from left atria of young adult (77 ± 7 day-old, mean ± SEM) and aged (624 ± 22 day-old) hamsters were compared to determine how beat-to-beat regulation of contractile force may be altered in aging heart. Atria were paced (1 Hz) and effects of interposing various test intervals (0.3-1800s) on a test beat following the interval were examined. The most prominent differences in FI curves were: (1) force at short intervals (<1s) was depressed in aged heart when compared to young heart and (2) rest depression was observed at long intervals (>100s) in young but not in aged heart. To quantify differences in FI curves they were fitted with an equation which used five parameters to define the shape of the curve. The parameter U_0 reflects force at short intervals and is believed to reflect Ca^{2+} content of the sarcoplasmic reticulum (SR). The parameter γ reflects rest depression at long intervals; rest depression is believed to occur as Ca^{2+} leaks from SR at rest and is extruded. Values of U_0 were significantly reduced in aged heart (young=2.4 ± 0.3 mN/mg, n=9; old=1.3 ± 0.2 mN/mg, n=8; p=0.005); this is consistent with either less Ca^{2+} influx or reduced Ca^{2+} sequestration by SR in aging heart. Values of γ also were significantly reduced in aged heart (young=0.0047 ± 0.0006 sec^{-1}, n=10; old=0.0028 ± 0.0003 sec^{-1}, n=11; p=0.02), suggesting Ca^{2+} efflux is reduced in aging heart, perhaps due to reduced Na^+-Ca^{2+} exchange.

M-Pos96

RELAXATION OF RAPID COOLING CONTRACTURES: ASSESSMENT OF INTRACELLULAR CALCIUM HANDLING IN HYPERTROPHIED GUINEA-PIG MYOCYTES.

((R.U. Naqvi and K.T. MacLeod)) National Heart and Lung Institute, University of London, Dovehouse Street, London, SW3 6LY, UK.

Abnormalities in the contraction of hypertrophied cardiac muscle have been shown in different mammalian species. Modifications to intracellular calcium handling could contribute to these contraction abnormalities. Rewarming to 22°C after the initiation of a rapid cooling contracture (RCC) brings about a lowering of cytoplasmic Ca and a relaxation of the cell. The process of relaxation is probably brought about by reuptake of Ca into the SR by the Ca ATPase and by efflux of Ca to the exterior of the cell by Na-Ca exchange. We have studied the time constants (τ) of relaxation of RCCs in cells obtained from a 2 kidney, 1 clip hypertensive model of hypertrophy. 64 ± 4 days after clipping, both blood pressure and cell size were found to be increased significantly ($p < 0.005$) in the hypertrophy (H) group compared with age and weight-matched controls (C). Cells were loaded with 10μM indo-1-AM, superfused with normal Tyrode (pH 7.4, 2mM Ca, 22°C, stimulated at 0.5Hz) and cell length measured by an edge-detection system. In H cells, rapid rewarming to 22°C in the presence of 10mM caffeine resulted in relaxation which was 725 ± 100% (n=5) slower than that in normal Tyrode whereas in C cells the caffeine-induced slowing of relaxation was 192 ± 48% (n=8) slower than control. This significant ($p < 0.005$) slowing of the H cells rewarming relaxation in caffeine together with the associated decline in intracellular Ca suggests abnormal calcium extrusion by mechanisms other than the SR, such as Na-Ca exchange.

M-Pos97

Na^+-CURRENT INDUCED Ca^{2+}-TRANSIENTS IN PATCH CLAMPED CARDIAC MYOCYTES REVEALED BY RATIOMETRIC CONFOCAL MICROSCOPY

P. Lipp & E. Niggli, Department of Physiology, University of Bern, 3012 Bern, Switzerland.

In heart muscle a critical link between electrical excitation and mechanical contraction is the activation of Ca^{2+}-release from the SR. Recently, indirect evidence has suggested an important functional role of short-lived subsarcolemmal concentration gradients for ec-coupling. This conclusion was derived from the observation that Na^+-currents could trigger Ca^{2+}-release from the SR in the absence of Ca^{2+} current, presumably by activating the Na-Ca exchange to transport Ca^{2+} into the cell. However, this hypothesis has not remained unquestioned. We used a new approach for time-resolved confocal microscopy with a mixture of the Ca^{2+} indicators Fluo-3 and Fura-Red to measure $[Ca^{2+}]_i$ ratiometrically. The fluorescence ratio was converted into Ca^{2+}-concentration by applying an in vitro calibration. The patch-clamp technique was used to dialyze the cells with the dyes and to measure membrane currents. Ca^{2+} transients induced by Ca^{2+}-currents or by Na^+-currents were analyzed in the absence and presence of 20 μM ryanodine. In agreement with the Ca^{2+}-induced Ca^{2+}-release concept the amplitude and time-course of the different types of Ca^{2+}-transients exhibited clearly distinguishable characteristics. Furthermore, we were able to detect, visualize and compare the small Ca^{2+}-transients resulting from Ca^{2+} and Na^+ currents alone (when the SR was inhibited by ryanodine). Under these conditions kinetic differences between Ca^{2+} and Na^+ current induced transients were revealed with the fast indicator Fluo-3 and appear to exclude the possibility of an uncontrolled activation of Ca^{2+}-channels by escape of the voltage-clamp during Na^+ currents. These results thus support the hypothesis that Na^+ current can activate the Na-Ca exchange and result in an increase of $[Ca^{2+}]_i$ that is large enough to trigger Ca^{2+}-release from the SR. These findings also support the view that a restricted space exists underneath the sarcolemmal membrane. Supported by SNF.

M-Pos98

DO INTERACTIONS BETWEEN PHOTOLABILE CA CHELATORS AND INDO-1 PREVENT SIMULTANEOUS MEASUREMENT AND MANIPULATION OF $[CA_i]$?

R.W. Hadley, M.S. Kirby, W.J. Lederer, J.P.Y. Kao, Dept. of Physiology, Univ. of Maryland School of Medicine, Baltimore, MD 21201.

Emission spectra of indo-1, DM-nitrophen (DM), nitr-5 (N5), diazo-2 (DZ), and various combinations of indo-1 and DM, N5 and DZ were obtained in a spectrometer using an excitation wavelength of 355 nm and a path length of 100 μ. The aim of these experiments was to determine if the absorbance or fluorescence of the photolabile Ca chelators interfered with the measurement of indo-1 fluorescence to such an extent that calibration became impossible or impractical. DM in its unaltered state is barely fluorescent, and does not affect the shape of the indo-1 emission spectra up to a ratio of 20:1 (chelator/indo-1). DZ was found to have similar properties. N5 is weakly fluorescent, with an emission peak at 520 nm. N5 did not significantly perturb the shape of the indo-1 emission spectra until a ratio of 20:1 was reached. However, all three photolabile Ca chelators absorbed excitation light, and thus diminished peak indo-1 fluorescence. This effect was negligible at a path length of 10 μ. Finally, the optical properties of the photoproducts of DM, DZ and N5 were studied. DZ still was negligibly fluorescent after complete photolysis. The photoproduct(s) of DM were more fluorescent than DM itself, but were still only 0.3% as fluorescent as indo-1. The photoproduct of N5 was more troublesome, as it was 2.2% as fluorescent as indo-1. It was concluded that: 1) DZ is nearly innocuous with respect to $[Ca_i]$ measurements using indo-1. 2) DM also would not affect indo-1 ratios until the concentration of photolyzed DM was ten times that of indo-1. 3) The use of N5 requires some care. The N5/indo-1 ratio should be no larger than 10:1, and the ratio of photolyzed N5/indo-1 should be no higher than 5:1.

M-Pos99

EFFECTS OF THAPSIGARGIN (TG) AND CYCLOPIAZONIC ACID (CPA) ON TWITCH FORCE AND SR Ca CONTENT OF RABBIT VENTRICULAR MUSCLE.

((S. Baudet, R. Shaoulian and D.M. Bers)) URA CNRS 1340, CP 3013, Nantes, France and Loyola Univ. Chicago, Maywood, IL, USA

TG and CPA are reported to be specific high affinity inhibitors of the SR Ca-pump in isolated membranes and cells, with TG causing complete pump inhibition at [nM]. To evaluate the effectiveness of TG and CPA in small multicellular cardiac preparations we used rapid cooling contractures (RCCs) to assess the SR Ca load at steady state. In striking contrast to observations in single myocytes (Bassani *et al.*, 1993, this issue) TG caused remarkably slow and incomplete SR Ca depletion in multicellular preparations. Even a 1 hr exposure to 500 μM TG at 30°C and 0.5 Hz stimulation only decreased RCCs by 76±5% (and 100 μM CPA reduced RCCs by 55±10%, mean±SEM). In contrast 10 min with 20 mM caffeine completely abolished RCCs. The time constant of rest decay of RCCs was accelerated by both TG (from 83±18 to 26±6 s) and CPA (from 68±11 to 10±5 s). This might be expected since Ca leaking from the SR during rest cannot be taken back up as efficiently, favoring Ca extrusion by the sarcolemmal Na/Ca exchanger. TG and CPA decreased twitch force (by 44±7% and 39±11% respectively) and increased twitch duration, presumably due to the SR effects. Time to peak force was increased by 28±7% and 81±9% for TG and CPA respectively. However, time to half relaxation was increased 56±10% by CPA, but not by TG (5±7%). While the lack of TG effect on relaxation may indicate that Na/Ca exchange can compensate for a weakened SR Ca-pump, the differential effects of CPA and TG on twitch time course raise the possibility that effects other than SR Ca-pump inhibition might occur at these high concentrations. We conclude that complete blockade of SR Ca uptake by TG or CPA in multicellular preparations cannot be assumed, even at high [TG] or [CPA], unless evaluated (e.g. by RCC).

M-Pos100

THE FRACTION OF SR Ca RELEASED AND REACCUMULATED DURING TWITCHES IN ISOLATED RABBIT MYOCYTES.

((José Wilson M. Bassani, Rosana A. Bassani and Donald M. Bers)) Loyola University, Maywood, IL 60153.

Using caffeine induced contractures (CafC) and thapsigargin (TG) we measured the number of twitches required to reload a depleted SR and what fraction of SR Ca is released at one twitch. Similar results were obtained for twitches or Ca_i transients using indo-1. Sustained exposure to 10 mM caffeine completely depletes the SR of Ca (as assessed by a second CafC). After such Ca depletion, 4-5 twitches are necessary to reload the SR to the steady state level (τ=1.6 twitches, left Fig). We also determined the time required for complete inhibition of the SR Ca pump by TG. After SR Ca depletion 5 μM TG was applied for various times prior to a train of "reloading" twitches. 90 s was sufficient to completely prevent CafC after these reloading twitches (TG left Fig). To assess SR Ca released at one twitch in cells with Ca loaded SR, 5 μM TG was applied for 90 s to prevent SR Ca reuptake. Then 1 or several twitches were activated (causing SR Ca release, but with no reuptake). After the twitch (or train) a CafC was used to assess remaining SR Ca. We found that one twitch released ~½ the Ca in the SR (right Fig), but the beat-dependence was biexponential (τ=0.9 and 60 twitches). The slower phase might represent a caffeine-sensitive pool of Ca not normally released during a twitch.

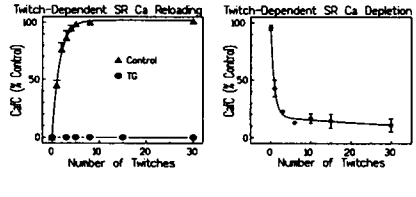

M-Pos101

ALTERATIONS OF INTRACELLULAR Ca^{2+} AND CONTRACTILITY IN AEQUORIN-LOADED VENTRICULAR MYOCYTES FROM THE FERRET HEART WITH PRESSURE-OVERLOAD HYPERTROPHY.

((J.X. Wang, K. Flemal, Z.H. Qiu, and J.P. Morgan)) Department of Medicine, Harvard Medical School, Boston, MA 02215.

To determine the alterations in contractility of the hypertrophied cardiac myocytes and the associated cellular mechanisms, experiments were performed in aequorin-loaded (chemical loading) left ventricular myocytes isolated from hypertrophied hearts (n=7) and age-matched control hearts (n=7). Five to six months after postvalvular aortic banding, significant left ventricular hypertrophy was present, as indicated by an increased cell width (20.9±0.5 vs 16.8±0.3μm; $p<0.001$) and left ventricular weight/body weight ratio (7.3±0.6 vs 3.7±0.2; $p<0.001$). Cell shortening and the intracellular Ca^{2+} transients (indicated by the aequorin light signal) were recorded. In comparison to controls, the hypertrophied myocytes demonstrated that 1) the peak shortening was decreased (5.4±0.4% vs 7.8±0.4%; $p<0.001$), which was associated with a reduced peak $[Ca^{2+}]_i$ (0.84±0.03 vs 1.06±0.03μM; $p<0.001$); 2) the contraction (from stimulus artifact to 50% relaxation time) was prolonged by ~37% ($p<0.001$), which was associated with a prolongation (~44%, $p<0.001$) of the intracellular Ca^{2+} transient; 3) the peak $[Ca^{2+}]_i$-peak shortening relation was shifted downward, suggesting a decrease in the myofilament Ca^{2+}-responsiveness; 4) isoproterenol ($5x10^{-9}$ M) produced equal increases in the peak $[Ca^{2+}]_i$ of control and hypertrophied myocytes (88.3±21.3% vs 90.0±18.6%; $p>0.05$) in contrast to smaller increases in the peak cell shortening (72.6±18.0% vs 170.1±32.3%; $p<0.02$) of the hypertrophied myocytes, suggesting cellular abnormality beyond the level of the β-receptors; and 5) of interest, the endothelin receptor agonist, endothelin-1 ($1x10^{-8}$ M) produced more pronounced increases in the peak cell shortening (95.0±12.2% vs 60.3±10.3%; $p<0.05$) in the hypertrophied myocytes, suggesting an altered behavior of the receptors for endothelin (Support: HL-31117, HL-01611, HL-07371).

M-Pos102

EFFECT OF ACIDOSIS ON CALCIUM UPTAKE AND EXTRUSION SYSTEMS IN ISOLATED GUINEA-PIG CARDIAC MYOCYTES.

((C.M.N. Terracciano and K.T. MacLeod)) Natl. Heart & Lung Inst., University of London, Dovehouse Street, London, SW3 6LY, U.K.

Intracellular Ca^{2+} handling during acidosis was studied in guinea-pig ventricular myocytes using rapid cooling contractures (RCCs). Rapid cooling of cardiac cells to 0°C in < 1sec induces Ca^{2+} release from the SR resulting in contracture. Under such conditions Ca^{2+} extrusion systems are inhibited. Rapid rewarming to room temperature re-activates the SR Ca^{2+} pump and the Na^+/Ca^{2+} exchanger, the main mechanisms producing relaxation. Applying another cooling period after 10sec, elicits a new RCC. The amplitude of this second contracture is dependent on Ca^{2+} taken up and re-released by the SR minus Ca^{2+} extruded from the cell via Na^+/Ca^{2+}exchange during the relaxation of the first RCC. Using the NH_4Cl rebound technique (15mM NH_4Cl) we produced an intracellular acidosis. In this condition (A), the second RCCs were significantly smaller than the first compared with control (C) (C-RCC_2/RCC_1 = 64.57 ± 7.94% (mean±SD), n=5; A-RCC_2/RCC_1 = 42.80 ± 9.98%, n=4; p=0.016). These results suggest that less $Ca^{2+}$is released from the SR during RCC_2, probably because SR uptake or release mechanisms are affected by acidosis. To study Na^+/Ca^{2+} exchange specifically in acidosis, we used a superfusing solution containing 10mM caffeine. In these conditions RCCs were elicited and $[Ca^{2+}]_i$ measured using Indo-1. During acidosis, the decline of $[Ca^{2+}]_i$ on rewarming was significantly slower than in control (C-$t_{½}$ = 955 ± 223 msec, n=4; A-$t_{½}$ = 1600 ± 349 msec, n=4; p=0.026). We conclude that acidosis can affect both Ca^{2+} handling at the SR and Na^+/Ca^{2+} exchange, leading to modifications of cellular Ca^{2+} homeostasis.

M-Pos103

RATE-DEPENDENT DECREASE OF TWITCH AMPLITUDE DURING HYPERCARBIC ACIDOSIS IN RAT CARDIAC MYOCYTES

((G.Gambassi, E.G. Lakatta, H.A. Spurgeon, M.C. Capogrossi)) Laboratory of Cardiovascular Science, Gerontology Research Center, NIA, NIH, Baltimore, MD.

Hypercarbic acidosis (HA) causes a variable decrease of myocardial contractility. The mechanisms for this variability are unknown. In rat cardiac myocytes we examined the effect of HA on twitch amplitude (TA), cytosolic $[Ca^{2+}]$, (Ca_i, measured by indo-1 free acid fluorescence) and cytosolic pH (pH_i, measured by SNARF-1 fluorescence). Cells were in bicarbonate buffer (5% or 20% CO_2; Ca^{2+} 1.5 mM), paced at 0.5 (n=5) or 1.5 Hz (n=11). HA for 10 min decreased pH_i .37±.05 units (n=6, control pH_i 7.33±.07) and the decrease was similar and stable in both groups. After HA for 10 min the decrease in TA was more marked at 1.5 than at 0.5 Hz (Fig, p<0.01) but systolic Ca_i (SYST) was increased at 0.5 Hz more than 1.5 Hz (Fig, p<0.05). In contrast, diastolic Ca_i (DIAST) was higher at 1.5 than at 0.5 Hz (Fig, p<0.05). Sarcoplasmic reticulum (SR) Ca^{2+} content, assessed by a 100 msec caffeine pulse (20 mM), was similar at both rates (n=3; not shown). Thus, a greater increase of diastolic Ca_i during HA at higher stimulation rate may inhibit SR Ca^{2+} release and explain the rate-dependence of TA decrease during myocardial acidosis.

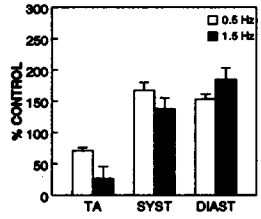

M-Pos104

Fluo-3 and BCECF fluorescence measurement in alkalinized or acidified single muscle fibers.

((P.Bolaños[1], M. DiFranco[2] and C.Caputo[1])). CBB. IVIC[1] and Facultad[2] de Ciencias, Universidad Central de Venezuela. Caracas

The fluorecent pH indicator BCECF was used to follow intracellular pH (pH_i) changes in single muscle fibers subjected to different experimental conditions. The fibers were loaded by exposing them to the AM form of the dye (4 μM for 10 minutes). Calibrations were carried out in vitro or in fibers exposed to nigericin. Exposure of the fibers to 10 mM NH_4Cl, caused an internal alkalinization of about 0.5 pH units, these changes only caused a slight potentiation of twitch tension. Exposure to CO_2 at different external pH values could cause a drop in pH_i of up to 0.6 units, which were accompanied by a marked reduction of twitch tension. After tetanic stimulation of 1 to 2 s duration, the pH_i baseline value increased by less than 0.01 pH unit. pH_i changes during contraction could not be measured due to movement artefact.

Other fibers, loaded with Fluo-3 AM were used to measure contractile force and calcium transients under conditions of internal alkalinization or acidification. During alkalinization, the Fluo3 baseline level diminished without marked changes in the transients associated with twitches. During intracellular acidification, the fluorescence basal level increased while the twitch transients (tension and fluorescence) showed a marked reduction both in magnitude and rate of rise and fall. Changes of this type were never observed following tetanic contractile activity in normal fibers, indicating that in non-fatigued fibers, contractile activity does not cause appreciable pH_i changes. Supported by CONICIT fund S1-2248 and S1-2289 and CDCH fund 03-34-2614-91

M-Pos105

INTRACELLULAR ACIDOSIS IN SKELETAL MUSCLE SLOWS RELAXATION OF FORCE AND CALCIUM SIGNALS AND DECREASES CALCIUM SENSITIVITY.

((A.J. Baker, R. Brandes* & M.W. Weiner)) Univ Calif. San Francisco, CA 94121 & *Loyola Univ Chicago, Maywood, IL 60153.

Muscle fatigue is associated with intracellular acidosis, but its role in fatigue is unclear. To investigate how acidosis affects contractility, acidosis was induced in whole frog skeletal muscle by raising the perfusate pCO_2 from 5% to 80%. Tetanic force and fluorescence were monitored in muscles (n=6) loaded with the fluorescent calcium indicator INDO-1. **Results** Fig.1 Intracellular acidosis (bold traces) did not appreciably decrease tetanic force, however relaxation was considerably slowed. Similarly, the fluorescence ratio (400/470nm) was not reduced but relaxation of the ratio was also slowed. Fig.2: The force-calcium relation during relaxation moved to the right with acidosis. **Conclusions:** 1) acidosis does not markedly decrease force in-vivo. 2) acidosis may slow force relaxation by slowing calcium removal from the myoplasm. 3) acidosis reduces calcium-sensitivity in-vivo.

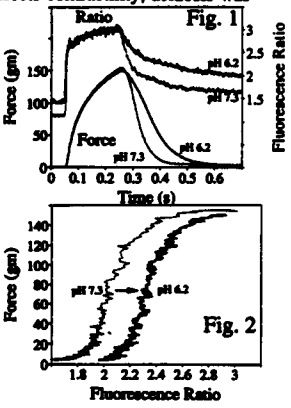

M-Pos106

EFFECTS OF HYPOXIA ON SODIUM/CALCIUM EXCHANGE IN ISOLATED GUINEA-PIG CARDIAC MYOCYTES.

((C.M.N. Terracciano, R.U.Naqvi and K.T.MacLeod)) Natl. Heart & Lung Inst., University of London, Dovehouse Street, London, SW3 6LY, U.K.

We have studied the ability of Na^+/Ca^{2+} exchange to efflux Ca^{2+} from guinea-pig ventricular myocytes subjected to hypoxia. When paired rapid cooling contractures (RCCs) are used, the amplitude of the second contracture is dependent on Ca^{2+}taken up and re-released by the SR minus Ca^{2+}extruded from the cell during the relaxation of the first RCC. The ratio RCC_2/RCC_1 is an index of the relative amount of relaxation brought about by non-SR mechanisms. Under control conditions RCC_2/RCC_1 = 66.8 ± 10.8%, (mean±SD), n=8; under Na-free conditions RCC_2/RCC_1 = 96.73 ± 4.24, n=7. This implies that, for guinea-pig myocytes at 22°C, SR Ca^{2+} uptake accounts for about 67% and Na^+/Ca^{2+}exchange accounts for about 30% relaxation.

Cardiac myocytes were superfused with a glucose-free Tyrode solution and were made hypoxic by bubbling N_2 vigorously in the superfusing solution and streaming the same gas across the top of the chamber containing the cells. Hypoxia was applied for up to 20 min and paired RCCs, as described above, were recorded every 5 min. The ratios RCC_2/RCC_1 after 15 min (H15) and after 20 min (H20) of hypoxia were significantly greater than in control (C) (C-RCC_2/RCC_1 = 66.12 ± 6.3%, n = 5; H15-RCC_2/RCC_1 = 79.03 ± 6.96%, n=5, p=0.018; H20-RCC_2/RCC_1 = 88.73 ± 3.27%, n=3, p=0.0011). We conclude that hypoxia in guinea-pig ventricular myocytes produces an inhibition of the Na^+/Ca^{2+} exchange.